

**DOCTORAL THESIS**

# Chemical Modification of Met and His Residues of Amyloid $\beta$ Peptide. Influence of Copper Ions and Effect on Fibrillization

Merlin Sardis

TALLINN UNIVERSITY OF TECHNOLOGY  
DOCTORAL THESIS  
19/2021

**Chemical Modification of Met and His  
Residues of Amyloid  $\beta$  Peptide. Influence  
of Copper Ions and Effect on Fibrillization**

MERLIN SARDIS



TALLINN UNIVERSITY OF TECHNOLOGY  
School of Science  
Department of Chemistry and Biotechnology

This dissertation was accepted for the defense of the degree of Philosophy in Gene Technology on 26.02.2021

**Supervisors:** Prof. Peep Palumaa  
Department of Chemistry and Biotechnology  
Tallinn University of Technology  
Tallinn, Estonia

**Co-supervisor:** Ph.D. Vello Tõugu  
Department of Chemistry and Biotechnology  
Tallinn University of Technology  
Tallinn, Estonia

**Opponents:** Prof. Jan Johansson  
Department of Bioscience and Nutrition  
Karolinska Institutet  
Stockholm, Sweden

Prof. Ago Rinken  
Institute of Chemistry  
Faculty of Science and Technology  
University of Tartu  
Tartu, Estonia

**Defence of the thesis:** 20.04.2021, Tallinn

**Declaration:**

Hereby I declare that this doctoral thesis, my original investigation and achievement, submitted for the doctoral degree at Tallinn University of Technology, has not been submitted for any academic degree.

Merlin Sardis



European Union  
European Regional  
Development Fund



Investing  
in your future

-----  
Signature

Copyright: Merlin Sardis, 2021  
ISSN 2585-6898 (publication)  
ISBN 978-9949-83-681-9 (publication)  
ISSN 2585-6901 (PDF)  
ISBN 978-9949-83-682-6 (PDF)  
Printed by Spin Press

TALLINNA TEHNIKAÜLIKOO  
DOKTORITÖÖ  
19/2021

**Metioniini ja histidiini jääkide keemiline  
modifitseerimine amüloid- $\beta$  peptiidis.  
Vaskioonide mõju ja efekt fibrillisatsioonile**

MERLIN SARDIS







# Contents

List of Publications .....	6
Introduction .....	8
Abbreviations .....	9
1 Review of the Literature.....	10
1.1 Alzheimer’s disease .....	10
1.1.1 Familial and sporadic AD.....	12
1.1.2 Treatment of AD .....	14
1.1.3 Molecular and pathological mechanisms of AD .....	15
1.1.3.1 Amyloid cascade hypothesis.....	15
1.1.3.2 Tau hypothesis.....	17
1.1.3.3 Neuroinflammation in AD.....	17
1.1.3.4 Mitochondrial dysfunction in AD.....	18
1.2 Amyloid $\beta$ peptides (A $\beta$ ) .....	18
1.2.1 Production of A $\beta$ peptide.....	19
1.2.2 A $\beta$ peptide assemblies .....	22
1.2.3 A $\beta$ peptide and metal ions.....	24
1.3 Oxidative stress .....	27
1.3.1 Oxidative stress in AD .....	28
1.4 Chemical modifications of A $\beta$ peptide .....	29
1.4.1 The oxidation of Met35 in A $\beta$ peptide.....	30
1.4.2 DEPC modification of His residues in A $\beta$ peptide .....	31
2 Aims of the study .....	33
3 Materials and Methods.....	34
4 Results .....	35
5 Discussion.....	37
Conclusions .....	40
References .....	41
Acknowledgments.....	57
Abstract.....	58
Kokkuvõte .....	60
Appendix .....	63
Publication I.....	63
Publication II.....	71
Publication III.....	81
Publication IV.....	87
CURRICULUM VITAE.....	107
ELULOOKIRJELDUS .....	109

## List of Publications

List of publications used in this thesis by Merlin Sardis (formerly Friedemann):

- I Tiiman, A., Noormagi, A., **Friedemann, M.**, Krishtal, J., Palumaa, P., & Tõugu, V. (2013). Effect of agitation on the peptide fibrillization: Alzheimer's amyloid-beta peptide 1-42 but not amylin and insulin fibrils can grow under quiescent conditions. *J Pept Sci*, 19(6), 386-391. doi: 10.1002/psc.2513
- II **Friedemann, M.**, Helk, E., Tiiman, A., Zovo, K., Palumaa, P., & Tõugu, V. (2015). Effect of methionine-35 oxidation on the aggregation of amyloid-beta peptide. *Biochem Biophys Res Commun*, 463(1), 94-99. doi: 10.1016/j.bbrep.2015.07.017
- III Tõugu, V., **Friedemann, M.**, Tiiman, A., & Palumaa, P. (2014). Copper(II) ions and the Alzheimer's amyloid- $\beta$  peptide: Affinity and stoichiometry of binding. *AIP Conference Proceedings*, 1618(1), 109-111. doi: 10.1063/1.4897689
- IV **Friedemann, M.**, Tõugu, V., & Palumaa, P. (2020). Cu(II) partially protects three histidine residues and the N-terminus of amyloid-beta peptide from diethyl pyrocarbonate (DEPC) modification. *FEBS Open Bio*. doi: 10.1002/2211-5463.12857

## Author's Contribution to the Publications

- I The author contributed to the planning of experiments and analysis of the data, performed the SDS-PAGE experiment.
- II The author performed the experimental work, analyzed the data, and participated in manuscript preparation
- III The author performed the experimental work of the A $\beta$ 1-16 peptide titration measurements with Cu(II) ions and analyzed the data.
- IV The author performed the experimental work, analyzed the data, and participated in manuscript preparation

## Other Publications

Taler-Vercic, A., Kirsipuu, T., **Friedemann, M.**, Noormagi, A., Polajnar, M., Smirnova, J., Znidaric, M. T., Zganec, M., Skarabot, M., Vilfan, A., Staniforth, R. A., Palumaa, P., & Zerovnik, E. (2013). The role of initial oligomers in amyloid fibril formation by human stefin B. [Research Support, Non-U.S. Gov't]. *International Journal of Molecular Sciences*, 14(9), 18362-18384. doi: 10.3390/ijms140918362

Wallin, C., **Friedemann, M.**, Sholts, S. B., Noormagi, A., Svantesson, T., Jarvet, J., Roos, P. M., Palumaa, P., Graslund, A., & Warmlander, S. (2019). Mercury and Alzheimer's Disease: Hg(II) Ions Display Specific Binding to the Amyloid-beta Peptide and Hinder Its Fibrillization. *Biomolecules*, 10(1). doi: 10.3390/biom10010044

Kirsipuu, T., Zadoroznaja, A., Smirnova, J., **Friedemann, M.**, Plitz, T., Tougu, V., & Palumaa, P. (2020). Copper(II)-binding equilibria in human blood. *Sci Rep*, 10(1), 5686. doi: 10.1038/s41598-020-62560-4

## Introduction

Protein fibrillization and amyloid formation is the hallmark of more than thirty different diseases, including neurodegenerative Alzheimer's disease (AD). AD is the most common form of dementia, with approximately 50 million people affected worldwide. Although enormous efforts have been directed to understanding the mechanisms behind AD pathology, there is still no cure.

According to the prevalent amyloid cascade hypothesis, AD starts with the pathological build-up of cerebral extracellular amyloid plaques composed of fibrillated amyloid  $\beta$  ( $A\beta$ ) peptides. Although the fibrillization of  $A\beta$  peptide has been intensively studied, the mechanism of amyloid formation and its propagation *in vivo* is still unsolved.  $A\beta$  peptide fibrillization process *in vitro* is affected by multiple factors such as temperature, pH, agitation, etc., which can give information about the fibrillization properties of  $A\beta$  peptide and gain an insight into the molecular mechanisms of AD. It has been generally accepted that the agitation of the solution substantially accelerates the peptide and protein fibrillization *in vitro*; however, the origin and variability of the accelerating effect in the case of different peptides has remained elusive. Stopping the agitation of different peptides in diverse stages of the fibrillization process can shed light on these critical aspects of the fibrillization process.

In AD pathogenesis, elevated oxidative stress has been observed in the AD brain, and the Met35 in  $A\beta$  peptide becomes oxidized to sulfoxide. Despite the research, there is still no consensus about the role of Met35 in oxidative stress and how the oxidation of Met35 affects  $A\beta$  peptide fibrillization.

Copper, one of the redox-active metals, has been implicated in AD pathology as the binding of Cu(II) ions to the  $A\beta$  peptide affects the onset and the rate of the  $A\beta$  peptide fibrillization. At the same time, there is no consensus about the stoichiometry of Cu(II) binding to  $A\beta$  peptide. The effect of pH on the binding curve of Cu(II) ions to  $A\beta$ 1-16 peptide could give reliable information about the stoichiometry of Cu(II) binding to  $A\beta$ . This interaction involves His6, His13, and His14 residues assumingly. Chemical modification of His residues with diethylpyrocarbonate (DEPC) can establish which His residues are protected by Cu(II) ions and estimate the role of His residues in the  $A\beta$  peptide fibrillization process.

In the current study, stopping the agitation of different peptides in the fibrillization process highlights the specific ability of  $A\beta$ 1-42 fibrils to grow under quiescent conditions after stopping the agitation. It was demonstrated that oxidative modification of Met35 in  $A\beta$  peptides by  $H_2O_2$  slows down  $A\beta$  peptide fibrillization; Cu(II) binding studies of  $A\beta$ 1-16 showed that the binding curve could be fitted by expecting binding of only one Cu(II) ion. Chemical modification of His residues in  $A\beta$  peptide with DEPC resulted in a decrease of the fibrillization and Cu(II) binding protected  $A\beta$  peptide from DEPC modification, indicating all His residues and peptide N-terminus are involved in Cu(II) binding.

Obtained *in vitro* results give new insight into the properties of  $A\beta$  peptide fibrillization that might help understand its role in AD pathogenesis.

## Abbreviations

AD	Alzheimer's disease
ADDLs	A $\beta$ -derived diffusible ligands
AICD	APP intracellular domain
ApoE	Apolipoprotein E
APP	Amyloid precursor protein
ATCUN	amino-terminal Cu(II) and Ni(II) binding motif
A $\beta$	Amyloid $\beta$ peptide
BBB	Blood-brain barrier
CSF	Cerebrospinal fluid
DEPC	Diethylpyrocarbonate
ER	Endoplasmatic reticulum
ESI MS/MS	Electrospray ionization tandem mass spectrometry
FAD	Familial Alzheimer's disease
HFIP	1,1,1,3,3,3-hexafluoro-2-propanol
MALDI MS	Matrix assisted laser desorption/ionization mass spectrometry
Met35	Methionine in the 35. position
NFT	Neurofibrillary tangles
NMDA	N-methyl-D-aspartate
PART	primary age-related tauopathy
PD	Parkinson's disease
PS-1	Presenilin-1 protein
PS-2	Presenilin-2 protein
ROS	Reactive oxygen species
SAD	Sporadic Alzheimer's disease
TEM	Transmission electron microscopy
ThT	Thioflavin T

# 1 Review of the Literature

## 1.1 Alzheimer's disease

Alzheimer's disease (AD) was first described by Alois Alzheimer, a psychiatrist, and neuropathologist, who linked a distinct clinical picture with peculiar histological findings in the post-mortem brain of his dementia patient Auguste Deter. These observations were published in 1907 in a paper called "Über eine eigenartige Erkrankung der Hirnrinde" (On an Unusual Illness of the Cerebral Cortex), which was translated into English in 1995. According to Stelzmann, Alzheimer noted that neurons, especially in the upper layer of the cortex, have entirely disappeared and that there were two types of depositions in the brain cortex (Alzheimer, Stelzmann et al. 1995).

Today we know that AD is the most common form of dementia, comprising 50-60% of all dementia cases (ADI 2018). In 2018, there were around 50 million cases in the world. AD is an age-dependent disease with no cure, and its prevalence in the current aging population is increasing. It is estimated that the number of people with AD will increase to 152 million by 2050 (ADI 2018). According to the World Alzheimer report in 2018, the current cost of the disease is one trillion US dollars a year, but it is predicted to double by the year 2030 (ADI 2018).

From a pathophysiological point of view, AD is an incurable neurodegenerative disorder characterized by progressive loss of long-term memory and cognitive decline resulting from the loss of neurons (Alzheimer, Stelzmann et al. 1995). The clinical symptoms of AD result from neuronal degeneration of selective cognitive and memory-related regions such as the hippocampus, amygdala, and cerebral cortex. The disease begins with the loss of pyramidal neurons and spreads to the hippocampus and parietal and temporal regions of the neocortex, the final stages of the disease are associated with the loss of GABA-containing neurons in the cerebellum (Francis, Palmer et al. 1999; Rub, Del Tredici et al. 2001). Based on clinical symptoms, AD is divided into six stages: I-II being mild (usually lasts 2-5 years); III-IV being moderate (lasts 2-4 years), and V-VI being severe AD (Braak and Braak 1991; Palmer 2002; Holtzman, Morris et al. 2011; Sperling, Aisen et al. 2011). The first symptoms are commonly mild cognitive difficulties and the loss of short-term memory. As the disease progresses, long-term memory becomes affected, and cognitive abilities decline, including decision-making, orientation, learning new things, and behavioral disturbances with communication problems resulting from the shrinking vocabulary. Reading and writing skills are progressively declining as the long-term memory is affected and remembering the family members' names becomes difficult (Tarawneh and Holtzman 2012). In this stage, controlling movements becomes impaired, and difficulty in fine motor tasks becomes evident (Holtzman, Morris et al. 2011). The patient goes from needing assistance or supervision to needing help with basic daily activities. In advanced stages, the loss of brain function becomes so severe that patients need constant care, and language consists only of simple phrases that are ultimately lost entirely. The patient depends on caregivers for dressing, eating, and using the bathroom (Tarawneh and Holtzman 2012). In the final stages, patients become bedbound and die in 7-10 years from the diagnosis (Holtzman, Morris et al. 2011).

From a histological point of view, the AD is characterized by two hallmarks in the AD brain: 1) occurrence of the extracellular amyloid plaques (also called senile and neuritic plaques) and 2) occurrence of intracellular neurofibrillary tangles (NFT)

(Alzheimer, Stelzmann et al. 1995). Amyloid plaques consist mainly of fibrillar amyloid  $\beta$  peptides ( $A\beta$ ) core surrounded by dystrophic neurites, microglia, and astrocytes (Glennner and Wong 1984; Masters, Multhaup et al. 1985; Masters, Simms et al. 1985; Wong, Quaranta et al. 1985; Holtzman, Morris et al. 2011).  $A\beta$  peptides in amyloid plaques contain mainly 42 residues ( $A\beta_{1-42}$ ) and 40 residues ( $A\beta_{1-40}$ ).  $A\beta$  peptides are produced during the enzymatic cleavage of amyloid precursor protein (APP) (described in Chapter 1.2.1). The size of amyloid plaques varies widely from 10 to 200  $\mu\text{m}$  (Selkoe 2001; Morgan, Colombres et al. 2004), whereas, larger plaque size distribution correlates with early onset of AD (Serrano-Pozo, Mielke et al. 2012). In the human monocytic cell line model, it was demonstrated that the amyloid plaques are initially formed intracellularly, and after cell death, the plaques are released into the extracellular space (Friedrich, Tepper et al. 2010). Amyloid plaques are associated with microglia and astrocytes, that contain in addition to  $A\beta$  peptides also small quantities of metal ions, amyloidogenic molecules like apolipoprotein E (ApoE) (Strittmatter, Saunders et al. 1993), proteoglycans, inflammatory and serum related molecules like cholinesterases, proteases, and some other proteins (Drummond, Nayak et al. 2017).  $A\beta$  peptides in amyloid plaques have been shown to contain post-translational modifications such as covalent cross-linking of Tyr10, oxidation of Met35, and pyroglutamated amino acids (Atwood, Martins et al. 2002; Kumar, Singh et al. 2015; Wildburger, Esparza et al. 2017). In addition to described tightly packed amyloid plaques, amorphous plaques were found in the late 1980s (Joachim, Morris et al. 1989). These amorphous plaques were named “diffuse” plaques or “preamyloid deposits” consisting mainly from  $A\beta_{42}$  and are usually smaller than 20  $\mu\text{m}$  (Castellani, Rolston et al. 2010). It is suggested that diffuse plaques may be the precursors of the amyloid plaques (Selkoe 2001; Atwood, Martins et al. 2002).

Intracellular neurofibrillary tangles (NFT) are composed of aggregated microtubule-associated hyperphosphorylated tau protein and contain clusters of paired helical filaments (Grundke-Iqbal, Iqbal et al. 1986; Kosik, Joachim et al. 1986). MW of Tau protein is 68 kDa, and it is expressed in all neurons, where it stabilizes cytoskeleton by binding to tubulin; however, hyperphosphorylation of tau proteins causes them to form NFT-s inside the neurons (Grundke-Iqbal, Iqbal et al. 1986). Most of these fibers are composed from pairs of 10 nm filaments wound into helices with a helical period of 160 nm (Selkoe 2001). NFTs characteristic to AD are also occurring in case of other neurodegenerative disorders referred to as tauopathies, including frontotemporal dementia, Parkinson’s disease (Palmer 2011), and tangle-predominant senile dementia termed as “primary age-related tauopathy” (PART) (Crary, Trojanowski et al. 2014). NFT in PART are indistinguishable from those occurring in AD (Crary, Trojanowski et al. 2014).



### 1.1.1 Familial and sporadic AD

There are two types of AD - early-onset familial Alzheimer's disease (FAD) and late-onset, sporadic Alzheimer's disease (SAD), which are responsible for 5% and 95% of cases, respectively (Avramopoulos 2009). FAD starts before the age of 65 and is caused by autosomal dominant mutations in the genes of APP (chromosome 21), presenilin 1 (PS-1) (*PSEN1* gene on chromosome 14), and presenilin 2 (PS-2) (*PSEN2* gene on chromosome 1). Mutations in the APP gene result in altered APP proteolytic processing (Selkoe 2001; Schellenberg and Montine 2012) or alter the propensity of A $\beta$  peptides to aggregate into amyloid fibrils. It is essential to mention that overexpression of normal APP in subjects with chromosome 21 trisomy (Down syndrome) also leads to classical AD pathology around the age of 40. At the same time, subjects with partial chromosome 21 trisomy (with Down syndrome phenotypic features but without the APP gene) showed no significant A $\beta$  deposition or other pathological features (Selkoe 2001). There are 39 APP gene mutations found, 6 of which being non-pathogenic (Cruts, Theuns et al. 2012). The APP mutations are divided into three categories: 1)  $\beta$ -secretase cleavage site mutations; 2)  $\gamma$ -secretase cleavage site mutations; and 3) the A $\beta$  domain mutations (Cheignon, Tomas et al. 2018). The  $\beta$ -secretase cleavage site mutations increase the rate of APP proteolysis by  $\beta$ -secretase, and the mutations in the  $\gamma$ -secretase cleavage site can alter the cleavage position and lead to an increase of the A $\beta$ 1-42/A $\beta$ 1-40 ratio. The mutations in the A $\beta$  region result in the altered propensity of A $\beta$  peptide to form oligomers and fibrils (Cheignon, Tomas et al. 2018).

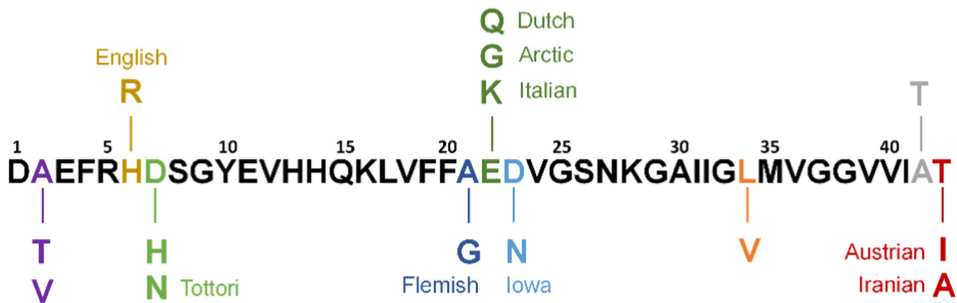


Figure 1. Mutations in A $\beta$  sequence. Figure from (Cheignon, Tomas et al. 2018), reproduction permitted by Elsevier.

Genes of PS-1 and PS-2 encode one subunit in the tetrameric  $\gamma$ -secretase complex. There are 185 mutations identified in the gene of PS-1 and 13 in the gene of PS-2 (Cruts, Theuns et al. 2012). PS-1 gene mutations cause the most aggressive form of AD with the onset before the age of 50 (Schellenberg and Montine 2012). Mutations in PS-1 and PS-2 genes increase the production of A $\beta$  peptides, and all PS-1 mutations associated with FAD increase the  $\gamma$ -secretase cleavage of APP, increase levels of A $\beta$  peptides or alter the A $\beta$ 1-42/A $\beta$ 1-40 ratio (Iversen, Mortishire-Smith et al. 1995).

The majority of AD cases are sporadic (SAD) and are not linked to defined genetic mutations but are affected by genetic and environmental factors that increase the risk of developing AD. The strongest genetic risk factor of SAD is the presence of the  $\epsilon$ 4 allele of the apolipoprotein E (ApoE) gene (chromosome 19) (Strittmatter, Saunders et al. 1993). ApoE consists of 299 amino acid residues and is coded in humans by three common alleles  $\epsilon$ 2,  $\epsilon$ 3, and  $\epsilon$ 4. The  $\epsilon$ 2 allele encodes Cys residues at positions 112 and

158,  $\epsilon 3$  encodes a Cys residue at position 112 and an Arg at position 158, while allele  $\epsilon 4$  encodes an Arg residue at both these locations. (Weisgraber, Rall et al. 1981; Schellenberg and Montine 2012). Inheritance of ApoE  $\epsilon 4$  allele increases the likelihood of developing AD up to five-fold or above five-fold in case of one or two copies, respectively (Selkoe 2001). The  $\epsilon 4$  allele has been shown to decrease the age of AD onset as compared to  $\epsilon 2$  and  $\epsilon 3$  alleles. The presence of  $\epsilon 2$  alleles delays the onset of AD or may even protect against the development of AD (Poirier 2003). Although the  $\epsilon 4$  allele increases the risk for AD (Strittmatter, Saunders et al. 1993), there are also examples that the subjects with two copies of  $\epsilon 4$  allele show no symptoms of AD in the later stages of life or the AD develops without the presence of one or both  $\epsilon 4$  alleles (Selkoe 2001).

ApoE is a plasma protein that is produced and secreted by astrocytes in CNS and plays a role in cholesterol (Weisgraber 1990) and phospholipid homeostasis (Georgiadou, Chroni et al. 2011), synaptic integrity, and neuronal survival (Strittmatter, Saunders et al. 1993; Poirier 2003; Avramopoulos 2009). After brain injury, the synthesis of ApoE is increased, which suggests that it has a role in the repair of the nervous system (Strittmatter, Saunders et al. 1993). ApoE knock-out mice have impaired recycling of cholesterol and synaptic plasticity, and aged animals show cognitive impairment (Poirier 2008). ApoE has been suggested to play a role in AD pathology as it is implicated in phosphorylation and accumulation of tau protein (Arboleda-Velasquez, Lopera et al. 2019), amyloid metabolism, A $\beta$  trafficking, and clearance from the brain by binding directly to A $\beta$  peptide (Strittmatter, Weisgraber et al. 1993; Strittmatter, Saunders et al. 1994; Poirier 2008; Schellenberg and Montine 2012; Cheignon, Tomas et al. 2018). ApoE4 has been shown to bind A $\beta$  peptide faster than ApoE3 (Strittmatter, Weisgraber et al. 1993). ApoE3 bound to A $\beta$ 1-40 peptide is suggested to delay the onset of fibril formation of A $\beta$  peptide *in vitro* but is not an amyloid inhibitor (Evans, Berger et al. 1995). Tau protein has been shown to bind ApoE3 avidly *in vitro* but not ApoE4 (Strittmatter, Saunders et al. 1994). ApoE4 has been shown to be less effective in neuronal repair and membrane lipid uptake than other isoforms.

Recently, homozygote ApoE3 Christchurch (APOE3ch) mutation (R136S) has been shown to postpone cognitive impairment by three decades in PS-1 mutation E280A carriers that cause A $\beta$ 1-42 overproduction and increased A $\beta$  plaque burden in the brain. The R136S mutation is located in the APOE region, known to bind to heparin sulfate proteoglycans and lipoprotein. Although the plaque burden was high, the tau burden and neurodegeneration were limited, and glucose metabolism was preserved compared to patients with AD (Arboleda-Velasquez, Lopera et al. 2019). It was postulated that APOE3ch has beneficial effects on downstream tau pathology and neurodegeneration, which is related to an altered affinity for heparin sulfate proteoglycans or other APOE receptors (Arboleda-Velasquez, Lopera et al. 2019).

Besides, ApoE4 also mutations in genes of cytokines, chemokines, and nitric oxide synthases are associated with increased risk for developing SAD (Domingues, da Cruz et al. 2017). Also, more women are suffering from SAD than men because of higher life expectancy and the decrease in estrogen levels caused by menopause (Janicki and Schupf 2010). It is still unclear how estrogen protects against the development of AD, but it has been observed that postmenopausal women receiving estrogen have reduced risk and delayed onset of AD (Tang, Jacobs D Fau - Stern et al. 1996; Baldereschi, Di Carlo A Fau - Lepore et al. 1998; Waring, Rocca Wa Fau - Petersen et al. 1999).

In addition, lifestyle choices, head injury, high level of blood cholesterol, cardiovascular diseases, and metal exposure, for example, have been related to increased risk for developing SAD (Arab and Sabbagh 2010).

### **1.1.2 Treatment of AD**

Despite the intensive investigations, the exact cause(s) of AD are unknown, and there is no cure. As AD is a multifactorial disease, a single treatment model might not work in all patients (Mullane and Williams 2018; Panza, Lozupone et al. 2019). During 20 years, only four drugs of two types have been approved for use out of 100 tested, but they can only manage some symptoms for some people (ADI 2018; Mullane and Williams 2018; Mullane and Williams 2018; Joe and Ringman 2019). The first type of drug is an NMDA receptor antagonist; the generic name is memantine (ADI 2018), which blocks the effects of the neurotransmitter glutamate, which is excessively released in the AD brains and is causing neuronal damage (Ankarcrona, Mangialasche et al. 2010). The other type of drugs are cholinesterase inhibitors (galantamine, donepezil, and rivastigmine) designed based on the cholinergic hypothesis to restore physiological levels of cholinergic transmission necessary for neuronal signaling and memory functioning (Joe and Ringman 2019). The cholinergic hypothesis is the oldest attempt to explain the cause and mechanism of the disease, where it was proposed that deficiency in the cholinergic signaling initiates the progression of the disease by causing the formation of plaques and tangles (Palmer and Gershon 1990; Francis, Palmer et al. 1999).

There is an urgent need for effective drugs for AD because currently, there are no disease-modifying drugs available, caused by the fact that the understanding of the molecular and pathological mechanisms of AD is incomplete. Our understanding of AD mechanisms could be improved with detailed studies of A $\beta$  peptides and their chemical properties.

### 1.1.3 Molecular and pathological mechanisms of AD

There are mainly four popular hypotheses trying to explain the cause and mechanism of the disease. The first, largest, and most widespread hypothesis is the amyloid cascade hypothesis, the second hypothesis is the tau hypothesis (Maccioni, Farias et al. 2010), the third is neuroinflammatory, and the fourth is the mitochondrial dysfunctioning hypothesis.

#### 1.1.3.1 Amyloid cascade hypothesis

A $\beta$  peptides were first sequenced from the plaques of blood vessels of AD patients in 1984 (Glennner and Wong 1984) and a year later from neuritic plaques (Wong, Quaranta et al. 1985) and senile plaques (Masters, Multhaup et al. 1985; Masters, Simms et al. 1985). It was initially believed that the degree of dementia correlates with the occurrence of plaques in grey matter (Blessed, Tomlinson et al. 1968). In 1992, Hardy and Higgins proposed an amyloid cascade hypothesis according to which neurodegeneration begins with the abnormal processing of the APP that results in the production, aggregation, and deposition of A $\beta$  peptides, which in turn leads to the formation of NFTs and neurodegeneration (Hardy and Higgins 1992). A $\beta$  peptides or their aggregates were believed to be neurotoxic, and the primary cause of neurodegeneration and the formation of NFTs of tau protein, synaptic dysfunction, and neuronal loss was proposed to occur downstream from A $\beta$  production (Hardy and Higgins 1992; Selkoe and Hardy 2016). The amyloid cascade hypothesis is supported by the genetic evidence of FAD combined with the evidence that individuals with chromosome 21 trisomy (Down syndrome) develop AD around the age of 40 because of the APP gene overexpression that locates in chromosome 21. In addition, all disease-causing mutations in FAD result in increased production of more amyloidogenic A $\beta$ 1-42 peptides, which leads to amyloid plaque formation. A $\beta$  deposits in AD patients without the NFTs, further point to the importance of A $\beta$  peptides. Unfortunately, there are also cases of AD and other observations, which are in apparent disagreement with the amyloid cascade hypothesis. For example, there are weak correlations between the time of AD onset and the number of plaques in the brain. Moreover, the appearance of amyloid plaques precedes the manifestation of clinical symptoms by several years. As a result, the amyloid cascade hypothesis focused on A $\beta$  deposits was refined, and small oligomeric amyloid species were declared to be the primary pathological agents (Figure 2) (Selkoe 2008). These oligomeric assemblies of A $\beta$  have been shown to be neurotoxic both *in vitro* and *in vivo* (Haass and Selkoe 2007), and they may be responsible for the loss of neurons and synaptic dysfunction (Tomaselli, Pagano et al. 2017; Xing, Feng et al. 2017).

## *Amyloid cascade hypothesis*

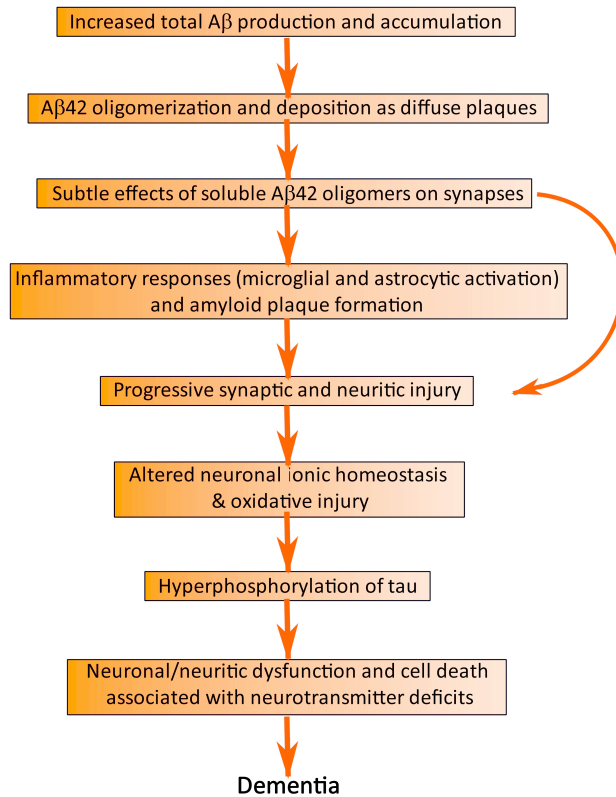


*Figure 2. Advanced amyloid cascade hypothesis events proposed by Hardy and Selkoe, where the curved violet arrow indicated that Aβ oligomers might directly injure the synapses and neuritis in the brain, in addition to activating microglia and astrocytes (Hardy and Selkoe 2002).*

Other contradictory cases have also been observed, which do not support the amyloid cascade hypothesis. For example, Aβ deposits alone can be seen in the brains of healthy elderly subjects (Coria, Castano et al. 1987; Sperling, Aisen et al. 2011), whereas NFTs have been observed without the amyloid deposits in less common neurodegenerative diseases and other disorders (Nelson, Abner et al. 2009; Kovacs, Milenkovic et al. 2013). Thus, it has been suggested that amyloid plaques and NFTs can also occur independently from each other. Consequently, the amyloid cascade hypothesis is now being challenged since it fails to provide a complete or sufficient explanation of the pathophysiology of AD (Palmer 2011).

### 1.1.3.2 *Tau hypothesis*

According to the tau hypothesis (Maccioni, Farias et al. 2010), tau protein is responsible for neurotoxicity based on the observation that tau hyperphosphorylation leads to the degradation of the cytoskeleton, formation of the tau aggregates act as toxic stimuli contributing to microglial activation and neuronal loss. The tau hypothesis is supported by the observation that the NFTs content correlates with disease severity, whereas the deposition of A $\beta$  peptides generally does not correlate with neuronal loss and the severity of AD (Ghoshal, Garcia-Sierra et al. 2002).

### 1.1.3.3 *Neuroinflammation in AD*

In addition to neuronal loss, amyloid plaques, and NFTs, there are also other neuropathological and molecular characteristics in the brain of AD such as disturbances in mitochondrial structure and function (Ankarcrona, Mangialasche et al. 2010), neuroinflammation (Giulian, Haverkamp et al. 1998; Nichols, St-Pierre et al. 2019), increased oxidative stress, disorders of metal ion metabolism, impairment of NMDA receptor-related signaling pathways, dysfunction of lipid metabolism and axonal transport (Crouch, Harding et al. 2008; Kozlov, Afonin et al. 2017), decreased glucose metabolism, and others. Some of these features are also part of typical aging (Coria, Castano et al. 1987; Kozlov, Afonin et al. 2017), but abnormal phenomena have been shown to contribute to AD pathology and are currently under intense investigation as previous hypotheses have not led to an understanding of AD at the molecular level or the development of effective drugs. Most of these processes are somehow linked to A $\beta$  peptides and are therefore connected to the amyloid cascade hypothesis.

The evidence of inflammatory changes in the AD brain are found in locations where neuritic and core plaques are surrounded by clusters of reactive microglia (Palmer 2002; Luca, Calandra et al. 2018; McQuade and Blurton-Jones 2019; Nichols, St-Pierre et al. 2019). Some studies claim A $\beta$  plaques initiate an inflammatory response (Halle, Hornung et al. 2008; Heneka, Kummer et al. 2013; Pereira, Santos et al. 2019) by activating microglia and stimulating the release of neurotoxic cytokines (Giulian, Haverkamp et al. 1996; Manocha, Floden et al. 2016; Chen, Xu et al. 2017; Holscher 2019), others state that microglia activation occurs prior to plaque formation in mice (Boza-Serrano, Yang et al. 2018). According to Prof. Combs and colleagues, APP protein can act as a proinflammatory receptor on monocytes and microglia by interacting with oligomeric A $\beta$  peptide and not with fibrillar A $\beta$  peptide to stimulate microglial activation and increase cytokine secretion (Manocha, Floden et al. 2016). A $\beta$  peptide binding to microglia has been shown to be associated with the HHQK sequence in the A $\beta$  peptide (A $\beta$ 13-16) and activating microglia through a cell-surface binding site involving heparin sulfate (Giulian, Haverkamp et al. 1998). Sequence RHQK in rodent A $\beta$ 40 was ineffective in activating microglia compared to human A $\beta$  (A $\beta$ 40, A $\beta$ 42) (Giulian, Haverkamp et al. 1996; Giulian, Haverkamp et al. 1998). In addition to increased concentrations of released pro-inflammatory cytokines, reactive microglia also releases proteolytic enzymes, free radicals, complement proteins, and nitric oxide (Giulian, Haverkamp et al. 1998). Microglia are usually located around the core of the plaques, whereas astrocytes often surround the outside of the plaque.

#### 1.1.3.4 Mitochondrial dysfunction in AD

Many lines of evidence suggest that mitochondria (Cenini, Lloret et al. 2019) have an important role in neurodegenerative disorders as mitochondrial dysfunction has been shown to occur in AD, Parkinson's, Huntington's, and ALS (Johri and Beal 2012). Mitochondria are abundant in presynaptic nerve terminals where they provide energy in the form of ATP for sustained neurotransmitter release and are crucial for cell survival as mitochondrial damage may lead to decreased ATP production, impaired calcium buffering capacity, and the release of death factors initiating apoptosis (Ankarcrona, Mangialasche et al. 2010). In addition to the role in ATP production, apoptosis, and calcium buffering, mitochondria are also a source of reactive oxygen species and place of lipid synthesis. It has been shown that A $\beta$  accumulation in mitochondria might lead to multiple effects like decrease in the number of mitochondria in the cell, mitochondrial fragmentation, increased ROS production, inhibition of complex IV, and therefore the toxic accumulation of A $\beta$  in the mitochondria is suggested to be the primary cause of mitochondrial dysfunction in AD (Ankarcrona, Mangialasche et al. 2010; Weidling and Swerdlow 2019).

In the early stages of AD, there is a reduced glucose metabolism that could result from reduced cerebral blood flow, deficient insulin signaling, impairment of glucose transport mechanisms, or dysfunction of glycolytic enzymes. Brain energy metabolism depends mainly on glucose. However, neurons cannot store glucose and are therefore dependent on its transport across the blood-brain-barrier (BBB). Glucose uptake by neurons is mediated by glucose transporters, which is insulin-dependent. Insulin is also essential for the transport of glucose into the brain across BBB, and the decrease of these receptors is an indication of insulin resistance (Frazier, Ghoweri et al. 2019). There is a well-established link between AD and type II diabetes mellitus, where type II diabetes patients have an increased risk for developing AD (Holscher 2019). It appears that functional insulin signaling is important for memory formation, and in AD brain areas related to memory, such as the hippocampus and medial temporal cortex, there are decreased levels of insulin receptors. Intranasal insulin administered to patients with early AD has shown improved working memory, attention, and functional status in the pilot study (Reger, Watson et al. 2008).

## 1.2 Amyloid $\beta$ peptides (A $\beta$ )

A $\beta$  peptides are amphipathic polypeptides prone to self-aggregation and fibril formation, which occur in two major forms - A $\beta$ 42 and A $\beta$ 40. A $\beta$ 42 is predominantly associated with AD as it has a higher tendency to form oligomers and fibrils and is also more toxic compared to A $\beta$ 40 (Harper, Wong et al. 1997; Walsh, Lomakin et al. 1997). As A $\beta$ 42 is more prone to aggregation, it is localized mainly in amyloid plaque cores, whereas A $\beta$ 40 is usually colocalized with A $\beta$ 42 (Selkoe 2001).

A $\beta$  sequence consists of a hydrophilic N-terminal region (A $\beta$ 1-28) that originates from the APP extracellular domain and a hydrophobic C-terminal region (A $\beta$ 29-42) that is APP transmembrane part. A $\beta$  peptide adopts essentially random coil structures in water; however, in SDS micelles, A $\beta$  peptide contains two helices: helix one is formed from residues 15-24 and helix two from residues 28-36 (Watson, Fairlie et al. 1998). Soluble unstructured A $\beta$  monomer needs to change into  $\beta$ -sheet conformation to fibrillize, as A $\beta$  insoluble fibrils display the cross-beta structure common to all amyloid

fibrils. Structural analysis of A $\beta$  peptides indicated that the unstructured N-terminal region around residues 1-17 is not important for amyloid fibril formation but is shown to be involved in the binding of metal ions (Habasescu, Jureschi et al. 2020).

### 1.2.1 Production of A $\beta$ peptide

A $\beta$  is derived from ubiquitously expressed transmembrane glycoprotein called amyloid precursor protein (APP) (Selkoe, Podlisny et al. 1988) by sequential proteolytic cleavage by  $\beta$ - (Vassar, Bennett et al. 1999) and  $\gamma$ -secretases (Wiley, Hudson et al. 2005). APP belongs to a larger evolutionary conserved APP superfamily found in different organisms and is expressed in almost all mammalian cell types (Selkoe, Podlisny et al. 1988; Monning, Konig et al. 1992; Sandbrink, Masters et al. 1994; Akaaboune, Allinquant et al. 2000; Sondag and Combs 2004; Galloway, Jian et al. 2007; Lee, Tharp et al. 2008). The APP gene of 290 kb is located on chromosome 21 containing 19 exons (Konig, Monning et al. 1992), of which exons 7, 8, and 15 can be sliced alternatively, leading to three major APP isoforms: APP<sub>695</sub>, APP<sub>751</sub>, and APP<sub>770</sub> (comprising from 695, 751 and 770 amino acid residues) of which the first (APP<sub>695</sub>) is most abundant in the brain, compared with other two isoforms (Tanaka, Shiojiri et al. 1989). APP<sub>751</sub> and APP<sub>770</sub> isoforms are widely expressed in peripheral organs (Selkoe, Podlisny et al. 1988). The ratio of different APP isoform mRNA in the human cortex is approximately APP<sub>770</sub>/APP<sub>751</sub>/APP<sub>695</sub>=1:10:20 (Tanaka, Shiojiri et al. 1989).

The physiological function of the APP is currently unknown. At the same time, it has been suggested that APP has functions in neuronal growth and axonal outgrowth (Billnitzer, Barskaya et al. 2013), neuronal regeneration, synaptogenesis (Priller, Bauer et al. 2006), cell adhesion (Soba, Eggert et al. 2005), migration (Rice, Townsend et al. 2012) and proliferation (Pietrzik, Hoffmann et al. 1998), and can function as a proinflammatory receptor on monocytes and microglia (Manocha, Floden et al. 2016). Predominantly, APP is located at synapses, and the lack of APP affects synapse transmission and formation in cultured hippocampal neuronal cells by increasing the number of functional synapses (Priller, Bauer et al. 2006). Another important function described for APP is maintaining neuronal calcium homeostasis (Santos, Pierrot et al. 2009) and iron regulation (Berggren, Agrawal et al. 2017); for example, APP can promote neuronal iron efflux (Duce, Tsatsanis et al. 2010). It has also been suggested that iron has a role in APP metabolism and that the APP itself has a role in copper homeostasis as copper can also regulate APP expression (Bellingham, Lahiri et al. 2004). APP has also been suggested to interact with Cu(II) ions to induce a localized increase in oxidative stress (White, Multhaup et al. 1999). APP knockout mice show the symptoms of minor weight loss, decreased motor activity, and non-specific degrees of reactive gliosis in the cortex (Zheng, Jiang et al. 1995). APP overexpression has been shown to promote cell growth, and as a result, enlarged neurons in transgenic mice have been seen (Oh, Savonenko et al. 2009). A link has been suggested between type 2 diabetes and AD: abnormal APP metabolism in the pancreas has been linked to the pathogenesis of type 2 diabetes and aggregated A $\beta$  peptide has been detected in type 2 diabetes Langerhans islets (Miklossy, Qing et al. 2010).

APP is synthesized in the endoplasmatic reticulum (ER) and transported to the Golgi complex and finally to the plasma membrane (Siman, Mistretta et al. 1993). The cleavage and processing of APP can be divided into naturally occurring pathways: a non-amyloidogenic and an amyloidogenic pathway (Siman, Mistretta et al. 1993).



In the common non-amyloidogenic pathway, APP is cleaved by  $\alpha$ - and then  $\gamma$ -secretase (Figure 3). Zinc metalloproteinase termed  $\alpha$ -secretase (Roberts, Ripellino et al. 1994) cleaves an 83 residues fragment from the C-terminus (cleavage site within A $\beta$  region) at the cell surface (Parvathy, Hussain et al. 1999), producing a large extracellular amino N-terminal ectodomain (sAPP $\alpha$ ) which displays neurotrophic and neuroprotective properties (Parvathy, Hussain et al. 1999; Turner, O'Connor et al. 2003; Stein, Anders et al. 2004; Nalivaeva and Turner 2013). sAPP $\alpha$  neuroprotective properties are derived from sAPP $\alpha$  protecting neuronal cultures from cell death and increasing the expression levels of several neuroprotective genes such as one of the transthyretins (Stein, Anders et al. 2004). The neuroprotective effect of sAPP $\alpha$  might arise from binding to BACE1, thereby decreasing soluble A $\beta$  and A $\beta$  peptide plaques (Obregon, Hou et al. 2012). The remaining C-terminal membrane-associated fragment in the membrane (CTF- $\alpha$ ; C83) is then cleaved into two pieces by the  $\gamma$ -secretase between Lys16 and Leu17 residues (Siman, Mistretta et al. 1993), producing a short fragment termed p3 (p83; A $\beta$ 17-40/42) and APP intracellular domain (AICD). The tetrameric  $\gamma$ -secretase complex contains PSEN (Presenilin, catalytic subunit), PEN-2 (presenilin enhancer 2), NCT (nicastrin), and APH1 (Anterior Pharynx Defective 1), with ratio 1:1:1:1 (Sato, Diehl et al. 2007).

The minor amyloidogenic pathway is an alternative cleavage pathway for APP, which leads to A $\beta$  generation by membrane-bound aspartyl proteinases termed  $\beta$ - and  $\gamma$ -secretases (Figure 3) (Parvathy, Hussain et al. 1999). These enzymes generate several other physiologically active metabolites in addition to A $\beta$ . The initial proteolysis of APP is performed by  $\beta$ -secretase (BACE) at a position of 99th amino acid residue from the C-terminus within the cell (Parvathy, Hussain et al. 1999). As a result, sAPP $\beta$  is released into the extracellular space, and the C-terminal fragment within the membrane (CTF- $\beta$ ; C99) with new N-terminus (corresponding to the N-terminus of A $\beta$ ) is subsequently cleavage by the  $\gamma$ -secretase between the residues 38 and 43, resulting in A $\beta$  peptides varying in length from A $\beta$ 1-38 to A $\beta$ 1-43, and AICD (Olsson, Schmidt et al. 2014). Mutations in C99 can increase the ratio of A $\beta$ 42/A $\beta$ 40, and the levels of soluble A $\beta$  peptides (Hu, Kienlen-Campard et al. 2017) and the interaction between nicastrin and C99 modulates A $\beta$  peptide length (Petit, Hitzzenberger et al. 2019). The further cleavage of AICD in both pathways by caspases can produce a neurotoxic peptide C31 and Jcasp fragment (between  $\gamma$ -secretase and caspase cleavage sites) (Lu, Rabizadeh et al. 2000; Park, Shaked et al. 2009). According to Prof. Koo's group and colleagues, the cascade of events that includes caspase activation and APP cleavage is initiated by A $\beta$  peptide-mediated toxicity (Lu, Soriano et al. 2003). In turn, caspase cleavage of APP seems to be crucial for A $\beta$  peptide-mediated toxicity concluded from the prevention of synaptic loss, astrogliosis, and behavioral abnormalities in the absence of C31 production, whereas A $\beta$  peptide production and plaque formation were unaltered in APP transgenic mice (Galvan, Gorostiza et al. 2006). Most of the A $\beta$  peptides produced are the A $\beta$ 40, whereas a small proportion (approximately 5-10%) is the A $\beta$ 42 (Jakob-Roetne and Jacobsen 2009; Bibl, Gallus et al. 2012). The generated A $\beta$  peptides are released from the membrane into the extracellular space or remain associated with the plasma membrane (Chen, Xu et al. 2017). A $\beta$  peptides released from the plasma membrane are secreted into the cerebrospinal fluid (CSF) and cleared from brain to blood plasma. Low production levels of A $\beta$  peptides are a normal metabolic event, and the peptides can be detected in both CSF and plasma in healthy subjects throughout the life in the range of 3-8 nM and under 500 pM, respectively (Selkoe 2001). Both A $\beta$ 40 and A $\beta$ 42 can be detected in these extracellular fluids (Selkoe 2001).

$\beta$ -Secretase competes with  $\alpha$ -secretase for the cleavage of APP (Selkoe and Schenk 2003) with the preferential formation of neuroprotective sAPP $\alpha$  and small amounts of A $\beta$ . Importantly, as the cleavage by the  $\alpha$ -secretase occurs within the A $\beta$  region, then the formation of A $\beta$  peptides is prevented. Although  $\beta$ -Secretase competes with  $\alpha$ -secretase, when the APP synthesis increases, the level of A $\beta$  peptides also increases (Kozlov, Afonin et al. 2017).

The third physiological APP processing pathway was discovered in 2015 that described the resulting newly identified APP fragments capable of inhibiting neuronal activity in the hippocampus (Willem, Tahirovic et al. 2015). In addition to previously known C-terminal fragments generated by  $\alpha$ -secretase (CTF- $\alpha$ ) and  $\beta$ -secretase (CTF- $\beta$ ), C-terminal fragments generated by  $\eta$ -secretase (CTF- $\eta$ ) were identified. CTF- $\eta$  is produced when  $\eta$ -secretase cleaves APP between amino acid residues 504 - 505 of APP<sub>695</sub> and subsequent cleavage by  $\alpha$ -secretase and  $\beta$ -secretase generates fragments A $\eta$ - $\alpha$  (108 amino acids long) containing the A $\beta$ 1-16 sequence at the end of the peptide and A $\eta$ - $\beta$  (92 amino acids long) (Figure 3) (Willem, Tahirovic et al. 2015).

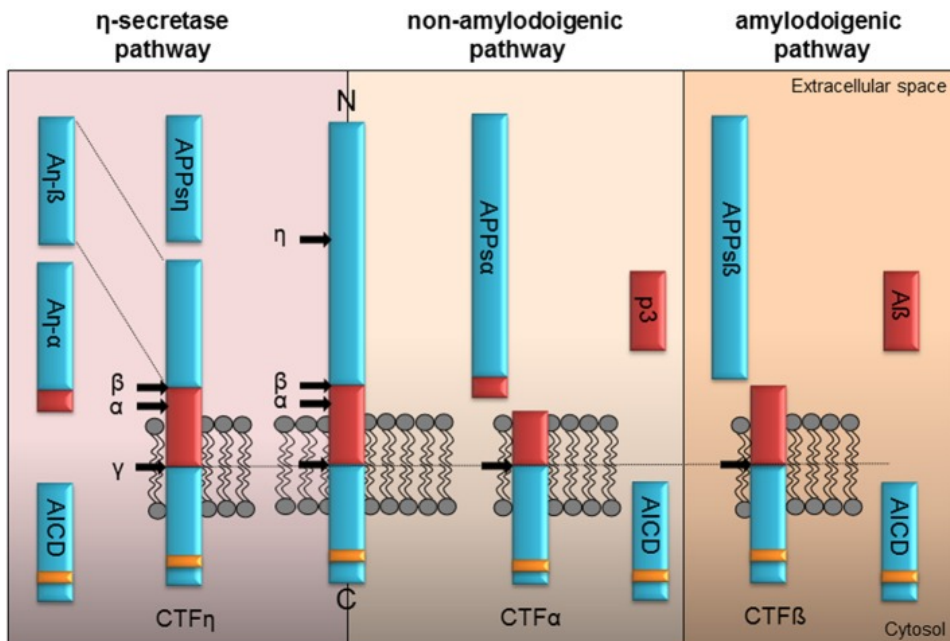


Figure 3. Proteolytic processing pathways of APP. Figure from (Ludewig and Korte 2016), reproduction permitted by Frontiers.

The function of A $\beta$  peptides produced in the amyloidogenic pathway is still unknown. It is generally known that A $\beta$ 1-42 is more amyloidogenic than A $\beta$ 1-40 and forms fibrils more avidly. In addition to fibrils, A $\beta$  peptide has been shown to form different assemblies.

### 1.2.2 A $\beta$ peptide assemblies

Interactions between the peptides and/or proteins are fundamental to the biological functions of all organisms, yet the same interactions can lead to the formation of aberrant protein aggregates, in particular, amyloid fibrils. Misfolding of proteins and their subsequent aggregation to cross  $\beta$ -sheet conformation are the hallmark of different diseases, including AD, Parkinson's disease (PD), Huntington's disease, Type II diabetes, and prion-related disorders. A $\beta$  peptide is present in the AD brain in soluble and insoluble forms (Glennner and Wong 1984; Kuo, Webster et al. 1998; Lambert, Barlow et al. 1998).

Soluble A $\beta$  monomers are shown to form various types of assemblies ranging from soluble oligomers and protofibrils to insoluble fibrils.

Relatively little is known about the structure of A $\beta$  oligomers because of their unstable nature that makes the structural characterization complicated as soluble oligomers are often prepared in the presence of detergents (Chen, Xu et al. 2017). The A $\beta$  oligomer size distribution varies from low-molecular-weight oligomers (dimers, trimers, tetramers, and pentamers) to midrange-molecular-weight oligomers (hexamers, nonamers, and dodecamers) (Chen, Xu et al. 2017). It has been shown that A $\beta$  oligomers may account for up to 45% of total species (Kuo, Emmerling et al. 1996; Roher, Chaney et al. 1996). Oligomers extracted from neuritic plaques are suggested to be SDS-resistant and covalently cross-linked dimeric and trimeric species (Roher, Chaney et al. 1996) linked in part through Tyr10 residue (Atwood, Martins et al. 2002).

In addition to oligomers, A $\beta$  also forms larger diffusible aggregates and "A $\beta$ -derived diffusible ligands" (ADDLs), with an estimated molecular weight of 17-42 kDa (Lambert, Barlow et al. 1998). The connection between A $\beta$  oligomers and fibrils remains to be established. It is unknown whether the oligomeric species are intermediates to fibril formation or are just in equilibrium with monomers, which form fibrils without oligomeric intermediates. It has been suggested that A $\beta$  monomers aggregate into fibrils through primary nucleation over oligomeric intermediates; however, when a certain concentration of fibrils is reached (10 nM), then the formation of the oligomers is catalyzed on fibrillar surfaces (secondary nucleation) (Cohen, Linse et al. 2013).

A $\beta$  insoluble fibrils isolated from amyloid plaques display the cross- $\beta$  structure common to all amyloid fibrils. The  $\beta$ -sheet-rich segments of amyloid fibrils are formed by the hydrophobic internal residues 18-26 and C-terminal residues 31-42 (Luhers, Ritter et al. 2005). A $\beta$ 19-28 (Burdick, Soreghan et al. 1992) and A $\beta$ 29-35 have been identified to form stable aggregates (Pike, Burdick et al. 1993; Pike, Walencewicz-Wasserman et al. 1995). Also, the N-truncated A $\beta$ 4-42 has been proposed to aggregate faster than A $\beta$ 1-42 (Pike, Overman et al. 1995). Fibril formation is concentration-dependent, which means that the level of A $\beta$  has to be above the critical concentration required for fibrillization (Williams, Shivaprasad et al. 2006; Brannstrom, Ohman et al. 2014). The critical concentration levels for A $\beta$ 40 have been determined to be around 100 nM and for A $\beta$ 42 even lower (Hasegawa, Ono et al. 2002; Brannstrom, Ohman et al. 2013). However, the A $\beta$  peptide extracellular concentrations in CSF are much lower, in the range of 3-8 nM (Selkoe 2001). In the plasma, the A $\beta$  peptides concentrations are even lower and under 500 pM (Selkoe 2001). In the critical concentration state, there is an equilibrium between monomers and oligomers called the lag phase. In order to start the fibrillization process, nucleation or seeding has to take place. Nucleation results in the formation of protofibrils that are 6-8 nm in diameter and less than 200 nm in length (Walsh, Lomakin et al. 1997), is followed by the fibril elongation phase and finally,

saturation phase where no more fibrils are formed (Walsh, Hartley et al. 1999). A $\beta$  fibrils are unbranched, with approximately 20 nm in diameter and varying lengths (Irie, Murakami et al. 2005). They consist of a cross- $\beta$  structure with characteristic  $\beta$ -sheet conformation and specific protofilament organization, where two filaments are twisted around each other in a left-handed helix orientation. Formed amyloid fibrils propagate autocatalytically and behave like prions inside the brain (Knowles, Waudby et al. 2009; Lu, Qiang et al. 2013); once the first fibrils are formed, the process will spread in the brain and lower the concentration of monomeric A $\beta$  in CSF (Andreasen, Hesse et al. 1999; Andreasen, Minthon et al. 1999; Boumenir, Cognat et al. 2019). Finally, these A $\beta$  peptide fibrils assemble into amyloid plaques in the brain, resistant to proteolysis. It has been proposed that A $\beta$ 1-42 peptide is toxic *in vivo* when the peptide fibrillizes in the growth media around the cells, whereas preformed A $\beta$ 1-42 peptide fibrils are non-toxic (Cohen, Arosio et al. 2015; Krishtal, Bragina et al. 2017). Therefore the process of A $\beta$  peptide fibrillization is still in the focus of *in vitro* studies.

Fibril formation *in vitro* has been shown to be affected by several factors such as peptide sequence and concentration, environmental factors like pH, temperature, presence of different molecules and certain metal ions (Bush, Pettingell et al. 1994; Atwood, Moir et al. 1998; Liu, Howlett et al. 1999; Tiiman, Krishtal et al. 2015) as well as by agitation. It has been generally accepted that the agitation of the solution substantially accelerates the peptide and protein *in vitro* fibrillization. The pH dependence of fibril formation has two outcomes. The rate of fibril formation increases at lower pH, which may indicate that fibril formation is favored within endosomes and lysosomes (Siman, Mistretta et al. 1993; Brannstrom, Islam et al. 2017). On the contrary, higher pH decreases the rate of fibril formation (Tiiman, Krishtal et al. 2015). Metal ions such as Zn(II) and Cu(II) have been shown to induce rapid aggregation of human A $\beta$  peptides (Miller, Ma et al. 2010) and have been implicated in the neurotoxicity of the formed metallated A $\beta$  aggregates. Rat A $\beta$  binds Zn(II) ions much less avidly than human A $\beta$ ; therefore, Zn(II) does not induce aggregation of rats A $\beta$ . Rat A $\beta$  differs from human A $\beta$  in three substitutions of R5G, Y10P, and H13R, from which His13 is suggested to be critical for the Zn(II) binding and Zn-induced aggregation (Bush, Pettingell et al. 1994; Liu, Howlett et al. 1999; Nalivaeva and Turner 2013). The research group of Anders Olofsson studied the contribution of His residues to fibrillar stability at neutral pH by substituting His residues (His6, His13, His14) to Alanine (Ala). The A $\beta$  peptide, with all three substitutions, showed the lowest fibril stability compared with each substitution individually. Substitution of His6 showed little lower fibril stability, and substitutions of His13 or His14 showed much lower fibril stability than normal A $\beta$  (Brannstrom, Islam et al. 2017). According to Prof. Cotman's group, I31L, I32L, G33A mutations in A $\beta$ 25-35 greatly reduced peptide aggregation, and M35Y, M35L, M35K prevented detectable aggregation, suggesting that these residues are also important for aggregation (Pike, Walencewicz-Wasserman et al. 1995).

A $\beta$  peptide fibrillization can be monitored by different methods, such as Thioflavin T (ThT) fluorescence, Congo red, light scattering, circular dichroism, electron and atomic force microscopy, X-ray diffraction. ThT fluorescence studies use a non-fluorescent agent ThT, which binds to fibrils and is characterized then by fluorescence emission centered at 482 nm after excitation at 450 nm. An increase in the ThT fluorescence levels reflects the increased level of amyloid fibrils (Figure 4) (Sebastiao, Quittot et al. 2017).

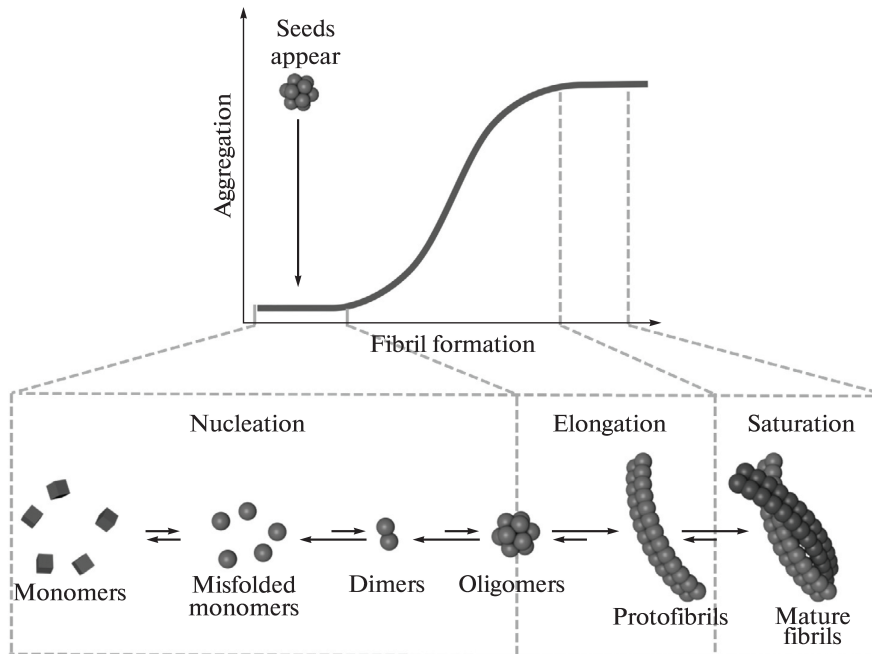


Figure 4. Schematic of A $\beta$  peptide fibril formation process. Figure from (Kulikova, Makarov et al. 2015), reproduced with permission from Springer Nature.

### 1.2.3 A $\beta$ peptide and metal ions

Metal ions are essential elements in all living organisms. Metal ions such as copper, zinc, and iron are used as catalytic cofactors by different enzymes and are also involved in protein structure stabilization. At the same time, excessive amounts of metal ions, especially iron and copper, are highly toxic and associated with various neurological disorders, including Wilson's disease (Cheignon, Tomas et al. 2018). Moreover, deficiency of copper ions is also harmful to the body and manifested as Menkes disease (Cheignon, Tomas et al. 2018). Also, dysfunction in metal ion homeostasis is believed to play a role in AD pathogenesis. Therefore the levels of metal ions have to be tightly regulated by metal transporters, metallochaperones, and buffering metalloproteins.

Copper, one of the redox-active metals, has been implicated in AD pathology in the following ways. It has been demonstrated that Cu(II) but also Zn(II) (Huang, Atwood et al. 1997; Atwood, Moir et al. 1998; Liu, Howlett et al. 1999; Danielsson, Pierattelli et al. 2007; Miller, Ma et al. 2010; Mold, Ouro-Gnao et al. 2013; Sharma, Pavlova et al. 2013; Hane, Hayes et al. 2016; Istrate, Kozin et al. 2016; Lee, Kim et al. 2018) and to a lesser extent Fe(III) (Atwood, Moir et al. 1998; Ha, Ryu et al. 2007; Lermyte, Everett et al. 2019; Everett, Brooks et al. 2020) modulate aggregation of A $\beta$  peptides. Precipitated A $\beta$ 40 has been shown to bind up to 3-4 Cu(II) ions at pH=7.0, and submicromolar concentration of Cu(II) has been shown to induce aggregation of nanomolar A $\beta$  peptide (Atwood, Moir et al. 1998). A $\beta$ 40 with His residues modified by diethylpyrocarbonate (DEPC) and rat A $\beta$ 40 has been shown not to aggregate in the presence of Cu(II) ions

(Atwood, Moir et al. 1998). Moreover, Cu(II) and other metal ions such as Zn(II) and Fe(III) have been found in high concentrations also in amyloid plaques extracted from AD brains (Mital, Wezrynfeld et al. 2015; Cheignon, Tomas et al. 2018). Amyloid-bound redox-active metal ions can induce the generation of reactive oxygen species and oxidative stress, which might lead to neurodegeneration (Cheignon, Jones et al. 2017).

The metal-binding region of A $\beta$  is located in the N-terminus of the peptide, which is hydrophilic, negatively charged, and contains three His residues (His 6, His 13, and His14) (Warmlander, Tiiman et al. 2013). Cu(II) binding to A $\beta$  peptide is suggested to result in component I and component II. In component I, Cu(II) is bound to A $\beta$  through N-terminal amino group of Asp1, imidazole ring of His6 and imidazole ring of either His13 or His14, and the carbonyl group of Asp1-Ala2 peptide bond (Alies, Conte-Daban et al. 2016; Yako, Young et al. 2017). Component II is divided into two: a) Cu(II) is bound to the carbonyl group of Ala2-Glu3 peptide bond and imidazole rings of all three His residues; b) Cu(II) is bound to N-terminal Asp1, the carbonyl group of Ala2, imidazole ring of only one His residue and the amide group of Asp1-Ala2 peptide bond (Yako, Young et al. 2017). Zn(II) binding has been shown to be tetrahedral at pH 7 involving 2 His residues (His6 and His13 or His14) and two carboxylate groups (Glu11 and Asp1) (Alies, Conte-Daban et al. 2016). His13 has been shown to be critical for the coordination of Zn(II) ions (Liu, Howlett et al. 1999), but the N-terminal amino group is not part of Zn(II) binding.

Peptide sequences with His at the third position are termed as the amino-terminal Cu(II) and Ni(II) binding (ATCUN) motifs (Xaa-Yaa-His) (Gonzalez, Bossak et al. 2018), which expose high binding affinity against Cu(II) ions. Such motif exists in many proteins and peptides, including human serum albumin (Mital, Wezrynfeld et al. 2015). Importantly ATCUN motif exists also in N-truncated A $\beta$ 4-42 peptide, which is a major truncated A $\beta$  isoform detected according to some publications, accounting for up to 60% of total A $\beta$  peptides in diseased brains (Glennier and Wong 1984; Masters, Multhaup et al. 1985; Masters, Simms et al. 1985; Naslund, Schierhorn et al. 1994; Lewis, Beher et al. 2006; Portelius, Bogdanovic et al. 2010; Wildburger, Esparza et al. 2017). It has been suggested that in addition to N-truncated A $\beta$ 4-42 peptide, truncation also happens at position 3 or 11, forming pyroglutamate (Liu, Solano et al. 2006; Portelius, Bogdanovic et al. 2010) that has been detected in the control and AD disease brains. Prof. Blennow's group and colleagues showed that A $\beta$ 4-42, A $\beta$ 1-42, pyroglutamated A $\beta$ 3-42, A $\beta$ 1-40, and their oxidized forms were detected from the control and AD brains, with one exception, that controls did not have A $\beta$ 1-40 in their brain (Portelius, Bogdanovic et al. 2010). A $\beta$ 4-x peptides have been demonstrated to bind Cu(II) three orders of magnitude more strongly than those reported for A $\beta$ 1-40 or A $\beta$ 1-42 peptides (Mital, Wezrynfeld et al. 2015; Teng, Stefaniak et al. 2020) due to the ATCUN motif. A $\beta$ 4-42 peptide also contains a second Cu(II) binding site HHQK (amino acids 13-16) that binds Cu(II) with an affinity that is lower by seven orders of magnitude, as compared with the N-terminal ATCUN site (Mital, Wezrynfeld et al. 2015). This site has also been shown to activate microglia through heparin-binding (Giulian, Haverkamp et al. 1998). It has been suggested that A $\beta$ 4-42 isoform in the brain has a physiological role in the maintenance of metal homeostasis in the central nervous system (Mital, Wezrynfeld et al. 2015).

Although the metal binding of A $\beta$  peptide has been intensively studied, there is no consensus about the stoichiometry and affinity of Cu(II) binding to A $\beta$  peptide. The fragment A $\beta$ 1-16 has the metal-binding region without the amyloidogenic

properties, which makes this peptide a good model for studying metal-binding properties of full-length A $\beta$  peptides (Lu, Prudent et al. 2010; Yako, Young et al. 2017). One possible method studying A $\beta$  peptide metal-binding properties is to monitor the decrease of Tyr10 fluorescence in response to Cu(II) ion addition (Garzon-Rodriguez, Yatsimirsky et al. 1999; Karr, Akintoye et al. 2005; Raman, Ban et al. 2005; Danielsson, Pierattelli et al. 2007; Young, Wijekoon et al. 2015). The obtained binding curve can be fitted to the Morrison equation (Kuzmj 2015), expecting the binding of one Cu(II) ion. Cu(II)-binding to A $\beta$  peptide has been proposed to form complexes with different binding stoichiometries. Dr. Hureau's group and colleagues claimed using this method that the A $\beta$ 1-16 peptide binds two Cu(II) ions according to the shape of the curve that can be divided into multiple sections (Alies, Renaglia et al. 2013).

A $\beta$  peptide in complex with redox-active metals such as Cu(II) is suggested to be able to catalyze the formation of ROS in the presence of reducing agents such as ascorbate and therefore has been linked to oxidative stress in AD.

All possible A $\beta$ -metal ion interactions and their influence on peptide fibrillization are presented in Figure 6.

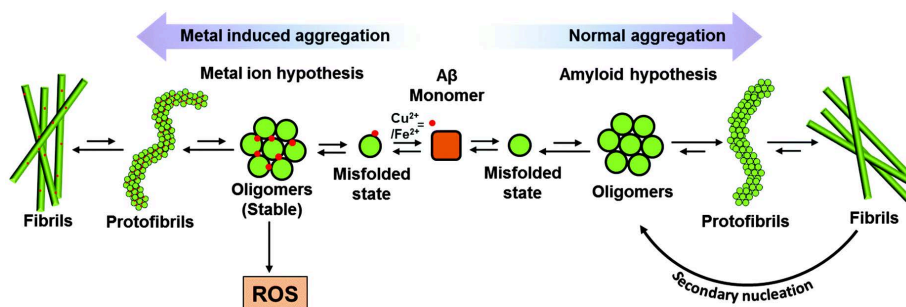
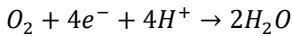


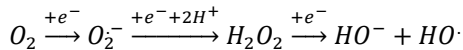
Figure 5. A $\beta$  peptide aggregation in normal aggregation and metal-induced aggregation. Figure from (Rajasekhar, Chakrabarti et al. 2015), reproduced with permission from ROYAL SOCIETY OF CHEMISTRY.

### 1.3 Oxidative stress

Redox reactions are one of the fundamental processes of life where electrons are passed in a chain from the first donor to the final acceptor through several intermediates. For aerobic cells, dioxygen is the final electron acceptor in the respiratory chain:



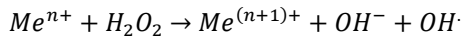
In partial  $O_2$  reduction reaction, reactive oxygen species (ROS) such as superoxide anion ( $O_2^-$ ), hydrogen peroxide ( $H_2O_2$ ) and hydroxyl radical ( $HO\cdot$ ) are produced (Cheignon, Tomas et al. 2018):



ROS are produced constantly in our body, mostly non-enzymatically (side reaction in the respiratory chain or Fenton chemistry) or enzymatically (by macrophages).

Redox-active metals such as Cu and Fe play a central role in oxidative stress and are known to be involved in ROS production as they cycle in physiological conditions between two redox states (Atrian-Blasco, Del Barrio et al. 2018). In the presence of reducing agents such as glutathione or ascorbate, Cu(II) and Fe(III) can be reduced to Cu(I) and Fe(II) (Cassagnes, Herve et al. 2013), which can then react with hydrogen peroxide to form hydroxyl radicals according to so-called Fenton reaction (Reybier, Ayala et al. 2016; Cheignon, Tomas et al. 2018).

Fenton reaction:



Produced hydroxyl radicals ( $OH\cdot$ ) are the most reactive oxygen species.

High levels of ROS are potentially dangerous, and thus their levels have to be controlled and kept at a low level as possible. Low levels of ROS are produced normally during aerobic metabolism and contribute to the normal aging process (Palmer 2002). However, the accumulation of ROS caused by overproduction or an insufficient elimination by antioxidant systems leads to oxidative stress, resulting in oxidative damage of various biomolecules such as proteins, DNA, RNA, and phospholipids (Cheignon, Tomas et al. 2018). In a normal organism, the formation of oxidants and anti-oxidants should be balanced. Moreover, oxidative stress through ROS can destroy biomolecules such as metalloproteins, which in return may lead to higher ROS production. Proteins are one of the main targets for ROS (Butterfield and Boyd-Kimball 2018). Oxidation can occur on the protein backbone as well as on amino acid side chains, which depend on the protein sequence, structure, and nature of the oxidant. The resulting oxidized protein might be functionally defective or can participate in damaging reactions and signal induction. The level of ROS is controlled by enzymatic antioxidants such as glutathione peroxidase, Mn- and Cu,Zn-superoxide dismutase, and chemical antioxidants such as uric acid, ascorbate, Vitamin E and C, melatonin, and resveratrol in plants.



### 1.3.1 Oxidative stress in AD

The human brain is due to the high oxygen consumption (20% of the total body consumption) particularly sensitive to oxidative stress and the generation of ROS such as  $H_2O_2$  and hydroxyl radicals (Cheignon, Tomas et al. 2018), that have been implicated in pathogenesis and neurotoxicity of AD. In proteins, oxidative damage involves post-translational modifications such as oxidation of amino acids.

Overproduction of ROS plays an important role in the pathogenesis of AD and leads to enhanced oxidative damage to biological macromolecules in the brain (Ramteke, Ginotra et al. 2013; Simunkova, Alwasel et al. 2019). Increased concentrations of these damaged molecules such as oxidated proteins and DNA or peroxidated lipids have been detected in post-mortem tissue from the AD brain.

Redox-active metal ions such as Cu and Fe can be coordinated to A $\beta$ , and the complex can catalyze the production of reactive oxygen species that may contribute to oxidative damage on the A $\beta$  peptide itself and surrounding molecules. ROS production of A $\beta$  peptide during this metal-catalyzed oxidation at the metal center has been mostly studied in the case of Cu ions (Kowalik-Jankowska, Ruta et al. 2004; Cheignon, Faller et al. 2016; Reybier, Ayala et al. 2016; Huang, Lou et al. 2019) because Fe-A $\beta$  complex has lower redox activity (Nakamura, Shishido et al. 2007). It has been hypothesized that oxidative stress is induced by the accumulation of A $\beta$  peptide complexes with redox-active metal ions (Butterfield and Boyd-Kimball 2004; Smith, Cappai et al. 2007; Rajasekhar, Chakrabarti et al. 2015). But according to Prof. Bal and colleagues, the Cu(II) bound to the A $\beta$ 4-x ATCUN motif is redox-inert and, therefore, does not generate ROS significantly (Teng, Stefaniak et al. 2020). Moreover, it has been shown that oxidative stress in AD might also contribute to A $\beta$  generation and the formation of NFTs (Butterfield 2002). On the other hand, the ascorbate-dependent hydroxyl radical generation by free Cu(II) has been shown to decrease in the presence of A $\beta$  peptides containing metal-binding region (Nakamura, Shishido et al. 2007). A $\beta$  peptide monomers and fibrils are claimed to have antioxidant properties, but oligomers are supposed to have pro-oxidant properties (Mitra, Prasad et al. 2018).

The primary targets for hydroxyl radicals in proteins are sulfur-containing amino acids such as methionine and cysteine. Also, other amino acids, such as tyrosine, histidine, lysine, aspartate, phenylalanine, and tryptophan, can be oxidized. In A $\beta$  peptide, the oxidations of Cu-binding amino acids have been seen, such as Asp and His residues. Two His residues (His13 and His14) involved in Cu(I) and Cu(II) binding have been shown to be oxidized during metal-catalyzed oxidation in the presence of ascorbate and  $H_2O_2$ ; however, His6 has not (Schoneich and Williams 2002; Kowalik-Jankowska, Ruta et al. 2004; Inoue, Garner et al. 2006; Cheignon, Hureau et al. 2018). Met35 oxidation has been proposed to occur after the oxidation of His13 and His14 in the presence of Cu(II) ions and ascorbate, but Tyr10 and His6 remain intact (Schoneich and Williams 2002). Asp1 oxidation has also been observed in the metal-catalyzed oxidation process (Cheignon, Hureau et al. 2018). In addition to previous amino acids, the amino acids not involved in Cu-binding have also been shown to be oxidized. For example, phenylalanines Phe19 and Phe20 are oxidized in A $\beta$  peptide during metal-catalyzed oxidation in the presence of ascorbate (Cassagnes, Herve et al. 2013; Cheignon, Hureau et al. 2018). Tyr10 has been shown to be sensitive to oxidation during metal-catalyzed oxidation in the presence of  $H_2O_2$  and results in dityrosine cross-linking of A $\beta$  peptide (Atwood, Perry et al. 2004), and the oxidation of Tyr10 has also been found to be promoted by Met35 in A $\beta$  peptide (Ali, Separovic et al. 2005). Dityrosine cross-linking is

suggested to impact A $\beta$  peptide aggregation by forming covalent A $\beta$  oligomers (Al-Hilaly, Williams et al. 2013). The oxidation of Tyr10 has been indicated in H<sub>2</sub>O<sub>2</sub> production, Cu-induced radicalization, and neurotoxicity, which are attenuated in the case of Tyr10Ala mutation of A $\beta$  peptide (Barnham, Haeffner et al. 2004). The oxidation of methionine in A $\beta$  peptides is discussed below.

#### 1.4 Chemical modifications of A $\beta$ peptide

Chemical modification has been a classical approach in protein science, determining the role of amino acid residues in the functioning of proteins and peptides. Commonly, chemical modification techniques such as covalent labeling, non-covalent labeling, and chemical cross-linking are used (Zhou and Vachet 2012). Non-covalent labeling such as hydrogen-deuterium exchange (HDE) provides information about the localization of protein backbone in protein structure (Mendoza and Vachet 2008). Cross-linking methods create intra- and intermolecular bonds and give information about the distance between two amino acid side chains in protein structure. Covalent labels are classified as non-specific or amino acid-specific. Non-specific labeling, such as oxidative footprinting, is based on protein reactions with radicals that modify many different amino acid residues, and residue-specific labels are reagents that have specific reactions with a particular amino acid side chain that is exposed to solvent in protein (Hnizda, Santrucek et al. 2008). Several different reagents have been used to modify all chemically reactive amino acid residues such as Arg, Cys, His, Lys, Trp, and Tyr (Mendoza and Vachet 2009). The modification reaction outcome depends on the reactivity of the labeling reagent and the reactivity and the accessibility of the amino acid side chains. The results give information about the protein structure and its interactions with ligands. Chemical modification can be monitored easily using the peptide mass fingerprinting with ESI or MALDI MS, and peptide sequencing could be performed with tandem ESI MS/MS. The number of reagent adducts bound to the protein can give information about the accessibility of the particular amino acid residues and therefore identify different protein states and structures.

A $\beta$  peptide in AD brains has been observed to contain post-translational modifications such as oxidation, glycosylation, isomerization, nitration, racemization, phosphorylation, and pyroglutamylation (Kummer and Heneka 2014) that may cause different physiological and pathological properties of A $\beta$  peptide. Chemical modification of amino acid residues affected by post-translational modification has been used to study A $\beta$  peptide properties. Different chemical modifications of A $\beta$  peptide have been used to study the catalytic properties of His, Ser, and Asp/Glu triad and oxidative activity related to residues His, Tyr, and Met (Brzyska, Bacia et al. 2001). His residues were modified with diethylpyrocarbonate (DEPC), Met was oxidized with chloramine T, Tyr was acetylated with N-acetylimidazole, Ser was modified with diisopropylfluorophosphate, and the carboxylic groups of Asp and Glu were modified by amidation (Brzyska, Bacia et al. 2001). Nitration of Tyr10 in A $\beta$ 1-42 peptide in the presence of nitrite and hydrogen peroxide has been used to study the A $\beta$  peptide toxicity related to Cu(II) binding (Zhao, Gao et al. 2019). The nitration of Tyr10 did not alter Cu(II) binding to A $\beta$  peptide but reduced the Cu(II)-induced aggregation and neurotoxicity of A $\beta$  peptide (Zhao, Gao et al. 2019). The effect of oxidation on A $\beta$  peptide Cu(II) binding properties have been studied using a pulse radiolysis study, showing oxidized dimeric and trimeric A $\beta$ 1-16 being produced through Tyr10

cross-linking, and it was demonstrated that the Cu(II)-binding properties of the oxidized peptide are similar to the nonoxidized peptide (Ramteke, Ginoira et al. 2013). Chemical modifications have also been used to study the aggregation and toxicity of A $\beta$  peptides. For example, naturally occurring N-terminal truncation and pyroglutamylation have been shown to reduce fibril length and accelerates A $\beta$ 3-42 and A $\beta$ 3-40 peptide fibrillization (Wulff, Baumann et al. 2016). A $\beta$  peptide backbone modification with a 2-nitrobenzyl group attached to glycine residue during peptide synthesis was used to study peptide aggregation and fibrillization. Chemical modification in the bend region resulted in decreased fibrillization but did not affect oligomer formation (Johnson, Lanning et al. 2016). Also, nitrotyrosination of A $\beta$  peptide results in decreased fibrillization and stabilization of oligomers. The nitrotyrosination was shown to increase A $\beta$  peptide synaptotoxicity (Guivernau, Bonet et al. 2016). Pyroglutamated A $\beta$ 3-42 has also been used to study the induction of synaptic dysfunction by A $\beta$  peptide (Grochowska, Yuanxiang et al. 2017). In addition to pyroglutamate, isoaspartate is also naturally occurring in A $\beta$  peptides in the aging brain. Both modifications of A $\beta$  peptides were increased in AD brains; however, isoaspartate accumulation is linked with aging, whereas pyroglutamate deposition is linked with AD (Moro, Phillips et al. 2018).

As Met residue at position 35 in A $\beta$  peptide has been shown to be oxidized in amyloid plaques and His residues with peptide N-terminus are essential for binding metal ions, it is important to understand the role of these amino acids in the properties of A $\beta$  peptide.

#### **1.4.1 The oxidation of Met35 in A $\beta$ peptide**

In proteins, oxidative damage involves post-translational chemical modifications, such as the oxidation of the Met side chain to the sulfoxides. For many proteins, the Met side chains are easily oxidized under physiological conditions; however, because sulfoxide can be converted enzymatically back to its reduced state by methionine sulfoxide reductase, it was proposed that surface-exposed Met residues may function for some proteins as antioxidants and protect other amino acids from irreversible oxidative damage (Watson, Fairlie et al. 1998; Hou, Kang et al. 2002).

A $\beta$  sequence contains Met in position 35, and it has been suggested that this residue is involved in oxidative damage and the toxicity of A $\beta$  peptide. It has been shown that oxidized Met35 forms 10-50% of the total A $\beta$  amount in the brain (Naslund, Schierhorn et al. 1994; Kuo, Kokjohn et al. 2001). In the case of Met35 oxidation of A $\beta$  peptide, the modification might affect fibrillization properties of the peptide, but the data regarding the effect of Met35 oxidation on A $\beta$  toxicity and on the aggregation or fibrillization are contradictory.

For example, Met35 residue has been shown to be critical to the free radical generation and neurotoxicity (Varadarajan, Yatin et al. 1999). Substitution of Met35 has been shown to attenuate the A $\beta$  peptide neurotoxic properties in oxidative stress (Yatin, Varadarajan et al. 1999). However, if Met35 is oxidized and then introduced to neuronal cells, the peptide is less neurotoxic (Varadarajan, Kanski et al. 2001; Ripoli, Piacentini et al. 2013); however, it still inhibits mitochondrial function (Varadarajan, Kanski et al. 2001). Also, Met35 has been shown to participate in the reduction of Cu(II) ions by A $\beta$  peptide (Curtain, Ali et al. 2001) and initiate the generation of ROS (Smith, Cappai et al. 2007). Other authors have proposed that Met35 has neuroprotective properties (Levine, Mosoni et al. 1996; Watson, Fairlie et al. 1998). Prof. Teplow's group

demonstrated that oxidation of Met35 blocked A $\beta$ 1-42 paranucleus formation and generated oligomers indistinguishable from those produced by A $\beta$ 1-40 (Bitan, Tarus et al. 2003).

The role of Met35 in aggregation and fibrillization is similarly unclear. Some reports have shown that oxidation of Met35 enhances aggregation (Snyder, Lador et al. 1994; Head, Garzon-Rodriguez et al. 2001); others demonstrate the opposite. According to those reports, oxidation of Met35 hampers A $\beta$  aggregation into protofibrils at physiological pH values (Watson, Fairlie et al. 1998; Varadarajan, Kanski et al. 2001; Hou, Kang et al. 2002; Palmblad, Westlind-Danielsson et al. 2002; Razzokov, Yusupov et al. 2019). It is suggested that critical interactions, which stabilize soluble oligomers, filaments, protofibrils, and mature fibrils are being affected, and therefore the morphology and stability of filaments, protofibrils, and fibrils are changed (Hou, Kang et al. 2002; Hou, Lee et al. 2013; Razzokov, Yusupov et al. 2019). This result is consistent with the reduced aggregation for A $\beta$ 40 upon Met35 oxidation due to hydrogen bonding or entropic destabilization (Bitan, Tarus et al. 2003). Additional results are in agreement with the presented data and specify that the oxidation of Met35 hinders the conformational transition from random coil to  $\beta$ -sheet, thus reducing the propensity for aggregation and fibril formation (Watson, Fairlie et al. 1998; Hou, Kang et al. 2002; Palmblad, Westlind-Danielsson et al. 2002). Watson et al. claim the effect of Met35 oxidation to A $\beta$ 42 is not the same as to A $\beta$ 40 as the conformational change in A $\beta$ 42ox from random coil to  $\beta$ -sheet occurs more quickly, highlighting the impact of residues Ile41 and Ala42 on the physiological properties of A $\beta$  peptide (Watson, Fairlie et al. 1998).

The role of metal ions in oxidative modification of Met35 in A $\beta$  is also not elucidated. Full-length A $\beta$  peptide, which contains N-terminal metal-binding His residues and C-terminal Met35 residue, has been shown to reduce Cu(II) to Cu(I). Truncated A $\beta$ , which either lacks the N-terminal His residues (A $\beta$ 25-35) or the Met35-containing C-terminus (A $\beta$ 1-28), has been shown not to reduce Cu(II) ions (Schoneich and Williams 2003).

#### **1.4.2 DEPC modification of His residues in A $\beta$ peptide**

As mentioned above, the metal-binding region of human A $\beta$  peptides is composed of His6, His13, His14, and peptide N-terminus (Faller, Hureau et al. 2013; Tiiman, Palumaa et al. 2013; Tiiman, Krishtal et al. 2015). His6, together with N-terminus in human A $\beta$  peptide, has been identified as a key ligand in the binding of Cu(II) ions. The binding of metal ions such as Zn(II) and Cu(II) ions to these amino acids has been shown to induce aggregation of the peptide (Faller, Hureau et al. 2013; Tiiman, Palumaa et al. 2013). In rat A $\beta$  peptide His13 is replaced with Arg13, and as a result, Zn(II)-induced aggregation is decreased compared with human A $\beta$  peptide (Liu, Howlett et al. 1999). Substoichiometric amounts of Cu(II) ions have been shown to accelerate A $\beta$  peptide fibrillization through binding to all three His residues (Sarell, Wilkinson et al. 2010), whereas His6 has been identified as a key ligand together with peptide N-terminus (Young, Kirchner et al. 2014). Binding and blocking of these residues can give information about the role they play in metal-induced aggregation.

Diethylpyrocarbonate (DEPC) has primarily been used to study the role of His residues in protein functioning because it allows to studying proteins under native conditions (Hegy, Premecz et al. 1974; Khananshvili and Grometelhanan 1983; Díaz, de Castro et al. 1993; Carneiro, Stauffer et al. 2003; Fang, Zhang et al. 2003; Mendoza

and Vachet 2009). However, it has to be taken into account that DEPC is not absolutely selective to His residue (Melchior and Fahrney 1970) and modifies other amino acid residues such as Lys, Tyr, Ser, Thr, Cys, the N-terminus, and occasionally Arg (Mendoza and Vachet 2008; Mendoza and Vachet 2009; Zhou and Vachet 2012). The majority of the modifications (except Lys and N-terminus) are reversible and could be removed by nucleophilic agents such as hydroxylamine (Melchior and Fahrney 1970; Evrard, Fastrez et al. 1999; Mendoza and Vachet 2009). DEPC has been shown to modify up to 25% of amino acid residues in the average protein sequence, located on the surface of the protein (Mendoza and Vachet 2008), while amino acid residues in the protein interior are inaccessible for DEPC and cannot be modified (Evrard, Fastrez et al. 1999; Hnizda, Santrucek et al. 2008; Zhou and Vachet 2012; Zhou and Vachet 2012). DEPC modification results in a carbethoxylated His residue, where the ethoxyformyl group is bound to the deprotonated nitrogen atom of the imidazole ring and N-ethoxyformylimidazole is formed (Hnizda, Santrucek et al. 2008; Yang, Li et al. 2015; Zhang, Liu et al. 2016). The reaction can be monitored with a spectrophotometer at 240 nm, where the intensity increases upon carbethoxylation of His residue (Díaz, de Castro et al. 1993). The reaction can precisely be observed in MALDI MS spectra by the m/z shift of 72 per one added modification (Kalkum, Przybylski et al. 1998; Hondal, Ma et al. 2001; Qin, Yang et al. 2002; Graziani, Bernauer et al. 2006) and the location of modification can be identified with peptide mass fingerprinting after tryptic digestion (Kalkum, Przybylski et al. 1998; Hondal, Ma et al. 2001; Hnizda, Santrucek et al. 2008; Karmakar and Das 2012; Zhou and Vachet 2012) or with tandem ESI MS/MS sequencing (Willard and Kinter 2001; Zhou and Vachet 2012).

The majority of studies use DEPC to investigate the role of His residues in the enzyme activity (Vik and Hatefi 1981; Coan and DiCarlo 1990; Díaz, de Castro et al. 1993; Evrard, Fastrez et al. 1999; Graziani, Bernauer et al. 2006) and in the metal-binding properties of proteins or peptides (Shoshan-Barmatz and Weil 1994; Qin, Yang et al. 2002; Fang, Zhang et al. 2003; Nakanishi, Takeuchi et al. 2008; Konkle, Elsenheimer et al. 2010; Karmakar and Das 2012). DEPC is also used for gaining the structural insight of proteins through covalent modification of accessible surface amino acids side chains (Duggan and Stephenson 1987; Evrard, Fastrez et al. 1999; Fang, Zhang et al. 2003; Hnizda, Santrucek et al. 2008; Mendoza and Vachet 2008; Konkle, Elsenheimer et al. 2010) and for characterizing protein-ligand interactions by observing the His residue modification level with DEPC in the presence and absence of a ligand (Duggan and Stephenson 1987; Hondal, Ma et al. 2001; Ginotra, Ramteke et al. 2012).

DEPC has also been used to study amyloidogenic peptides (Qin, Yang et al. 2002; Arndt, Kondalaji et al. 2015; Zhang, Liu et al. 2016), among them A $\beta$  (Ginotra, Ramteke et al. 2012; Ramteke, Ginotra et al. 2013) and insulin (Kalkum, Przybylski et al. 1998; Yang, Li et al. 2015). Insulin HisB5 residue modification with DEPC has been shown to increase the amyloidogenicity of the peptide at neutral pH (Yang, Li et al. 2015). DEPC has been used to study His residue role in human A $\beta$ 1-16 peptide metal-binding properties, and His6 has been proposed as a key ligand in the binding of Cu(II) ions (Ginotra, Ramteke et al. 2012). As previously mentioned, the human A $\beta$  peptide metal-binding region has been determined to be located at positions His6, His13, His14, and peptide N-terminus (Faller, Hureau et al. 2013; Tiiman, Palumaa et al. 2013; Tiiman, Krishtal et al. 2015). Studying of DEPC modification of all these residues in the absence and presence of Cu(II) ions is essential for the elucidation of their role in Cu(II) binding and in fibrillization of A $\beta$ .

## 2 Aims of the study

To shed more light on the mechanism of A $\beta$  peptide fibrillization and metal ion binding *in vivo*, the current *in vitro* study has been focused on the following aims:

- ✓ Determination of the effect of stopping the agitation in diverse stages of the *in vitro* fibrillization process of different peptides.
- ✓ Determination of the effect of Met35 oxidation to sulfoxide by H<sub>2</sub>O<sub>2</sub> on the A $\beta$  peptide fibrillization and effect of oxidized Met35 on the radical generating mechanism in the presence of H<sub>2</sub>O<sub>2</sub> and Cu(II) ions.
- ✓ Determination of the *in vitro* stoichiometry of Cu(II) ion binding to A $\beta$  peptide through studying the effect of pH on Cu(II) binding curve monitored by the decrease of the Tyr10 fluorescence.
- ✓ Determination of the DEPC modification sites in A $\beta$  peptide using tandem mass spectrometry and their participation in the binding of Cu(II) ions as well as establishing the fibrillization propensity of the DEPC modified A $\beta$  peptide.

### 3 Materials and Methods

Publication I - Effect of agitation on the peptide fibrillization: Alzheimer's amyloid-beta peptide 1-42 but not amylin and insulin fibrils can grow under quiescent conditions.

- ✓ Fluorescence spectrometric measurements of A $\beta$  peptide fibrillization with ThT.
- ✓ Bicine/Tris SDS-PAGE.
- ✓ Data analysis and kinetics of fibril formation.

Publication II - Effect of methionine-35 oxidation on the aggregation of amyloid-beta peptide.

- ✓ Fluorescence spectroscopic measurements of fibrillization for oxidized and native A $\beta$  peptide with ThT.
- ✓ Data analysis and kinetics of fibril formation.
- ✓ TEM of A $\beta$  peptide fibrils.
- ✓ Analysis of A $\beta$  peptide oxidation kinetics with MALDI MS.
- ✓ ESI MS/MS sequencing of oxidized A $\beta$  peptide.
- ✓ Bicine/Tris SDS-PAGE.

Publication III - Copper(II) Ions and the Alzheimer's Amyloid-beta Peptide: Affinity and Stoichiometry of Binding.

- ✓ Fluorescence spectroscopic measurements of Cu(II) binding curve through the quenching of fluorescence for Tyr10 residue.
- ✓ UV-VIS spectroscopic measurements of Cu(II) ion levels with Zincon dye
- ✓ Data analysis.

Publication IV - Cu(II) partially protects three histidine residues and the N-terminus of amyloid-beta peptide from diethyl pyrocarbonate (DEPC) modification.

- ✓ Analysis of DEPC modification kinetics with MALDI MS.
- ✓ Fluorescence spectroscopic measurements of fibrillization for DEPC-modified A $\beta$  peptide with ThT.
- ✓ ESI MS/MS sequencing of DEPC modified A $\beta$  peptide.

## 4 Results

Publication I - Effect of agitation on the peptide fibrillization: Alzheimer's amyloid-beta peptide 1-42 but not amylin and insulin fibrils can grow under quiescent conditions.

- ✓ Lyophilized A $\beta$  peptide pre-treatment with HFIP is necessary to disassemble preformed aggregates.
- ✓ The agitation of A $\beta$ 1-42 affects the formation of new seeds and/or fibrils but not the fibril growth.
- ✓ The agitation results for A $\beta$ 1-40 were somewhat different from A $\beta$ 1-42 in the fibril growth phase. A $\beta$ 1-40 fibrillization rate was enhanced by agitation throughout the whole fibrillization process.
- ✓ Insulin and amylin require agitation in all phases of the fibrillization process.

Publication II - Effect of methionine-35 oxidation on the aggregation of amyloid-beta peptide.

- ✓ In the absence of Cu(II) ions, Met35 residue was readily oxidized to sulfoxide.
- ✓ Oxidation of Met35 inhibited A $\beta$  fibrillization. Fibrillization rate constant value was threefold lower than that of the native peptide and the lag-phase for the oxidized peptide was also longer.
- ✓ The location of oxidation was confirmed with ESI MS/MS sequencing that indicated the involvement of Met35 residue.
- ✓ The oxidation pattern of A $\beta$  in the presence of Cu(II) ions was more complicated: the addition of the first oxygen was the fastest process; however, it was accompanied by unspecific modifications of several other residues in the peptide.
- ✓ Met35 oxidation had no effect on the oxidative behavior of the A $\beta$  complex with Cu(II) ions – when Met35 was oxidized in the absence of Cu(II) ions, the addition of copper ions still led to the appearance of a diverse spectrum of oxidized peptides. Thus, it can be concluded that Met35 residue is not a part of the radical generating mechanism of the A $\beta$ -Cu(II) complex.

Publication III - Copper(II) Ions and the Alzheimer's Amyloid-beta Peptide: Affinity and Stoichiometry of Binding.

- ✓ One equivalent of the A $\beta$  peptide can precipitate two equivalents of Cu(II) ions; however, in the presence of glycine, the amount of Cu(II) decreases to one equivalent.
- ✓ Experimental data about quenching of Tyr10 fluorescence by Cu(II) ions can be fitted to the binding curve expecting the binding of one Cu(II) ion.



Publication IV - Cu(II) partially protects three histidine residues and the N-terminus of amyloid-beta peptide from diethyl pyrocarbonate (DEPC) modification.

- ✓ DEPC modification level of A $\beta$  peptide is higher at pH 7.4 compared to pH 6.8.
- ✓ Modification of A $\beta$  peptide with a 30-fold excess of DEPC resulted in 5 total modifications at pH 7.4, which were identified as peptide N-terminus, 1 Lys, and 3 His residues according to ESI MS/MS sequencing.
- ✓ Hydroxylamine treatment removed DEPC modifications from His residues but not from peptide N-terminus and Lys residue.
- ✓ The binding of Cu(II) ions protects all involved A $\beta$  peptide residues from DEPC modification.
- ✓ DEPC modification increases the aggregation of the A $\beta$  peptide.

## 5 Discussion

A $\beta$  peptide is implicated in AD pathogenesis; however, it is still unknown what role it plays in the mechanism of AD onset or neurodegeneration. Initially, it was considered that the fibrillar form of A $\beta$  peptide is neurotoxic and the causative agent in AD pathogenesis since it is the major component in amyloid plaques, and the amyloid cascade hypothesis was formulated (Hardy and Higgins 1992). According to this hypothesis, deposition of A $\beta$  peptide results in the formation of neurofibrillary tangles, neuronal loss, vascular damage, and dementia (Hardy and Higgins 1992). Later, the primary focus has shifted to oligomeric A $\beta$  species due to the observation that in animal models, the symptoms often appear before the plaque formation, and in the *in vitro* experiments, the neurotoxicity of A $\beta$  oligomers is higher than that of the fibrils (Ono, Condron et al. 2009; Yang, Wang et al. 2017). In the search for other toxic forms of A $\beta$  peptides, a large variety of oligomeric A $\beta$  forms have been defined, and an “oligomer” hypothesis for AD has been formulated (Lambert, Barlow et al. 1998). However, the concentration of such species in the brain must be low because the initially formed amyloid fibrils propagate autocatalytically and behave like prions inside the brain (Knowles, Waudby et al. 2009; Lu, Qiang et al. 2013), which leaves very little space for the formation of nonfibrillar aggregates in higher amounts: once the first fibrils are formed, the process will spread in the brain and lower the concentration of monomeric A $\beta$  in CSF (Andreasen, Hesse et al. 1999; Andreasen, Minthon et al. 1999; Boumenir, Cognat et al. 2019).

In multiple experiments, the low toxicity of fibrillar A $\beta$  aggregates *in vitro* may be caused by the absence of bound redox-active Cu(II) ions and, therefore, the inability of A $\beta$  peptides to produce ROS (Dahlgren, Manelli et al. 2002; Tiiman, Palumaa et al. 2013). It has been proposed that A $\beta$ 1-42 peptide is toxic *in vivo* when the peptide fibrillizes in the growth media around the cells, whereas preformed A $\beta$ 1-42 peptide fibrils are non-toxic (Cohen, Arosio et al. 2015; Krishtal, Bragina et al. 2017) and therefore, the process of A $\beta$  peptide fibrillization is still in the focus of *in vitro* studies. A $\beta$  peptide fibrillization process *in vitro* is affected by multiple factors such as peptide concentration and agitational state, temperature, pH, metal ions, etc. The corresponding studies can give information about the nature of A $\beta$  fibrillization and gain an insight into the molecular mechanisms of AD.

The most principal requirement for all *in vitro* experiments with A $\beta$  peptides is to obtain reproducible results. The most critical factor affecting the reproducibility is the requirement that the A $\beta$  peptide is monomeric before the experiment is started. To obtain a stable monomeric A $\beta$  peptide solution, HFIP treatment of lyophilized peptide is a necessary step to disassemble preformed aggregates (Publication I, Figure 2). The *in vitro* fibrillization of A $\beta$  in quiescent conditions takes a long time, making the experiments time-consuming; moreover, the beginning of visible fibrillization can be stochastic and irreproducible. It has been confirmed that the agitation of the solution substantially accelerates the peptide and protein fibrillization *in vitro*; however, the origin of the accelerating effect has remained elusive. We aimed to study the effect of agitation on fibrillization of different amyloidogenic peptides *in vitro* monitored by ThT fluorescence. The results show that A $\beta$ 1-42 (Publication I, Figure 5) has distinct fibrillization properties compared to insulin and amylin (Publication I, Figure 6). A $\beta$ 1-42 (and with some reservations also A $\beta$ 1-40) needed agitation only for the initial phase of the process, in the lag phase where new seed and/or fibrils are formed (Publication I,

Figure 5). The elongation of A $\beta$ 1-42 fibrils and other subsequent processes were not affected by agitation, which probably means that agitation is most likely needed for the propagation of the initial fibrillary seeds formed and that their fibrils can easily grow without vigorous agitation, e.g., also in biological *in vivo* conditions. Unlike A $\beta$  peptides, the growth of amylin and insulin fibrils required agitation in all phases of the process (Publication I, Figure 6). The *in vitro* results of A $\beta$ 1-42 peptide fibrillization in quiescent conditions give a new aspect to higher amyloidogenicity of A $\beta$ 1-42 peptide as compared with A $\beta$ 1-40, which is important for initiation of the amyloid cascade in AD. Together with published results that A $\beta$ 1-42 peptide is toxic *in vivo* when the peptide fibrillizes in the growth medium around the cells (Cohen, Arosio et al. 2015; Krishtal, Bragina et al. 2017) most likely suggests that the initial fibrils *in vivo* are probably propagated on the biological membranes since the fibrillization occurs in the presence of cells without agitation (Krishtal, Bragina et al. 2017).

In AD pathogenesis, elevated oxidative stress has been observed in the AD brain, and in this process, the Met35 residue in A $\beta$  peptide becomes oxidized to sulfoxide (Naslund, Schierhorn et al. 1994; Kuo, Kokjohn et al. 2001). Despite the research, there was no consensus about the role of Met35 in oxidative stress and the effect of the oxidation of Met35 on the amyloidogenicity of A $\beta$  peptide. It has even been suggested that A $\beta$  mediated generation of ROS is initiated by the Met35 residue (Smith, Cappai et al. 2007). On the other hand, a particular function of Met35 in neuroprotection was also proposed due to the antioxidant properties of the thioether group. We studied the oxidation of A $\beta$  peptide in the presence of two physiologically relevant redox-active compounds, H<sub>2</sub>O<sub>2</sub> and Cu(II) ions, by using MALDI TOF MS (Publication II). Our results show that the oxidation of Met35 to sulfoxide by H<sub>2</sub>O<sub>2</sub> was the only oxidation process occurring in the absence of Cu(II) ions (Publication II, Figure 1). The A $\beta$  with oxidized Met35 residue showed an approximately threefold lower fibrillization rate and a longer lag-phase (Publication II, Figure 3). In the presence of Cu(II) ions, the oxidation was more complex. The addition of the oxygen to Met35 was still the fastest process; however, the following steps led to multiple unspecific modifications of several other residues in the peptide (Publication II, Figure 2). Met35 oxidation did not affect the oxidative behavior of the A $\beta$  peptide complex in the presence of Cu(II) ions – when Met35 was oxidized in the absence of Cu(II) ions, the addition of Cu(II) ions still leads to the formation of a whole spectrum of oxidized peptides. This indicates that Met35 residue does not participate as a reducing agent in the copper-mediated radical generating mechanism.

Fibrillization of A $\beta$  peptide is also affected by metal ions. A $\beta$  peptide forms metal-induced amorphous aggregates in the presence of copper and zinc ions, which tend to form fibrils over time (Tougu, Karafin et al. 2009). Copper, one of the redox-active metal ions, is found in amyloid plaques in addition to zinc and iron and is believed to be linked to oxidative stress. Studying the interactions of full-length A $\beta$  peptides with redox-active metals are essential due to the ability of these complexes to generate ROS. Cu(II)-binding to A $\beta$  peptide has been proposed to form complexes with different binding stoichiometries. The fluorescence of Tyr10 residue can be used to monitor Cu(II) binding *in vitro* (Garzon-Rodriguez, Yatsimirsky et al. 1999; Raman, Ban et al. 2005). As the Cu(II) binding region of A $\beta$  peptide locates in the first 16 residues, A $\beta$ 1-16 peptide is more suitable for metal-binding studies using Tyr10 fluorescence compared to A $\beta$ 1-42 since A $\beta$ 1-16 does not fibrillize in contrast to A $\beta$ 1-42. Dr. Hureau's group and colleagues claimed using this method that A $\beta$ 1-16 peptide binds two Cu(II) ions

according to the shape of the binding curve that can be divided into multiple phases (Alies, Renaglia et al. 2013). As Cu(II)-binding curve should depend on the pH, we aimed to use the change of pH to investigate the phenomena observed by Dr. Hureau's group and colleagues (Alies, Renaglia et al. 2013) and hoping that the models expecting the binding of one or more Cu(II) ions can be discriminated. Our results from A $\beta$ 1-16 Tyr10 fluorescence experiments at different pH values showed reduced Cu(II)-binding in acidic conditions that confirm the involvement of His residues in Cu(II)-binding (Publication III). The Cu(II) titration curve obtained from Tyr10 fluorescence quenching could be fitted to the Morrison equation (Kuzmj 2015) that indicated binding one Cu(II) ion to A $\beta$ 1-16 (Publication III, Figure 1). We also showed that in agreement to Alies et al., one A $\beta$ 1-40 peptide is binding two equivalents of Cu(II) while precipitating; however, in the presence of glycine, which forms a weak complex with Cu(II) ions, Cu(II) levels decreased to one equivalent (Publication III, Figure 2). Therefore we concluded that *in vivo* the peptide cannot bind more than one Cu(II) ion; however, further investigations are needed to confirm this assumption. For example, the application of inductively coupled plasma mass spectrometry (ICP MS) could be used for these studies.

The binding of Cu(II) ions to A $\beta$  peptide has been suggested to occur with the involvement of residues His6, His13, His14, and peptide N-terminus, whereas His residues have also been shown to have a role in A $\beta$  peptide fibrillization (Alies, Hureau et al. 2013; Faller, Hureau et al. 2013). Chemical modification of His residues with DEPC can be used to estimate the role of His residues in the A $\beta$  peptide fibrillization process, and DEPC modification in the presence of Cu(II) ions can be used to establish which His residues are participating in the binding of Cu(II) ions. DEPC modification of insulin has been shown to increase peptide fibrillization at neutral pH and a decrease in acidic conditions (Yang, Li et al. 2015); however, the DEPC-modified A $\beta$  peptide fibrillization properties have not been studied. DEPC modification of His residues in A $\beta$ 1-42 peptide resulted in decreased fibrillization in ThT studies (Publication IV, Figure 4), but an increase in peptide aggregation was determined with semi-quantitative MALDI MS (Publication IV, Figure 3). His residues that are bound to Cu(II) ions were established from the protection studies of the residues from DEPC modification by Cu(II) ions in Ginotra et al. research article, showing that only His6 participates in Cu(II) binding to A $\beta$ 1-16 peptide (Ginotra, Ramteke et al. 2012). Tandem ESI MS/MS fragmentation results of Cu(II)-protected and DEPC-modified A $\beta$ 1-16 confirm that Cu(II) binding protected A $\beta$  peptide from DEPC modification but indicated that all A $\beta$  peptide His residues and peptide N-terminus are partially protected by Cu(II) ions (Publication IV, Figure S6-S8). Results did not indicate that some His residues are specifically protected by Cu(II) ions, and therefore we can conclude that all residues are involved in Cu(II) binding at pH=7.4.

Obtained *in vitro* results in the current thesis give some new information about the chemical properties of A $\beta$  peptides and their propensity for fibrillization, which could be together with the results of follow-up studies lead to a better understanding of amyloid cascade in AD and finding of strategies for its halting or prevention.

## Conclusions

- It was demonstrated that A $\beta$ 1-42 has distinct fibrillization properties compared to insulin and amylin. A $\beta$ 1-42 (and with some reservations also A $\beta$ 1-40) needed agitation only for the initial phase of the process, in the lag phase where new seed and/or fibrils are formed. The elongation of A $\beta$ 1-42 fibrils and other subsequent processes were not affected by agitation. Unlike A $\beta$  peptides, the growth of amylin and insulin fibrils required agitation in all phases of the process (Publication I).
- It was shown that in the oxidation of A $\beta$  peptides by H<sub>2</sub>O<sub>2</sub> the conversion of Met35 to sulfoxide was the only oxidation process occurring in the absence of Cu(II) ions. The A $\beta$  with oxidized Met35 residue showed an approximately threefold lower fibrillization rate and a longer lag-phase. In the presence of Cu(II) ions, the oxidation was more complex. The addition of the oxygen to Met35 was still the fastest process; however, the following steps led to multiple unspecific modifications of several other residues in the peptide. Met35 oxidation did not affect the oxidative behavior of the A $\beta$  peptide complex in the presence of Cu(II) ions - when Met35 was oxidized in the absence of Cu(II) ions, the addition of Cu(II) ions still leads to the formation of a whole spectrum of oxidized peptides. This indicates that Met35 residue does not participate as a reducing agent in the copper-mediated radical generating mechanism (Publication II).
- From the results of A $\beta$ 1-16 fluorescence experiments, it was shown that A $\beta$  peptide has reduced Cu(II)-binding in acidic conditions, which confirms the involvement of His residues in Cu(II)-binding. The Cu(II) titration curve obtained from Tyr10 fluorescence quenching could be fitted to the Morrison equation (Kuzmj 2015) that indicated binding one Cu(II) ion to A $\beta$ 1-16. It was demonstrated that one A $\beta$ 1-40 peptide is binding two equivalents of Cu(II) while precipitating; however, in the presence of glycine, Cu(II) stoichiometry decreased to one equivalent. Therefore we concluded that *in vivo* the A $\beta$  peptide cannot bind more than one Cu(II) ion (Publication III).
- It was established that A $\beta$ 1-42 could be modified with a maximum of five DEPC molecules affecting three His residues (His6, His13, His14), Lys16, and peptide N-terminus. DEPC modification of A $\beta$ 1-42 peptide resulted in decreased fibrillization in ThT studies, but an increase in peptide aggregation as determined with semi-quantitative MALDI MS. The results of Cu(II)-protection confirmed that Cu(II) binding protects A $\beta$  peptide from DEPC modification and indicated that all A $\beta$  peptide His residues and peptide N-terminus are partially protected by Cu(II) ions (Publication IV).

## References

- ADI (2018). "World Alzheimer Report 2018. The state of the art of dementia research: New frontiers." Alzheimer's Disease International (ADI), London.
- Akaaboune, M., B. Allinquant, et al. (2000). "Developmental regulation of amyloid precursor protein at the neuromuscular junction in mouse skeletal muscle." Mol Cell Neurosci **15**(4): 355-367.
- Al-Hilaly, Y. K., T. L. Williams, et al. (2013). "A central role for dityrosine crosslinking of Amyloid-beta in Alzheimer's disease." Acta Neuropathol Commun **1**: 83.
- Ali, F. E., F. Separovic, et al. (2005). "Methionine regulates copper/hydrogen peroxide oxidation products of Aβeta." J Pept Sci **11**(6): 353-360.
- Alies, B., A. Conte-Daban, et al. (2016). "Zinc(II) Binding Site to the Amyloid-beta Peptide: Insights from Spectroscopic Studies with a Wide Series of Modified Peptides." Inorg Chem **55**(20): 10499-10509.
- Alies, B., C. Hureau, et al. (2013). "The role of metal ions in amyloid formation: general principles from model peptides." Metallomics **5**(3): 183-192.
- Alies, B., E. Renaglia, et al. (2013). "Cu(II) affinity for the Alzheimer's peptide: tyrosine fluorescence studies revisited." Anal Chem **85**(3): 1501-1508.
- Alzheimer, A., R. A. Stelzmann, et al. (1995). "An English translation of Alzheimer's 1907 paper, "Uber eine eigenartige Erkrankung der Hirnrinde"." Clin Anat **8**(6): 429-431.
- Andreasen, N., C. Hesse, et al. (1999). "Cerebrospinal fluid beta-amyloid((1-42)) in Alzheimer disease - Differences between early- and late-onset Alzheimer disease and stability during the course of disease." Archives of Neurology **56**(6): 673-680.
- Andreasen, N., L. Minthon, et al. (1999). "Cerebrospinal fluid tau and A beta 42 as predictors of development of Alzheimer's disease in patients with mild cognitive impairment." Neuroscience Letters **273**(1): 5-8.
- Ankarcrona, M., F. Mangialasche, et al. (2010). "Rethinking Alzheimer's disease therapy: are mitochondria the key?" J Alzheimers Dis **20 Suppl 2**: S579-590.
- Arab, L. and M. N. Sabbagh (2010). "Are certain lifestyle habits associated with lower Alzheimer's disease risk?" J Alzheimers Dis **20**(3): 785-794.
- Arboleda-Velasquez, J. F., F. Lopera, et al. (2019). "Resistance to autosomal dominant Alzheimer's disease in an APOE3 Christchurch homozygote: a case report." Nat Med.
- Arndt, J. R., S. G. Kondalaji, et al. (2015). "Huntingtin N-Terminal Monomeric and Multimeric Structures Destabilized by Covalent Modification of Heteroatomic Residues." Biochemistry **54**(28): 4285-4296.
- Atrian-Blasco, E., M. Del Barrio, et al. (2018). "Ascorbate Oxidation by Cu(Amyloid-beta) Complexes: Determination of the Intrinsic Rate as a Function of Alterations in the Peptide Sequence Revealing Key Residues for Reactive Oxygen Species Production." Anal Chem **90**(9): 5909-5915.
- Atwood, C. S., R. N. Martins, et al. (2002). "Senile plaque composition and posttranslational modification of amyloid-beta peptide and associated proteins." Peptides **23**(7): 1343-1350.
- Atwood, C. S., R. D. Moir, et al. (1998). "Dramatic aggregation of Alzheimer abeta by Cu(II) is induced by conditions representing physiological acidosis." J Biol Chem **273**(21): 12817-12826.

- Atwood, C. S., G. Perry, et al. (2004). "Copper mediates dityrosine cross-linking of Alzheimer's amyloid-beta." Biochemistry **43**(2): 560-568.
- Avramopoulos, D. (2009). "Genetics of Alzheimer's disease: recent advances." Genome Med **1**(3): 34.
- Baldereschi, M., V. Di Carlo A Fau - Lepore, et al. (1998). "Estrogen-replacement therapy and Alzheimer's disease in the Italian Longitudinal Study on Aging." Neurology **50**(0028-3878 (Print)): 996-1002.
- Barnham, K. J., F. Haeffner, et al. (2004). "Tyrosine gated electron transfer is key to the toxic mechanism of Alzheimer's disease beta-amyloid." FASEB J **18**(12): 1427-1429.
- Bellingham, S. A., D. K. Lahiri, et al. (2004). "Copper depletion down-regulates expression of the Alzheimer's disease amyloid-beta precursor protein gene." J Biol Chem **279**(19): 20378-20386.
- Berggren, K., S. Agrawal, et al. (2017). "Amyloid Precursor Protein Haploinsufficiency Preferentially Mediates Brain Iron Accumulation in Mice Transgenic for The Huntington's Disease Mutation." J Huntingtons Dis **6**(2): 115-125.
- Bibl, M., M. Gallus, et al. (2012). "Characterization of cerebrospinal fluid aminoterminally truncated and oxidized amyloid-beta peptides." Proteomics Clin Appl **6**(3-4): 163-169.
- Billnitzer, A. J., I. Barskaya, et al. (2013). "APP independent and dependent effects on neurite outgrowth are modulated by the receptor associated protein (RAP)." Journal of Neurochemistry **124**(1): 123-132.
- Bitan, G., B. Tarus, et al. (2003). "A molecular switch in amyloid assembly: Met35 and amyloid beta-protein oligomerization." J Am Chem Soc **125**(50): 15359-15365.
- Blessed, G., B. E. Tomlinson, et al. (1968). "The association between quantitative measures of dementia and of senile change in the cerebral grey matter of elderly subjects." Br J Psychiatry **114**(512): 797-811.
- Boza-Serrano, A., Y. Yang, et al. (2018). "Innate immune alterations are elicited in microglial cells before plaque deposition in the Alzheimer's disease mouse model 5xFAD." Sci Rep **8**(1): 1550.
- Boumenir, A., E. Cognat, et al. (2019). "CSF level of beta-amyloid peptide predicts mortality in Alzheimer's disease." Alzheimers Res Ther **11**(1): 29.
- Braak, H. and E. Braak (1991). "Neuropathological staging of Alzheimer-related change." Acta Neuropathol **82**(4): 239-259.
- Brannstrom, K., T. Islam, et al. (2017). "The role of histidines in amyloid beta fibril assembly." FEBS Lett **591**(8): 1167-1175.
- Brannstrom, K., A. Ohman, et al. (2013). "Ca(2+) enhances Abeta polymerization rate and fibrillar stability in a dynamic manner." Biochem J **450**(1): 189-197.
- Brannstrom, K., A. Ohman, et al. (2014). "The N-terminal region of amyloid beta controls the aggregation rate and fibril stability at low pH through a gain of function mechanism." J Am Chem Soc **136**(31): 10956-10964.
- Brzyska, M., A. Bacia, et al. (2001). "Oxidative and hydrolytic properties of beta-amyloid." Eur J Biochem **268**(12): 3443-3454.
- Burdick, D., B. Soreghan, et al. (1992). "Assembly and aggregation properties of synthetic Alzheimer's A4/beta amyloid peptide analogs." J Biol Chem **267**(1): 546-554.
- Bush, A. I., W. H. Pettingell, et al. (1994). "Rapid induction of Alzheimer A beta amyloid formation by zinc." Science **265**(5177): 1464-1467.

- Butterfield, D. A. (2002). "Amyloid beta-peptide (1-42)-induced oxidative stress and neurotoxicity: implications for neurodegeneration in Alzheimer's disease brain. A review." *Free Radic Res* **36**(12): 1307-1313.
- Butterfield, D. A. and D. Boyd-Kimball (2004). "Amyloid beta-peptide(1-42) contributes to the oxidative stress and neurodegeneration found in Alzheimer disease brain." *Brain Pathol* **14**(4): 426-432.
- Butterfield, D. A. and D. Boyd-Kimball (2018). "Oxidative Stress, Amyloid-beta Peptide, and Altered Key Molecular Pathways in the Pathogenesis and Progression of Alzheimer's Disease." *J Alzheimers Dis* **62**(3): 1345-1367.
- Carneiro, F. A., F. Stauffer, et al. (2003). "Membrane fusion induced by vesicular stomatitis virus depends on histidine protonation." *J Biol Chem* **278**(16): 13789-13794.
- Cassagnes, L. E., V. Herve, et al. (2013). "The catalytically active copper-amyloid-Beta state: coordination site responsible for reactive oxygen species production." *Angew Chem Int Ed Engl* **52**(42): 11110-11113.
- Castellani, R. J., R. K. Rolston, et al. (2010). "Alzheimer disease." *Dis Mon* **56**(9): 484-546.
- Cenini, G., A. Lloret, et al. (2019). "Oxidative Stress in Neurodegenerative Diseases: From a Mitochondrial Point of View." *Oxid Med Cell Longev* **2019**: 2105607.
- Cheignon, C., P. Faller, et al. (2016). "Metal-catalyzed oxidation of A $\beta$  and the resulting reorganization of Cu binding sites promote ROS production." *Metallomics* **8**(10): 1081-1089.
- Cheignon, C., C. Hureau, et al. (2018). "Real-time evolution of A $\beta$ 40 metal-catalyzed oxidation reveals Asp1 as the main target and a dependence on metal binding site." *Inorganica Chimica Acta* **472**: 111-118.
- Cheignon, C., M. Jones, et al. (2017). "Identification of key structural features of the elusive Cu-A $\beta$  complex that generates ROS in Alzheimer's disease." *Chem Sci* **8**(7): 5107-5118.
- Cheignon, C., M. Tomas, et al. (2018). "Oxidative stress and the amyloid beta peptide in Alzheimer's disease." *Redox Biology* **14**: 450-464.
- Chen, G. F., T. H. Xu, et al. (2017). "Amyloid beta: structure, biology and structure-based therapeutic development." *Acta Pharmacologica Sinica* **38**(9): 1205-1235.
- Coan, C. and R. DiCarlo (1990). "Effect of diethyl pyrocarbonate modification on the calcium binding mechanism of the sarcoplasmic reticulum ATPase." *J Biol Chem* **265**(10): 5376-5384.
- Cohen, S. I., S. Linse, et al. (2013). "Proliferation of amyloid-beta42 aggregates occurs through a secondary nucleation mechanism." *Proc Natl Acad Sci U S A* **110**(24): 9758-9763.
- Cohen, S. I. A., P. Arosio, et al. (2015). "A molecular chaperone breaks the catalytic cycle that generates toxic A $\beta$  oligomers." *Nat Struct Mol Biol* **22**(3): 207-213.
- Coria, F., E. M. Castano, et al. (1987). "Brain amyloid in normal aging and cerebral amyloid angiopathy is antigenically related to Alzheimer's disease beta-protein." *American Journal of Pathology* **129**(3): 422-428.
- Crary, J. F., J. Q. Trojanowski, et al. (2014). "Primary age-related tauopathy (PART): a common pathology associated with human aging." *Acta Neuropathol* **128**(6): 755-766.



- Crouch, P. J., S. M. Harding, et al. (2008). "Mechanisms of A beta mediated neurodegeneration in Alzheimer's disease." Int J Biochem Cell Biol **40**(2): 181-198.
- Cruts, M., J. Theuns, et al. (2012). "Locus-specific mutation databases for neurodegenerative brain diseases." Hum Mutat **33**(9): 1340-1344.
- Curtain, C. C., F. Ali, et al. (2001). "Alzheimer's disease amyloid-beta binds copper and zinc to generate an allosterically ordered membrane-penetrating structure containing superoxide dismutase-like subunits." J Biol Chem **276**(23): 20466-20473.
- Dahlgren, K. N., A. M. Manelli, et al. (2002). "Oligomeric and fibrillar species of amyloid-beta peptides differentially affect neuronal viability." J Biol Chem **277**(35): 32046-32053.
- Danielsson, J., R. Pierattelli, et al. (2007). "High-resolution NMR studies of the zinc-binding site of the Alzheimer's amyloid beta-peptide." FEBS J **274**(1): 46-59.
- Díaz, I., I. N. de Castro, et al. (1993). "An experiment on the chemical modification of essential histidine residues of lactate dehydrogenase." Biochemical Education **21**(4): 219-220.
- Domingues, C., E. S. O. A. B. da Cruz, et al. (2017). "Impact of Cytokines and Chemokines on Alzheimer's Disease Neuropathological Hallmarks." Curr Alzheimer Res **14**(8): 870-882.
- Drummond, E., S. Nayak, et al. (2017). "Proteomic differences in amyloid plaques in rapidly progressive and sporadic Alzheimer's disease." Acta Neuropathol **133**(6): 933-954.
- Duce, J. A., A. Tsatsanis, et al. (2010). "Iron-export ferroxidase activity of beta-amyloid precursor protein is inhibited by zinc in Alzheimer's disease." Cell **142**(6): 857-867.
- Duggan, M. J. and F. A. Stephenson (1987). "Diethylpyrocarbonate Modification of the Central Benzodiazepine Binding-Site of Bovine Brain." Biochemical Society Transactions **15**(6): 1151-1151.
- Evans, K. C., E. P. Berger, et al. (1995). "Apolipoprotein E is a kinetic but not a thermodynamic inhibitor of amyloid formation: implications for the pathogenesis and treatment of Alzheimer disease." Proc Natl Acad Sci U S A **92**(3): 763-767.
- Everett, J., J. Brooks, et al. (2020). "Iron stored in ferritin is chemically reduced in the presence of aggregating Abeta(1-42)." Sci Rep **10**(1): 10332.
- Evrard, C., J. Fastrez, et al. (1999). "Histidine modification and mutagenesis point to the involvement of a large conformational change in the mechanism of action of phage lambda lysozyme." FEBS Lett **460**(3): 442-446.
- Faller, P., C. Hureau, et al. (2013). "Role of metal ions in the self-assembly of the Alzheimer's amyloid-beta peptide." Inorg Chem **52**(21): 12193-12206.
- Fang, J., B. Zhang, et al. (2003). "Chemical modification of contractile 3-nm-diameter filaments in Vorticella spasmoneme by diethyl-pyrocarbonate and its reversible renaturation by hydroxylamine." Biochem Biophys Res Commun **310**(4): 1067-1072.
- Francis, P. T., A. M. Palmer, et al. (1999). "The cholinergic hypothesis of Alzheimer's disease: a review of progress." J Neurol Neurosurg Psychiatry **66**(2): 137-147.
- Frazier, H. N., A. O. Ghoweri, et al. (2019). "Broadening the definition of brain insulin resistance in aging and Alzheimer's disease." Exp Neurol **313**: 79-87.

- Friedrich, R. P., K. Tepper, et al. (2010). "Mechanism of amyloid plaque formation suggests an intracellular basis of Abeta pathogenicity." Proc Natl Acad Sci U S A **107**(5): 1942-1947.
- Galloway, S., L. Jian, et al. (2007). "beta-amyloid or its precursor protein is found in epithelial cells of the small intestine and is stimulated by high-fat feeding." J Nutr Biochem **18**(4): 279-284.
- Galvan, V., O. F. Gorostiza, et al. (2006). "Reversal of Alzheimer's-like pathology and behavior in human APP transgenic mice by mutation of Asp664." Proc Natl Acad Sci U S A **103**(18): 7130-7135.
- Garzon-Rodriguez, W., A. K. Yatsimirsky, et al. (1999). "Binding of Zn(II), Cu(II), and Fe(II) ions to Alzheimer's A beta peptide studied by fluorescence." Bioorg Med Chem Lett **9**(15): 2243-2248.
- Georgiadou, D., A. Chroni, et al. (2011). "Biophysical analysis of apolipoprotein E3 variants linked with development of type III hyperlipoproteinemia." Plos One **6**(11): e27037.
- Ghoshal, N., F. Garcia-Sierra, et al. (2002). "Tau conformational changes correspond to impairments of episodic memory in mild cognitive impairment and Alzheimer's disease." Exp Neurol **177**(2): 475-493.
- Ginotra, Y. P., S. N. Ramteke, et al. (2012). "Mass spectral studies reveal the structure of Abeta1-16-Cu<sup>2+</sup> complex resembling ATCUN motif." Inorg Chem **51**(15): 7960-7962.
- Giulian, D., L. J. Haverkamp, et al. (1998). "The HHQK domain of beta-amyloid provides a structural basis for the immunopathology of Alzheimer's disease." J Biol Chem **273**(45): 29719-29726.
- Giulian, D., L. J. Haverkamp, et al. (1996). "Specific domains of beta-amyloid from Alzheimer plaque elicit neuron killing in human microglia." J Neurosci **16**(19): 6021-6037.
- Glenner, G. G. and C. W. Wong (1984). "Alzheimer's-Disease - Initial Report of the Purification and Characterization of a Novel Cerebrovascular Amyloid Protein." Biochem Biophys Res Commun **120**(3): 885-890.
- Gonzalez, P., K. Bossak, et al. (2018). "N-Terminal Cu-Binding Motifs (Xxx-Zzz-His, Xxx-His) and Their Derivatives: Chemistry, Biology and Medicinal Applications." Chemistry **24**(32): 8029-8041.
- Graziani, S., J. Bernauer, et al. (2006). "Catalytic mechanism and structure of viral flavin-dependent thymidylate synthase ThyX." J Biol Chem **281**(33): 24048-24057.
- Grochowska, K. M., P. Yuanxiang, et al. (2017). "Posttranslational modification impact on the mechanism by which amyloid-beta induces synaptic dysfunction." EMBO Rep **18**(6): 962-981.
- Grundke-Iqbal, I., K. Iqbal, et al. (1986). "Abnormal phosphorylation of the microtubule-associated protein tau (tau) in Alzheimer cytoskeletal pathology." Proc Natl Acad Sci U S A **83**(13): 4913-4917.
- Guivernau, B., J. Bonet, et al. (2016). "Amyloid-beta Peptide Nitrotyrosination Stabilizes Oligomers and Enhances NMDAR-Mediated Toxicity." J Neurosci **36**(46): 11693-11703.
- Ha, C., J. Ryu, et al. (2007). "Metal ions differentially influence the aggregation and deposition of Alzheimer's beta-amyloid on a solid template." Biochemistry **46**(20): 6118-6125.

- Haass, C. and D. J. Selkoe (2007). "Soluble protein oligomers in neurodegeneration: lessons from the Alzheimer's amyloid beta-peptide." Nat Rev Mol Cell Biol **8**(2): 101-112.
- Habasescu, L., M. Jureschi, et al. (2020). "Histidine-Lacked A beta(1-16) Peptides: pH-Dependent Conformational Changes in Metal Ion Binding." International Journal of Peptide Research and Therapeutics **26**(4): 2529-2546.
- Halle, A., V. Hornung, et al. (2008). "The NALP3 inflammasome is involved in the innate immune response to amyloid-beta." Nat Immunol **9**(8): 857-865.
- Hane, F. T., R. Hayes, et al. (2016). "Effect of Copper and Zinc on the Single Molecule Self-Affinity of Alzheimer's Amyloid-beta Peptides." Plos One **11**(1): e0147488.
- Hardy, J. and G. Higgins (1992). "Alzheimer's disease: the amyloid cascade hypothesis." Science **256**: 184-185.
- Hardy, J. and D. J. Selkoe (2002). "The amyloid hypothesis of Alzheimer's disease: progress and problems on the road to therapeutics." Science **297**(5580): 353-356.
- Harper, J. D., S. S. Wong, et al. (1997). "Observation of metastable A $\beta$  amyloid protofibrils by atomic force microscopy." Chem Biol **4**(2): 119-125.
- Hasegawa, K., K. Ono, et al. (2002). "Kinetic modeling and determination of reaction constants of Alzheimer's beta-amyloid fibril extension and dissociation using surface plasmon resonance." Biochemistry **41**(46): 13489-13498.
- Head, E., W. Garzon-Rodriguez, et al. (2001). "Oxidation of A $\beta$  and plaque biogenesis in Alzheimer's disease and Down syndrome." Neurobiol Dis **8**(5): 792-806.
- Hegy, G., G. Premecz, et al. (1974). "Selective carbethoxylation of the histidine residues of actin by diethylpyrocarbonate." Eur J Biochem **44**(1): 7-12.
- Heneka, M. T., M. P. Kummer, et al. (2013). "NLRP3 is activated in Alzheimer's disease and contributes to pathology in APP/PS1 mice." Nature **493**(7434): 674-678.
- Hnizda, A., J. Santrucek, et al. (2008). "Reactivity of histidine and lysine side-chains with diethylpyrocarbonate - a method to identify surface exposed residues in proteins." J Biochem Biophys Methods **70**(6): 1091-1097.
- Holscher, C. (2019). "Insulin Signaling Impairment in the Brain as a Risk Factor in Alzheimer's Disease." Front Aging Neurosci **11**: 88.
- Holtzman, D. M., J. C. Morris, et al. (2011). "Alzheimer's disease: the challenge of the second century." Sci Transl Med **3**(77): 77sr71.
- Hondal, R. J., S. Ma, et al. (2001). "Heparin-binding histidine and lysine residues of rat selenoprotein P." J Biol Chem **276**(19): 15823-15831.
- Hou, L., I. Kang, et al. (2002). "Methionine 35 oxidation reduces fibril assembly of the amyloid abeta-(1-42) peptide of Alzheimer's disease." J Biol Chem **277**(43): 40173-40176.
- Hou, L., H. G. Lee, et al. (2013). "Modification of amyloid-beta1-42 fibril structure by methionine-35 oxidation." J Alzheimers Dis **37**(1): 9-18.
- Hu, Y., P. Kienlen-Campard, et al. (2017). "beta-Sheet Structure within the Extracellular Domain of C99 Regulates Amyloidogenic Processing." Sci Rep **7**(1): 17159.
- Huang, H., X. Lou, et al. (2019). "A comprehensive study on the generation of reactive oxygen species in Cu-A $\beta$ -catalyzed redox processes." Free Radic Biol Med **135**: 125-131.
- Huang, X., C. S. Atwood, et al. (1997). "Zinc-induced Alzheimer's A $\beta$ 1-40 aggregation is mediated by conformational factors." J Biol Chem **272**(42): 26464-26470.

- Inoue, K., C. Garner, et al. (2006). "Liquid chromatography/tandem mass spectrometry characterization of oxidized amyloid beta peptides as potential biomarkers of Alzheimer's disease." *Rapid Commun Mass Spectrom* **20**(5): 911-918.
- Irie, K., K. Murakami, et al. (2005). "Structure of beta-amyloid fibrils and its relevance to their neurotoxicity: implications for the pathogenesis of Alzheimer's disease." *J Biosci Bioeng* **99**(5): 437-447.
- Istrate, A. N., S. A. Kozin, et al. (2016). "Interplay of histidine residues of the Alzheimer's disease Aβ peptide governs its Zn-induced oligomerization." *Sci Rep* **6**: 21734.
- Iversen, L. L., R. J. Mortishire-Smith, et al. (1995). "The toxicity in vitro of beta-amyloid protein." *Biochem J* **311** ( Pt 1): 1-16.
- Jakob-Roetne, R. and H. Jacobsen (2009). "Alzheimer's disease: from pathology to therapeutic approaches." *Angew Chem Int Ed Engl* **48**(17): 3030-3059.
- Janicki, S. C. and N. Schupf (2010). "Hormonal influences on cognition and risk for Alzheimer's disease." *Curr Neurol Neurosci Rep* **10**(5): 359-366.
- Joachim, C. L., J. H. Morris, et al. (1989). "Diffuse senile plaques occur commonly in the cerebellum in Alzheimer's disease." *American Journal of Pathology* **135**(2): 309-319.
- Joe, E. and J. M. Ringman (2019). "Cognitive symptoms of Alzheimer's disease: clinical management and prevention." *BMJ* **367**: l6217.
- Johnson, E. C., J. D. Lanning, et al. (2016). "Peptide backbone modification in the bend region of amyloid-beta inhibits fibrillogenesis but not oligomer formation." *J Pept Sci* **22**(5): 368-373.
- Johri, A. and M. F. Beal (2012). "Mitochondrial dysfunction in neurodegenerative diseases." *J Pharmacol Exp Ther* **342**(3): 619-630.
- Kalkum, M., M. Przybylski, et al. (1998). "Structure characterization of functional histidine residues and carbethoxylated derivatives in peptides and proteins by mass spectrometry." *Bioconjug Chem* **9**(2): 226-235.
- Karmakar, S. and K. P. Das (2012). "Identification of histidine residues involved in Zn(2+) binding to alphaA- and alphaB-crystallin by chemical modification and MALDI TOF mass spectrometry." *Protein J* **31**(7): 623-640.
- Karr, J. W., H. Akintoye, et al. (2005). "N-Terminal deletions modify the Cu<sup>2+</sup> binding site in amyloid-beta." *Biochemistry* **44**(14): 5478-5487.
- Khananashvili, D. and Z. Grometelhanan (1983). "Modification of Histidine-Residues by Diethyl Pyrocarbonate Leads to Inactivation of the Rhodospirillum-Rubrum Rrf1-ATPase." *FEBS Lett* **159**(1-2): 271-274.
- Knowles, T. P., C. A. Waudby, et al. (2009). "An analytical solution to the kinetics of breakable filament assembly." *Science* **326**(5959): 1533-1537.
- Konig, G., U. Monning, et al. (1992). "Identification and differential expression of a novel alternative splice isoform of the beta A4 amyloid precursor protein (APP) mRNA in leukocytes and brain microglial cells." *J Biol Chem* **267**(15): 10804-10809.
- Konkle, M. E., K. N. Elsenheimer, et al. (2010). "Chemical modification of the Rieske protein from *Thermus thermophilus* using diethyl pyrocarbonate modifies ligating histidine 154 and reduces the [2Fe-2S] cluster." *Biochemistry* **49**(34): 7272-7281.

- Kosik, K. S., C. L. Joachim, et al. (1986). "Microtubule-associated protein tau (tau) is a major antigenic component of paired helical filaments in Alzheimer disease." Proc Natl Acad Sci U S A **83**(11): 4044-4048.
- Kozlov, S., A. Afonin, et al. (2017). "Alzheimer's disease: as it was in the beginning." Rev Neurosci **28**(8): 825-843.
- Kovacs, G. G., I. Milenkovic, et al. (2013). "Non-Alzheimer neurodegenerative pathologies and their combinations are more frequent than commonly believed in the elderly brain: a community-based autopsy series." Acta Neuropathol **126**(3): 365-384.
- Kowalik-Jankowska, T., M. Ruta, et al. (2004). "Products of Cu(II)-catalyzed oxidation in the presence of hydrogen peroxide of the 1-10, 1-16 fragments of human and mouse beta-amyloid peptide." J Inorg Biochem **98**(6): 940-950.
- Krishtal, J., O. Bragina, et al. (2017). "In situ fibrillizing amyloid-beta 1-42 induces neurite degeneration and apoptosis of differentiated SH-SY5Y cells." Plos One **12**(10): e0186636.
- Kulikova, A. A., A. A. Makarov, et al. (2015). "Roles of zinc ions and structural polymorphism of  $\beta$ -amyloid in the development of Alzheimer's disease." Molecular Biology **49**(2): 217-230.
- Kumar, A., A. Singh, et al. (2015). "A review on Alzheimer's disease pathophysiology and its management: an update." Pharmacol Rep **67**(2): 195-203.
- Kummer, M. P. and M. T. Heneka (2014). "Truncated and modified amyloid-beta species." Alzheimers Res Ther **6**(3): 28.
- Kuo, Y. M., M. R. Emmerling, et al. (1996). "Water-soluble A $\beta$  (N-40, N-42) oligomers in normal and Alzheimer disease brains." J Biol Chem **271**(8): 4077-4081.
- Kuo, Y. M., T. A. Kokjohn, et al. (2001). "Comparative analysis of amyloid-beta chemical structure and amyloid plaque morphology of transgenic mouse and Alzheimer's disease brains." J Biol Chem **276**(16): 12991-12998.
- Kuo, Y. M., S. Webster, et al. (1998). "Irreversible dimerization/tetramerization and post-translational modifications inhibit proteolytic degradation of A $\beta$  peptides of Alzheimer's disease." Biochim Biophys Acta **1406**(3): 291-298.
- Kuzmij, P. (2015). History, variants and usage of the Morrison equation in enzyme inhibition kinetics.
- Lambert, M. P., A. K. Barlow, et al. (1998). "Diffusible, nonfibrillar ligands derived from A $\beta$ 1-42 are potent central nervous system neurotoxins." Proc Natl Acad Sci U S A **95**(11): 6448-6453.
- Lee, M., J. I. Kim, et al. (2018). "Metal ions affect the formation and stability of amyloid aggregates at multiple length scales." Physical Chemistry Chemical Physics **20**(13): 8951-8961.
- Lee, Y. H., W. G. Tharp, et al. (2008). "Amyloid precursor protein expression is upregulated in adipocytes in obesity." Obesity (Silver Spring) **16**(7): 1493-1500.
- Lermyte, F., J. Everett, et al. (2019). "Emerging Approaches to Investigate the Influence of Transition Metals in the Proteinopathies." Cells **8**(10).
- Levine, R. L., L. Mosoni, et al. (1996). "Methionine residues as endogenous antioxidants in proteins." Proc Natl Acad Sci U S A **93**(26): 15036-15040.
- Lewis, H., D. Beher, et al. (2006). "Quantification of Alzheimer pathology in ageing and dementia: age-related accumulation of amyloid-beta(42) peptide in vascular dementia." Neuropathol Appl Neurobiol **32**(2): 103-118.

- Liu, K., I. Solano, et al. (2006). "Characterization of Abeta11-40/42 peptide deposition in Alzheimer's disease and young Down's syndrome brains: implication of N-terminally truncated Abeta species in the pathogenesis of Alzheimer's disease." Acta Neuropathol **112**(2): 163-174.
- Liu, S. T., G. Howlett, et al. (1999). "Histidine-13 is a crucial residue in the zinc ion-induced aggregation of the A beta peptide of Alzheimer's disease." Biochemistry **38**(29): 9373-9378.
- Lu, D. C., S. Rabizadeh, et al. (2000). "A second cytotoxic proteolytic peptide derived from amyloid beta-protein precursor." Nat Med **6**(4): 397-404.
- Lu, D. C., S. Soriano, et al. (2003). "Caspase cleavage of the amyloid precursor protein modulates amyloid beta-protein toxicity." Journal of Neurochemistry **87**(3): 733-741.
- Lu, J. X., W. Qiang, et al. (2013). "Molecular structure of beta-amyloid fibrils in Alzheimer's disease brain tissue." Cell **154**(6): 1257-1268.
- Lu, Y., M. Prudent, et al. (2010). "Copper(I) and copper(II) binding to beta-amyloid 16 (Abeta16) studied by electrospray ionization mass spectrometry." Metallomics **2**(7): 474-479.
- Luca, A., C. Calandra, et al. (2018). "Molecular Bases of Alzheimer's Disease and Neurodegeneration: The Role of Neuroglia." Aging Dis **9**(6): 1134-1152.
- Ludewig, S. and M. Korte (2016). "Novel Insights into the Physiological Function of the APP (Gene) Family and Its Proteolytic Fragments in Synaptic Plasticity." Front Mol Neurosci **9**: 161.
- Luhrs, T., C. Ritter, et al. (2005). "3D structure of Alzheimer's amyloid-beta(1-42) fibrils." Proc Natl Acad Sci U S A **102**(48): 17342-17347.
- Maccioni, R. B., G. Farias, et al. (2010). "The revitalized tau hypothesis on Alzheimer's disease." Arch Med Res **41**(3): 226-231.
- Manocha, G. D., A. M. Floden, et al. (2016). "APP Regulates Microglial Phenotype in a Mouse Model of Alzheimer's Disease." J Neurosci **36**(32): 8471-8486.
- Masters, C. L., G. Multhaup, et al. (1985). "Neuronal origin of a cerebral amyloid: neurofibrillary tangles of Alzheimer's disease contain the same protein as the amyloid of plaque cores and blood vessels." EMBO J **4**(11): 2757-2763.
- Masters, C. L., G. Simms, et al. (1985). "Amyloid plaque core protein in Alzheimer disease and Down syndrome." Proc Natl Acad Sci U S A **82**(12): 4245-4249.
- McQuade, A. and M. Blurton-Jones (2019). "Microglia in Alzheimer's Disease: Exploring How Genetics and Phenotype Influence Risk." J Mol Biol.
- Melchior, W. B., Jr. and D. Fahrney (1970). "Ethoxyformylation of proteins. Reaction of ethoxyformic anhydride with alpha-chymotrypsin, pepsin, and pancreatic ribonuclease at pH 4." Biochemistry **9**(2): 251-258.
- Mendoza, V. L. and R. W. Vachet (2008). "Protein surface mapping using diethylpyrocarbonate with mass spectrometric detection." Anal Chem **80**(8): 2895-2904.
- Mendoza, V. L. and R. W. Vachet (2009). "Probing protein structure by amino acid-specific covalent labeling and mass spectrometry." Mass Spectrom Rev **28**(5): 785-815.
- Miklossy, J., H. Qing, et al. (2010). "Beta amyloid and hyperphosphorylated tau deposits in the pancreas in type 2 diabetes." Neurobiol Aging **31**(9): 1503-1515.

- Miller, Y., B. Ma, et al. (2010). "Zinc ions promote Alzheimer Abeta aggregation via population shift of polymorphic states." Proc Natl Acad Sci U S A **107**(21): 9490-9495.
- Mital, M., N. E. Wezynfeld, et al. (2015). "A Functional Role for Abeta in Metal Homeostasis? N-Truncation and High-Affinity Copper Binding." Angew Chem Int Ed Engl **54**(36): 10460-10464.
- Mitra, S., P. Prasad, et al. (2018). "A Unified View of Assessing the Pro-oxidant versus Antioxidant Nature of Amyloid Beta Conformers." Chembiochem **19**(22): 2360-2371.
- Mold, M., L. Ouro-Gnao, et al. (2013). "Copper prevents amyloid-beta(1-42) from forming amyloid fibrils under near-physiological conditions in vitro." Sci Rep **3**: 1256.
- Monning, U., G. Konig, et al. (1992). "Alzheimer beta A4-amyloid protein precursor in immunocompetent cells." J Biol Chem **267**(33): 23950-23956.
- Morgan, C., M. Colombres, et al. (2004). "Structure and function of amyloid in Alzheimer's disease." Prog Neurobiol **74**(6): 323-349.
- Moro, M. L., A. S. Phillips, et al. (2018). "Pyroglutamate and Isoaspartate modified Amyloid-Beta in ageing and Alzheimer's disease." Acta Neuropathol Commun **6**(1): 3.
- Mullane, K. and M. Williams (2018). "Alzheimer's disease (AD) therapeutics - 1: Repeated clinical failures continue to question the amyloid hypothesis of AD and the current understanding of AD causality." Biochem Pharmacol **158**: 359-375.
- Mullane, K. and M. Williams (2018). "Alzheimer's disease (AD) therapeutics - 2: Beyond amyloid - Re-defining AD and its causality to discover effective therapeutics." Biochem Pharmacol **158**: 376-401.
- Nakamura, M., N. Shishido, et al. (2007). "Three histidine residues of amyloid-beta peptide control the redox activity of copper and iron." Biochemistry **46**(44): 12737-12743.
- Nakanishi, N., F. Takeuchi, et al. (2008). "Characterization of heme-coordinating histidyl residues of an engineered six-coordinated myoglobin mutant based on the reactivity with diethylpyrocarbonate, mass spectrometry, and electron paramagnetic resonance spectroscopy." J Biosci Bioeng **105**(6): 604-613.
- Nalivaeva, N. N. and A. J. Turner (2013). "The amyloid precursor protein: a biochemical enigma in brain development, function and disease." FEBS Lett **587**(13): 2046-2054.
- Naslund, J., A. Schierhorn, et al. (1994). "Relative abundance of Alzheimer A beta amyloid peptide variants in Alzheimer disease and normal aging." Proc Natl Acad Sci U S A **91**(18): 8378-8382.
- Nelson, P. T., E. L. Abner, et al. (2009). "Brains with medial temporal lobe neurofibrillary tangles but no neuritic amyloid plaques are a diagnostic dilemma but may have pathogenetic aspects distinct from Alzheimer disease." J Neuropathol Exp Neurol **68**(7): 774-784.
- Nichols, M. R., M. K. St-Pierre, et al. (2019). "Inflammatory Mechanisms in Neurodegeneration." Journal of Neurochemistry.
- Obregon, D., H. Hou, et al. (2012). "Soluble amyloid precursor protein-alpha modulates beta-secretase activity and amyloid-beta generation." Nat Commun **3**: 777.
- Oh, E. S., A. V. Savonenko, et al. (2009). "Amyloid precursor protein increases cortical neuron size in transgenic mice." Neurobiol Aging **30**(8): 1238-1244.

- Olsson, F., S. Schmidt, et al. (2014). "Characterization of intermediate steps in amyloid beta (Abeta) production under near-native conditions." J Biol Chem **289**(3): 1540-1550.
- Ono, K., M. M. Condrón, et al. (2009). "Structure-neurotoxicity relationships of amyloid beta-protein oligomers." Proc Natl Acad Sci U S A **106**(35): 14745-14750.
- Palmlblad, M., A. Westlind-Danielsson, et al. (2002). "Oxidation of methionine 35 attenuates formation of amyloid beta -peptide 1-40 oligomers." J Biol Chem **277**(22): 19506-19510.
- Palmer, A. M. (2002). "Pharmacotherapy for Alzheimer's disease: progress and prospects." Trends Pharmacol Sci **23**(9): 426-433.
- Palmer, A. M. (2011). "Neuroprotective therapeutics for Alzheimer's disease: progress and prospects." Trends Pharmacol Sci **32**(3): 141-147.
- Palmer, A. M. and S. Gershon (1990). "Is the neuronal basis of Alzheimer's disease cholinergic or glutamatergic?" FASEB J **4**(10): 2745-2752.
- Panza, F., M. Lozupone, et al. (2019). "Amyloid-beta immunotherapy for alzheimer disease: Is it now a long shot?" Ann Neurol **85**(3): 303-315.
- Park, S. A., G. M. Shaked, et al. (2009). "Mechanism of cytotoxicity mediated by the C31 fragment of the amyloid precursor protein." Biochem Biophys Res Commun **388**(2): 450-455.
- Parvathy, S., I. Hussain, et al. (1999). "Cleavage of Alzheimer's amyloid precursor protein by alpha-secretase occurs at the surface of neuronal cells." Biochemistry **38**(30): 9728-9734.
- Pereira, C. F., A. E. Santos, et al. (2019). "Is Alzheimer's disease an inflammasomopathy?" Ageing Res Rev **56**: 100966.
- Petit, D., M. Hitzengerber, et al. (2019). "Extracellular interface between APP and Nicastrin regulates Abeta length and response to gamma-secretase modulators." EMBO J **38**(12).
- Pietrzik, C. U., J. Hoffmann, et al. (1998). "From differentiation to proliferation: the secretory amyloid precursor protein as a local mediator of growth in thyroid epithelial cells." Proc Natl Acad Sci U S A **95**(4): 1770-1775.
- Pike, C. J., D. Burdick, et al. (1993). "Neurodegeneration induced by beta-amyloid peptides in vitro: the role of peptide assembly state." J Neurosci **13**(4): 1676-1687.
- Pike, C. J., M. J. Overman, et al. (1995). "Amino-terminal deletions enhance aggregation of beta-amyloid peptides in vitro." J Biol Chem **270**(41): 23895-23898.
- Pike, C. J., A. J. Walencewicz-Wasserman, et al. (1995). "Structure-activity analyses of beta-amyloid peptides: contributions of the beta 25-35 region to aggregation and neurotoxicity." Journal of Neurochemistry **64**(1): 253-265.
- Poirier, J. (2003). "Apolipoprotein E and cholesterol metabolism in the pathogenesis and treatment of Alzheimer's disease." Trends Mol Med **9**(3): 94-101.
- Poirier, J. (2008). "Apolipoprotein E represents a potent gene-based therapeutic target for the treatment of sporadic Alzheimer's disease." Alzheimers Dement **4**(1 Suppl 1): S91-97.
- Portelius, E., N. Bogdanovic, et al. (2010). "Mass spectrometric characterization of brain amyloid beta isoform signatures in familial and sporadic Alzheimer's disease." Acta Neuropathol **120**(2): 185-193.
- Priller, C., T. Bauer, et al. (2006). "Synapse formation and function is modulated by the amyloid precursor protein." J Neurosci **26**(27): 7212-7221.



- Qin, K., Y. Yang, et al. (2002). "Mapping Cu(II) binding sites in prion proteins by diethyl pyrocarbonate modification and matrix-assisted laser desorption ionization-time of flight (MALDI-TOF) mass spectrometric footprinting." *J Biol Chem* **277**(3): 1981-1990.
- Rajasekhar, K., M. Chakrabarti, et al. (2015). "Function and toxicity of amyloid beta and recent therapeutic interventions targeting amyloid beta in Alzheimer's disease." *Chem Commun (Camb)* **51**(70): 13434-13450.
- Raman, B., T. Ban, et al. (2005). "Metal ion-dependent effects of clioquinol on the fibril growth of an amyloid {beta} peptide." *J Biol Chem* **280**(16): 16157-16162.
- Ramteke, S. N., Y. P. Ginotra, et al. (2013). "Effects of oxidation on copper-binding properties of Abeta1-16 peptide: a pulse radiolysis study." *Free Radic Res* **47**(12): 1046-1053.
- Razzokov, J., M. Yusupov, et al. (2019). "Oxidation destabilizes toxic amyloid beta peptide aggregation." *Sci Rep* **9**(1): 5476.
- Reger, M. A., G. S. Watson, et al. (2008). "Intranasal insulin improves cognition and modulates beta-amyloid in early AD." *Neurology* **70**(6): 440-448.
- Reybier, K., S. Ayala, et al. (2016). "Free Superoxide is an Intermediate in the Production of H<sub>2</sub>O<sub>2</sub> by Copper(I)-Abeta Peptide and O<sub>2</sub>." *Angew Chem Int Ed Engl* **55**(3): 1085-1089.
- Rice, H. C., M. Townsend, et al. (2012). "Pancortins interact with amyloid precursor protein and modulate cortical cell migration." *Development* **139**(21): 3986-3996.
- Ripoli, C., R. Piacentini, et al. (2013). "Effects of different amyloid beta-protein analogues on synaptic function." *Neurobiol Aging* **34**(4): 1032-1044.
- Roberts, S. B., J. A. Ripellino, et al. (1994). "Non-amyloidogenic cleavage of the beta-amyloid precursor protein by an integral membrane metalloendopeptidase." *J Biol Chem* **269**(4): 3111-3116.
- Roher, A. E., M. O. Chaney, et al. (1996). "Morphology and toxicity of Abeta-(1-42) dimer derived from neuritic and vascular amyloid deposits of Alzheimer's disease." *J Biol Chem* **271**(34): 20631-20635.
- Rub, U., K. Del Tredici, et al. (2001). "The autonomic higher order processing nuclei of the lower brain stem are among the early targets of the Alzheimer's disease-related cytoskeletal pathology." *Acta Neuropathol* **101**(6): 555-564.
- Sandbrink, R., C. L. Masters, et al. (1994). "Beta A4-amyloid protein precursor mRNA isoforms without exon 15 are ubiquitously expressed in rat tissues including brain, but not in neurons." *J Biol Chem* **269**(2): 1510-1517.
- Santos, S. F., N. Pierrot, et al. (2009). "Expression of human amyloid precursor protein in rat cortical neurons inhibits calcium oscillations." *J Neurosci* **29**(15): 4708-4718.
- Sarell, C. J., S. R. Wilkinson, et al. (2010). "Substoichiometric levels of Cu<sup>2+</sup> ions accelerate the kinetics of fiber formation and promote cell toxicity of amyloid- $\beta$  from Alzheimer disease." *J Biol Chem* **285**(53): 41533-41540.
- Sato, T., T. S. Diehl, et al. (2007). "Active gamma-secretase complexes contain only one of each component." *J Biol Chem* **282**(47): 33985-33993.
- Schellenberg, G. D. and T. J. Montine (2012). "The genetics and neuropathology of Alzheimer's disease." *Acta Neuropathol* **124**(3): 305-323.
- Schoneich, C. and T. D. Williams (2002). "Cu(II)-catalyzed oxidation of beta-amyloid peptide targets His13 and His14 over His6: Detection of 2-Oxo-histidine by HPLC-MS/MS." *Chem Res Toxicol* **15**(5): 717-722.

- Schoneich, C. and T. D. Williams (2003). "Cu(II)-catalyzed oxidation of Alzheimer's disease beta-amyloid peptide and related sequences: remarkably different selectivities of neurotoxic betaAP1-40 and non-toxic betaAP40-1." Cell Mol Biol (Noisy-le-grand) **49**(5): 753-761.
- Sebastiao, M., N. Quittot, et al. (2017). "Thioflavin T fluorescence to analyse amyloid formation kinetics: Measurement frequency as a factor explaining irreproducibility." Anal Biochem **532**: 83-86.
- Selkoe, D. J. (2001). "Alzheimer's disease: genes, proteins, and therapy." Physiol Rev **81**(2): 741-766.
- Selkoe, D. J. (2008). "Soluble oligomers of the amyloid beta-protein impair synaptic plasticity and behavior." Behav Brain Res **192**(1): 106-113.
- Selkoe, D. J. and J. Hardy (2016). "The amyloid hypothesis of Alzheimer's disease at 25 years." EMBO Mol Med **8**(6): 595-608.
- Selkoe, D. J., M. B. Podlisny, et al. (1988). "Beta-amyloid precursor protein of Alzheimer disease occurs as 110- to 135-kilodalton membrane-associated proteins in neural and nonneural tissues." Proc Natl Acad Sci U S A **85**(19): 7341-7345.
- Selkoe, D. J. and D. Schenk (2003). "Alzheimer's disease: molecular understanding predicts amyloid-based therapeutics." Annu Rev Pharmacol Toxicol **43**: 545-584.
- Serrano-Pozo, A., M. L. Mielke, et al. (2012). "Stable size distribution of amyloid plaques over the course of Alzheimer disease." J Neuropathol Exp Neurol **71**(8): 694-701.
- Sharma, A. K., S. T. Pavlova, et al. (2013). "The effect of Cu(2+) and Zn(2+) on the Abeta42 peptide aggregation and cellular toxicity." Metallomics **5**(11): 1529-1536.
- Shoshan-Barmatz, V. and S. Weil (1994). "Diethyl pyrocarbonate modification of the ryanodine receptor/Ca<sup>2+</sup> channel from skeletal muscle." Biochem J **299 ( Pt 1)**: 177-181.
- Siman, R., S. Mistretta, et al. (1993). "Processing of the beta-amyloid precursor. Multiple proteases generate and degrade potentially amyloidogenic fragments." J Biol Chem **268**(22): 16602-16609.
- Simunkova, M., S. H. Alwasel, et al. (2019). "Management of oxidative stress and other pathologies in Alzheimer's disease." Arch Toxicol **93**(9): 2491-2513.
- Smith, D. G., R. Cappai, et al. (2007). "The redox chemistry of the Alzheimer's disease amyloid beta peptide." Biochim Biophys Acta **1768**(8): 1976-1990.
- Snyder, S. W., U. S. Lador, et al. (1994). "Amyloid-beta aggregation: selective inhibition of aggregation in mixtures of amyloid with different chain lengths." Biophys J **67**(3): 1216-1228.
- Soba, P., S. Eggert, et al. (2005). "Homo- and heterodimerization of APP family members promotes intercellular adhesion." EMBO J **24**(20): 3624-3634.
- Sondag, C. M. and C. K. Combs (2004). "Amyloid precursor protein mediates proinflammatory activation of monocytic lineage cells." J Biol Chem **279**(14): 14456-14463.
- Sperling, R. A., P. S. Aisen, et al. (2011). "Toward defining the preclinical stages of Alzheimer's disease: recommendations from the National Institute on Aging-Alzheimer's Association workgroups on diagnostic guidelines for Alzheimer's disease." Alzheimers Dement **7**(3): 280-292.
- Stein, T. D., N. J. Anders, et al. (2004). "Neutralization of transthyretin reverses the neuroprotective effects of secreted amyloid precursor protein (APP) in APPSW mice resulting in tau phosphorylation and loss of hippocampal neurons: support for the amyloid hypothesis." J Neurosci **24**(35): 7707-7717.

- Strittmatter, W. J., A. M. Saunders, et al. (1994). "Isoform-specific interactions of apolipoprotein E with microtubule-associated protein tau: implications for Alzheimer disease." Proc Natl Acad Sci U S A **91**(23): 11183-11186.
- Strittmatter, W. J., A. M. Saunders, et al. (1993). "Apolipoprotein E: high-avidity binding to beta-amyloid and increased frequency of type 4 allele in late-onset familial Alzheimer disease." Proc Natl Acad Sci U S A **90**(5): 1977-1981.
- Strittmatter, W. J., K. H. Weisgraber, et al. (1993). "Binding of human apolipoprotein E to synthetic amyloid beta peptide: isoform-specific effects and implications for late-onset Alzheimer disease." Proc Natl Acad Sci U S A **90**(17): 8098-8102.
- Zhang, X., J. Liu, et al. (2016). "How the imidazole ring modulates amyloid formation of islet amyloid polypeptide: A chemical modification study." Biochim Biophys Acta **1860**(4): 719-726.
- Zhao, J., W. Gao, et al. (2019). "Nitration of amyloid-beta peptide (1-42) as a protective mechanism for the amyloid-beta peptide (1-42) against copper ion toxicity." J Inorg Biochem **190**: 15-23.
- Zheng, H., M. Jiang, et al. (1995). "beta-Amyloid precursor protein-deficient mice show reactive gliosis and decreased locomotor activity." Cell **81**(4): 525-531.
- Zhou, Y. and R. W. Vachet (2012). "Diethylpyrocarbonate labeling for the structural analysis of proteins: label scrambling in solution and how to avoid it." J Am Soc Mass Spectrom **23**(5): 899-907.
- Zhou, Y. and R. W. Vachet (2012). "Increased protein structural resolution from diethylpyrocarbonate-based covalent labeling and mass spectrometric detection." J Am Soc Mass Spectrom **23**(4): 708-717.
- Tanaka, S., S. Shiojiri, et al. (1989). "Tissue-specific expression of three types of beta-protein precursor mRNA: enhancement of protease inhibitor-harboring types in Alzheimer's disease brain." Biochem Biophys Res Commun **165**(3): 1406-1414.
- Tang, M. X., Y. Jacobs D Fau - Stern, et al. (1996). "Effect of oestrogen during menopause on risk and age at onset of Alzheimer's disease." Lancet **348**(0140-6736 (Print)): 429-432.
- Tarawneh, R. and D. M. Holtzman (2012). "The clinical problem of symptomatic Alzheimer disease and mild cognitive impairment." Cold Spring Harb Perspect Med **2**(5): a006148.
- Teng, X., E. Stefaniak, et al. (2020). "Hierarchical binding of copper(II) to N-truncated Aβ<sub>4-16</sub> peptide." Metalomics **12**(4): 470-473.
- Tiiman, A., J. Krishtal, et al. (2015). "In vitro fibrillization of Alzheimer's amyloid-β peptide (1-42)." AIP Advances **5**(9): 092401.
- Tiiman, A., P. Palumaa, et al. (2013). "The missing link in the amyloid cascade of Alzheimer's disease - metal ions." Neurochem Int **62**(4): 367-378.
- Tomaselli, S., K. Pagano, et al. (2017). "Evidence of Molecular Interactions of A beta 1-42 with N-Terminal Truncated Beta Amyloids by NMR." ACS Chemical Neuroscience **8**(4): 759-765.
- Tougu, V., A. Karafin, et al. (2009). "Zn(II)- and Cu(II)-induced non-fibrillar aggregates of amyloid-beta (1-42) peptide are transformed to amyloid fibrils, both spontaneously and under the influence of metal chelators." Journal of Neurochemistry **110**(6): 1784-1795.
- Turner, P. R., K. O'Connor, et al. (2003). "Roles of amyloid precursor protein and its fragments in regulating neural activity, plasticity and memory." Prog Neurobiol **70**(1): 1-32.

- Walsh, D. M., D. M. Hartley, et al. (1999). "Amyloid beta-protein fibrillogenesis. Structure and biological activity of protofibrillar intermediates." J Biol Chem **274**(36): 25945-25952.
- Walsh, D. M., A. Lomakin, et al. (1997). "Amyloid beta-protein fibrillogenesis. Detection of a protofibrillar intermediate." J Biol Chem **272**(35): 22364-22372.
- Varadarajan, S., J. Kanski, et al. (2001). "Different mechanisms of oxidative stress and neurotoxicity for Alzheimer's A beta(1--42) and A beta(25--35)." J Am Chem Soc **123**(24): 5625-5631.
- Varadarajan, S., S. Yatin, et al. (1999). "Methionine residue 35 is important in amyloid beta-peptide-associated free radical oxidative stress." Brain Res Bull **50**(2): 133-141.
- Waring, S. C., R. C. Rocca Wa Fau - Petersen, et al. (1999). "Postmenopausal estrogen replacement therapy and risk of AD: a population-based study." Neurology **52**(0028-3878 (Print)): 965-970.
- Warmlander, S., A. Tiiman, et al. (2013). "Biophysical studies of the amyloid beta-peptide: interactions with metal ions and small molecules." Chembiochem **14**(14): 1692-1704.
- Vassar, R., B. D. Bennett, et al. (1999). "Beta-secretase cleavage of Alzheimer's amyloid precursor protein by the transmembrane aspartic protease BACE." Science **286**(5440): 735-741.
- Watson, A. A., D. P. Fairlie, et al. (1998). "Solution structure of methionine-oxidized amyloid beta-peptide (1-40). Does oxidation affect conformational switching?" Biochemistry **37**(37): 12700-12706.
- Weidling, I. and R. H. Swerdlow (2019). "Mitochondrial Dysfunction and Stress Responses in Alzheimer's Disease." Biology (Basel) **8**(2).
- Weisgraber, K. H. (1990). "Apolipoprotein E distribution among human plasma lipoproteins: role of the cysteine-arginine interchange at residue 112." Journal of Lipid Research **31**(8): 1503-1511.
- Weisgraber, K. H., S. C. Rall, Jr., et al. (1981). "Human E apoprotein heterogeneity. Cysteine-arginine interchanges in the amino acid sequence of the apo-E isoforms." J Biol Chem **256**(17): 9077-9083.
- White, A. R., G. Multhaup, et al. (1999). "The Alzheimer's disease amyloid precursor protein modulates copper-induced toxicity and oxidative stress in primary neuronal cultures." J Neurosci **19**(21): 9170-9179.
- Vik, S. B. and Y. Hatefi (1981). "Possible occurrence and role of an essential histidyl residue in succinate dehydrogenase." Proc Natl Acad Sci U S A **78**(11): 6749-6753.
- Wildburger, N. C., T. J. Esparza, et al. (2017). "Diversity of Amyloid-beta Proteoforms in the Alzheimer's Disease Brain." Sci Rep **7**(1): 9520.
- Wiley, J. C., M. Hudson, et al. (2005). "Familial Alzheimer's disease mutations inhibit gamma-secretase-mediated liberation of beta-amyloid precursor protein carboxy-terminal fragment." Journal of Neurochemistry **94**(5): 1189-1201.
- Willard, B. B. and M. Kinter (2001). "Effects of the position of internal histidine residues on the collision-induced fragmentation of triply protonated tryptic peptides." J Am Soc Mass Spectrom **12**(12): 1262-1271.
- Willem, M., S. Tahirovic, et al. (2015). "eta-Secretase processing of APP inhibits neuronal activity in the hippocampus." Nature **526**(7573): 443-447.

- Williams, A. D., S. Shivaprasad, et al. (2006). "Alanine scanning mutagenesis of Abeta(1-40) amyloid fibril stability." J Mol Biol **357**(4): 1283-1294.
- Wong, C. W., V. Quaranta, et al. (1985). "Neuritic plaques and cerebrovascular amyloid in Alzheimer disease are antigenically related." Proc Natl Acad Sci U S A **82**(24): 8729-8732.
- Wulff, M., M. Baumann, et al. (2016). "Enhanced Fibril Fragmentation of N-Terminally Truncated and Pyroglutamyl-Modified Abeta Peptides." Angew Chem Int Ed Engl **55**(16): 5081-5084.
- Xing, Y., X. Z. Feng, et al. (2017). "A sensitive and selective electrochemical biosensor for the determination of beta-amyloid oligomer by inhibiting the peptide-triggered in situ assembly of silver nanoparticles." International Journal of Nanomedicine **12**: 3171-3179.
- Yako, N., T. R. Young, et al. (2017). "Copper binding and redox chemistry of the Abeta16 peptide and its variants: insights into determinants of copper-dependent reactivity." Metallomics **9**(3): 278-291.
- Yang, A., C. Wang, et al. (2017). "Attenuation of beta-Amyloid Toxicity In Vitro and In Vivo by Accelerated Aggregation." Neurosci Bull **33**(4): 405-412.
- Yang, X., Y. Li, et al. (2015). "Diethylpyrocarbonate modification reveals HisB5 as an important modulator of insulin amyloid formation." J Biochem **157**(1): 45-51.
- Yatin, S. M., S. Varadarajan, et al. (1999). "In vitro and in vivo oxidative stress associated with Alzheimer's amyloid beta-peptide (1-42)." Neurobiol Aging **20**(3): 325-330; discussion 339-342.
- Young, T. R., A. Kirchner, et al. (2014). "An integrated study of the affinities of the Abeta16 peptide for Cu(I) and Cu(II): implications for the catalytic production of reactive oxygen species." Metallomics **6**(3): 505-517.
- Young, T. R., C. J. Wijekoon, et al. (2015). "A set of robust fluorescent peptide probes for quantification of Cu(ii) binding affinities in the micromolar to femtomolar range." Metallomics **7**(3): 567-578.

## Acknowledgments

First and foremost, I would like to express my sincere gratitude to my supervisors Prof. Peep Palumaa and Dr. Vello Tõugu, for the guidance, immense knowledge, valuable critics, patience, and support during my Ph.D. studies.

My sincere thanks also goes to all my colleagues in the metalloproteomics lab; without your support, it would not have been possible. I especially like to thank Andra and Julia for your support, and our talks on science and other subjects were highly appreciated. Also, I would like to thank co-authors of my publications and colleagues from the Department of Chemistry and Biotechnology.

I would like to thank Aivar Lõokene, for reviewing the thesis.

I would also like to thank Estonian Research Council, the World Federation of Scientists (WFS), the Archimedes Foundation, and the Graduate School on Biomedicine and Biotechnology for financial support. This work has been partially supported by “TUT Institutional Development Program for 2016-2022” Graduate School in Biomedicine and Biotechnology receiving funding from the European Regional Development Fund under program ASTRA 2014-2020.4.01.16-0032 in Estonia.

Finally, I would like to thank my husband, my family, and friends for their support and patience during this process.

## Abstract

### Chemical modification of Met and His residues of Amyloid $\beta$ peptide. Influence of copper ions and effect on fibrillization

Alzheimer's disease (AD) is the most common form of dementia, with approximately 50 million people affected worldwide. Although enormous efforts have been directed to understanding the mechanisms behind AD pathology, there is still no cure. According to the prevalent amyloid cascade hypothesis, AD starts with the pathological build-up of cerebral extracellular amyloid plaques composed of fibrillated amyloid  $\beta$  (A $\beta$ ) peptide; however, it is still not known what role it plays in the mechanism of sporadic AD onset or neurodegeneration. Although the fibrillization of A $\beta$  peptide has been intensively studied, the mechanism of amyloid formation and its propagation *in vivo* is still unsolved. A $\beta$  peptide fibrillization process *in vitro* is affected by multiple factors such as temperature, pH, agitation, etc., which can give information about the properties of A $\beta$  peptide and gain an insight into the molecular mechanisms of AD. It has been generally accepted that the agitation of the solution substantially accelerates the peptide and protein fibrillization *in vitro*; however, the origin and variability of the accelerating effect in the case of different peptides has remained elusive. In the current study, Thioflavin T (ThT) fluorescence was used to study the effect of agitation on insulin, amylin, and A $\beta$  peptide *in vitro* fibrillization in diverse stages. Results show that agitation significantly accelerated the onset of fibrillization of all the peptides. Insulin and amylin required agitation throughout the whole process. A $\beta$ 1-42 fibrils grow under quiescent conditions when the agitation is stopped after the onset of fibrillization. The agitation affects the formation of new seeds and/or fibrils but not the fibril growth monitored by ThT fluorescence. A $\beta$ 1-40 also needed agitation for fibrillization throughout the whole process, including the fibril growth phase; however, differently from insulin, A $\beta$ 1-40 fibrillization continued with a reduced rate even when the agitation was stopped.

In AD pathogenesis, an elevated level of oxidative stress has been observed in the AD brain, and the Met35 in A $\beta$  peptide becomes oxidized to sulfoxide. Despite the research, there was still no consensus about the role of Met35 in oxidative stress. Is the oxidation of Met35 a result of oxidative stress, or does the oxidation of Met35 affect the level of oxidative stress, A $\beta$  peptide fibrillization, and subsequent deposition in the brain? We demonstrated that oxidative modification of Met35 in A $\beta$  peptides to sulfoxides by hydrogen peroxide (H<sub>2</sub>O<sub>2</sub>) slows down A $\beta$  peptide fibrillization monitored by ThT fluorescence; however, according to MALDI MS, Met35 residue is not part of a radical generating mechanism in the presence of H<sub>2</sub>O<sub>2</sub> and Cu(II) ions. Therefore, the oxidation of Met35 to sulfoxide is the result of oxidative stress.

Copper, one of the redox-active metals, has been implicated in AD pathology as the binding of Cu(II) ions to the A $\beta$  peptide by causing A $\beta$  peptide aggregation *in vitro* and catalysis of ROS. At the same time, there is no consensus about the stoichiometry and affinity of Cu(II) binding to A $\beta$  peptide. In the current study, the binding curve of Cu(II) to A $\beta$ 1-16 peptide followed by the decrease in Tyr10 fluorescence on different pH values was investigated that could give reliable information about the stoichiometry of Cu(II) binding to A $\beta$ . Results showed that the binding curve in all pH values could be fitted to the Morrison equation (Kuzmj 2015), expecting the binding of one Cu(II) ion. Cu(II) binding to A $\beta$  peptide involves His6, His13, and His14 residues assumingly.

Chemical modification of His residues with diethylpyrocarbonate (DEPC) can establish which His residues are protected by Cu(II) ions after sequencing with tandem ESI MS/MS and estimate the role of His residues in the A $\beta$  peptide fibrillization process. Chemical modification of His residues in A $\beta$  peptide with DEPC resulted in a decrease of the fibrillization monitored by ThT fluorescence and Cu(II) binding protected A $\beta$  peptide N-terminus and all His residues from DEPC modification, indicating their involvement in Cu(II) binding.

Studying the *in vitro* fibrillization mechanism and modification of A $\beta$  peptides is crucial due to their central role in AD pathogenesis and may contribute to finding effective strategies for halting or prevention of amyloid cascade, characteristic for AD.



## Kokkuvõte

### Metioniini ja histidiini jääkide keemiline modifitseerimine amüloid- $\beta$ peptiidis. Vaskioonide mõju ja efekt fibrillisatsioonile

Alzheimeri tõbi (AT) on kõige levinum dementsuse vorm maailmas, mille all kannatab hinnanguliselt 50 miljonit inimest. Kuigi AT patoloogiliste mehhanismide uurimiseks on tehtud suuri jõupingutusi, pole sellele tõele ravi veel leitud. Amüloidi kaskaadi hüpoteesi kohaselt algab AT valdavalt fibrilleerunud amüloid- $\beta$  ( $A\beta$ ) peptiidist koosnevate patoloogiliste rakuväliste naastude kuhjumisega ajus. Seejuures ei ole teada, mis on  $A\beta$  algse agregatsiooni põhjuseks haiguse sporaadilise vormi korral ja ei ole selge mehhanism, mille kaudu naastud põhjustavad neurodegeneratsiooni. Vaatamata eelnenud uuringute rohkusele, pole siiski veel selge amüloidi moodustumise mehhanism ning selle levimine *in vivo*.  $A\beta$  peptiidi *in vitro* fibrillisatsiooni protsess on mõjutatud paljude erinevate tegurite poolt nagu temperatuur, pH, segamine jne. Nende tegurite mõju uurimine võib anda informatsiooni  $A\beta$  peptiidi käitumise ja AT molekulaarsete mehhanismide kohta. Üldiselt peaks segamine peptiidi ja valgu *in vitro* fibrillisatsiooni kui tahke faasi teket kiirendama, kuid täpsem mõju mehhanism ja selle muutlikus erinevate peptiidide korral pole teada. Kasutades fibrillide kvantiseerimiseks ThT fluorestsentsi uuriti segamise mõju insuliini, amüliini ja  $A\beta$  peptiidi fibrillisatsiooni erinevatele staadiumitele. Tulemused näitavad, et segamine kiirendas oluliselt kõigi nende peptiidide puhul fibrillisatsiooni käivitumist. Insuliin ja amüliin vajasid segamist fibrillisatsioon kulgemiseks kogu protsessi vältel.  $A\beta$ 1-42 fibrillid aga jätkasid kasvu ka segamise peatamisel juhul kui seda tehti peale fibrillisatsiooni käivitumist. Segamine mõjutas  $A\beta$ 1-42 uute fibrillisatsiooni algete ja/või fibrillide moodustumist.  $A\beta$ 1-40 vajab segamist pidevalt fibrillisatsiooni kestel, kaasa arvatud kasvufaasis, kuid erinevalt insuliinist toimus kas ka peale segamise peatamist, kuid väiksema kiirusega.

AT patogeneesis on täheldatud oksüdatiivse stressi taseme tõusu ajus ning samal ajal ka  $A\beta$  peptiidi Met35 kõrvalahela oksüdeerimist sulfoksiidiks. Vaatamata arvukatele uuringutele puudub ühene arusaam sellest, kas Met35 oksüdatsioon on vaid stressi tulemus või mõjutab see stressi taset ja/või  $A\beta$  peptiidi fibrillisatsiooni ning seeläbi kuhjumist ajus. Töös näidati, et Met35 oksüdeerimine sulfoksiidiks aeglustab  $A\beta$  peptiidi fibrillisatsiooni. Oksüdatsiooni uurimine MALDI MS meetodiga näitas, et Met35 ei osale vesinikperoksiidi ( $H_2O_2$ ) ja Cu(II) juuresolekul toimivas radikaalide moodustumise protsessis. Seega on Met35 oksüdeerumine vaid oksüdatiivse stressi tagajärg ega võimenda AT puhul olulisi oksüdatiivseid protsesse.

AT patogeneesis on arvatavasti oma roll ka  $A\beta$  seonduvatel vaskioonidel, mis põhjustavad peptiidi kiiret agregatsiooni *in vitro* ning oma elektrokeemilise aktiivsuse tõttu katalüüsivad reaktiivsete hapnikuühendite teket. Kuigi vask(II) seondumist  $A\beta$  peptiidiga on palju uuritud, puudub ühene arusaam vask(II) ionide sidumise stöhhiomeetriast ja afiinsusest. Käesolevas töös jälgiti Tyr10 jäägi fluorestsentsi kahanemist vask(II) ionide seondumise tulemusena erinevatel pH väärtustel. Tiitrimiskõveraid oli võimalik kirjeldada Morrisoni valemiga eeldades ühe vask(II)iooni sidumist  $A\beta$ 1-16 peptiidiga kõigil pH väärtustel. Vask(II) sidumisel kaasatakse oletatavalt  $A\beta$  peptiidi järjestuses olevad His6, His13 ja His14, millede modifitseerimine dietüülpürokarbonaadiga (DEPC) annab võimaluse hinnata nende rolli  $A\beta$  peptiidi fibrillisatsioonis. Samal ajal on tandem elektropihustusionsatsiooni mass spektromeetria

(ESI MS/MS) abil peptiidi sekveneerides võimalik määrata ka vask(II) ionide kaitsvat toimet DEPC modifitseerimise eest. Tulemused näitavad, et vask(II) ioonid kaitsesid A $\beta$  peptiidi N-terminust ja kõiki kolme His jääki modifitseerimise eest, millest võib järeldada, et vask(II) seondumisest võtavad osa nii A $\beta$  peptiidi N-terminus kui ka kõik His jäägid. Samuti näidati, et A $\beta$  peptiidi His jääkide modifitseerimine DEPC poolt põhjustab ThT fluorestsentsi kaudu jälgitava peptiidi fibrillatsiooni aeglustumist.

*In vitro* fibrillatsiooni ja modifitseerimise uurimine on oluline, tema keske rolli tõttu AT patogeneesis ja võib kaasa aidata AT patogeneesi mehhanismi väljaselgitamisele ning strateegiate väljatöötamisele AT-le omase amüloidse kaskaadi pidurdamiseks või preventsooniks.



## Appendix

### Publication I

Tiiman, A., Noormagi, A., **Friedemann, M.**, Krishtal, J., Palumaa, P., & Tõugu, V. (2013). Effect of agitation on the peptide fibrillization: Alzheimer's amyloid-beta peptide 1-42 but not amylin and insulin fibrils can grow under quiescent conditions. [Research Support, Non-U.S. Gov't]. *J Pept Sci*, *19*(6), 386-391. doi: 10.1002/psc.2513



# Effect of agitation on the peptide fibrillization: Alzheimer's amyloid- $\beta$ peptide 1-42 but not amylin and insulin fibrils can grow under quiescent conditions

Ann Tiiman,<sup>a\*</sup> Andra Noormägi,<sup>a,b</sup> Merlin Friedemann,<sup>a</sup> Jekaterina Krishtal,<sup>a</sup> Peep Palumaa<sup>a,b</sup> and Vello Tõugu<sup>a</sup>

Many peptides and proteins can form fibrillar aggregates *in vitro*, but only a limited number of them are forming pathological amyloid structures *in vivo*. We studied the fibrillization of four peptides – Alzheimer's amyloid- $\beta$  ( $A\beta$ ) 1-40 and 1-42, amylin and insulin. In all cases, intensive mechanical agitation of the solution initiated fast fibrillization. However, when the mixing was stopped during the fibril growth phase, the fibrillization of amylin and insulin was practically stopped, and the rate for  $A\beta_{40}$  substantially decreased, whereas the fibrillization of  $A\beta_{42}$  peptide continued to proceed with almost the same rate as in the agitated conditions. The reason for the different sensitivity of the *in vitro* fibrillization of these peptides towards agitation in the fibril growth phase remains elusive. Copyright © 2013 European Peptide Society and John Wiley & Sons, Ltd.

**Keywords:** Alzheimer's amyloid- $\beta$ ; insulin; amylin; fibrillization; agitation

## Introduction

The formation of amyloid aggregates by peptides and proteins has attracted a great deal of attention because the presence of the resulting proteinaceous deposits with a fibrillar structure is characteristic to over 25 human diseases. Some of these amyloidogenic diseases, such as AD, Parkinson's disease and type II diabetes exert remarkable clinical relevance because of their dramatic prevalence in the elderly population [1]. The number of proteins that can misfold and aggregate into amyloid assemblies *in vitro* is considerably larger than the number of proteins involved in amyloid diseases. Moreover, it has been shown that most proteins can form fibrils under specific experimental conditions and fibrillization is suggested to be a generic property of polypeptide chains [2]. One of the most important questions in the studies of amyloid peptides/proteins is to find molecular and physicochemical characteristics that distinguish the peptides and proteins that are causing severe amyloid pathology from those that can fibrillize only in the *in vitro* conditions.

As a rule, protein fibrillization *in vitro* is characterized by a sigmoidal growth curve typical to autocatalytic processes [3,4]. The autocatalysis means that the addition of monomers to the ends of an existing fibril is faster than the formation of new fibrils from the monomers and, accordingly, the rate of the process depends on the number of fibril ends. Analysis of the kinetics of the self assembly of filamentous structures demonstrates that amyloid growth can often be dominated by secondary rather than primary nucleation events, for instance, fragmentation of early fibrils [5].

One of the important environmental factors that has a significant impact on the fibrillization kinetics and can also enhance fibril fragmentation is the agitation of the reaction mixture [6–8]. In this paper, we determined the effect of agitation on the different stages of fibrillization of four amyloidogenic peptides *in vitro*. The experimental conditions were similar for all four peptides, but optimized individually for each peptide, to obtain adequate fibrillization in the same time scale. For all the peptides studied, intensive agitation was required in the initial exponential phase of the reaction where the fibrillar 'seeds' and primary fibrils are formed that grow during the next elongation phase.  $A\beta_{42}$  was the only peptide that did not require agitation during this elongation phase as stopping of the agitation did not affect fibril elongation rate. Fibrillization of insulin and amylin stopped when agitation was stopped in this phase and fibrillization of  $A\beta_{40}$  proceeded with a significantly lower rate. We assume that the profound ability of  $A\beta_{42}$  fibrils to grow under quiescent

\* Correspondence to: Ann Tiiman, Department of Gene Technology, Tallinn University of Technology, Akadeemia 15, Tallinn 12618, Estonia. E-mail: ann.tiiman@ttu.ee

a Department of Gene Technology, Tallinn University of Technology, Akadeemia tee 15, Tallinn 12618, Estonia

b Competence Center on Reproductive Medicine and Biology, Tiigi 61 b, Tartu 50410, Estonia

**Abbreviations:**  $A\beta$ , amyloid- $\beta$  peptide; AD, Alzheimer's disease; ThT, Thioflavin T; HFIP, 1,1,1,3,3,3-hexafluoro-2-propanol

conditions is responsible for their high propensity to form pathological aggregates *in vivo*.

## Materials and Methods

### Materials

Lyophilized  $A\beta_{42}$  peptide TFA salt,  $A\beta_{40}$  NaOH salt and amylin (ultrapure, recombinant) were purchased from rPeptide (Bogart, Georgia, USA). Lyophilized insulin was from Sigma-Aldrich (St. Louis, Missouri, USA). 4-(2-hydroxyethyl)-1-piperazineethanesulfonic acid (HEPES), Ultrapure, MB Grade was from USB Corporation (Cleveland, Ohio, USA). 1,1,1,3,3,3-hexafluoro-2-propanol (HFIP) and thioflavin T (ThT) were from Sigma-Aldrich. NaCl was extra pure from Scharlau (Barcelona, Spain). All solutions were prepared in fresh MilliQ water.

### Sample Preparation

Stock solution of peptides was prepared as follows: 1 mg of the  $A\beta$  peptide was dissolved in HFIP at a concentration 500  $\mu\text{M}$  to disassemble preformed aggregates [9]. The solution was divided into aliquots, HFIP was evaporated in vacuum, and the tubes with the peptide film were kept at  $-80^\circ\text{C}$  until used. Before usage, the  $A\beta$  HFIP film was dissolved in water containing 0.02%  $\text{NH}_3$  at a concentration of 10–20  $\mu\text{M}$ . After 5 min of incubation, the  $A\beta$  stock solution was filtrated through a 0.45  $\mu\text{m}$  pore size Millex syringe-driven filter, dissolved with buffer and used for experiments. Insulin and amylin were dissolved in 20 mM HEPES and 100 mM NaCl, pH 7.4 at a concentration of 50  $\mu\text{M}$ . After 30 min of incubation, the peptide stock solution was diluted with buffer and used for experiments.

### Spectroscopy

Fluorescence spectra were collected on a Perkin–Elmer LS-45 fluorescence spectrophotometer equipped in house with a magnetic stirrer with constant stirring rate 250 rpm or equipped with a variable speed stirrer. Hellma semimicro cells were used. It is important to note that the stirring rate that is sufficient for a fast fibrillization depends not only on the stirrer speed but also varies with the cuvette and stirrer rod type used. We also noticed that in spectrofluorimeters equipped with built-in stirrers, the stirring speed should be 600–800 rpm to achieve fast aggregation (Figure 1). In our custom system, the movement of the stirrer rod was irregular because of a 2 mm shift of the rotation axis of the magnetic stirrer with respect to the center of the cell that caused the stirrer bar to flip against the walls of the quartz cell. Fibrillization was monitored using ThT fluorescence. If not otherwise stated, fresh  $A\beta$  stock solution was diluted in 20 mM HEPES and 100 mM NaCl, pH 7.4 containing 3.3  $\mu\text{M}$  of ThT to a final concentration of 5  $\mu\text{M}$  in the case of  $A\beta_{42}$  and 10  $\mu\text{M}$  in the case of  $A\beta_{40}$ . The final concentration of insulin and amylin was 2.5  $\mu\text{M}$  and 10  $\mu\text{M}$ , respectively. Of each sample, 400  $\mu\text{l}$  was incubated at constant temperature. ThT fluorescence was measured at 480 nm using excitation at 445 nm.

### Bicine/Tris SDS-PAGE

The SDS-PAGE was performed using 15%T/5%C gel on *Mini-PROTEAN Tetra System* (Bio-Rad) over 1.5 h. Gel consisted of separation gel, stacking gel and comb gel, thickness, 0.75 mm,

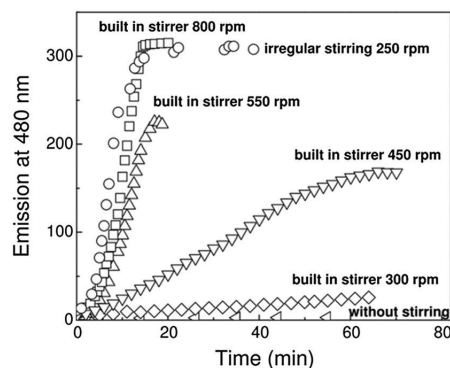


**Figure 1.** The effect of agitation on the  $A\beta$  fibrillization followed by ThT fluorescence. Aggregation of 5  $\mu\text{M}$   $A\beta_{42}$  in 20 mM HEPES and 100 mM NaCl, 25  $^\circ\text{C}$ , pH 7.4 with irregular stirring at a constant stirring rate of 250 rpm or with a built-in stirrer with various stirring speeds. Fluorescence measurement was carried out on a Perkin–Elmer LS-45 fluorescence spectrophotometer in a Hellma semimicro cells.

that were made according to Wiltfang J. *et al.* 1997 [10] with minor modifications: Separation gel was made without urea. Of samples containing 10  $\mu\text{M}$   $A\beta$ , 20  $\mu\text{l}$  were mixed with 5  $\mu\text{l}$  of 5 $\times$  loading buffer (1.8 M bistris, 0.265 M bicine, 75% glycerol, 5% SDS, 0.02% bromophenol blue) and heated to 95  $^\circ\text{C}$  for 5 min. The SDS-PAGE gel was resolved in Cathode buffer with 0.1% SDS at 110 V for 1.5 h (room temperature). After electrophoresis, gel was fixed in glutaraldehyde/sodium borate/phosphate buffer solution for 45 min at room temperature (glutaraldehyde 0.25%). Silver staining was carried out by a modified Dunn, M. silver staining method [11].

### Data Analysis and Kinetics of Fibril Formation

The kinetics of  $A\beta$  fibrillization could be described as sigmoid curves, and the aggregation parameters were determined by fitting the plot of fluorescence intensity versus time to Boltzmann curve

$$y = \frac{A_2 - A_1}{1 + e^{(t-t_0) \times k}} + A_2 \quad (1)$$

where  $A_1$  is the initial fluorescence level,  $A_2$  corresponds to the fluorescence at maximal fibrillization level,  $t_0$  is the time  $t$  when fluorescence is reached half maximum and  $k$  is the apparent rate constant for the growth of fibrils [12,13].

## Results

### Effect of Agitation on the Fibrillization of $A\beta$ Peptides

The time curves of  $A\beta_{42}$  fibrillization are presented in Figures 1 and 2. As a rule, the lyophilized  $A\beta_{42}$  preparations without HFIP pretreatment showed comparably high initial ThT-fluorescence levels indicating high content of fibrillar material (Figure 2). Different peptide preparations with different counterions had similar fibrillization curves after pretreatment of lyophilized peptides with HFIP (Figure 2).  $A\beta$  peptides, pretreated with HFIP to disassemble preformed aggregates, form stable solutions where the formation of ThT reactive material was not observed during several (2–4) days. The changes in the ThT fluorescence of  $A\beta_{40}$  were parallel to changes on the light scattering (Figure 3)

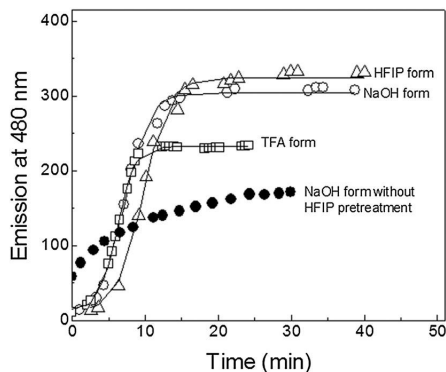


**Figure 2.** The effect of  $A\beta$  preparation on the fibrillization. The aggregation of  $5\ \mu\text{M}$   $A\beta_{42}$  in 20 mM HEPES and 100 mM NaCl, pH 7.4, at  $25\ ^\circ\text{C}$  in the presence of  $3.3\ \mu\text{M}$  ThT with irregular stirring at a constant stirring rate of 250 rpm. Open symbols – different  $A\beta$  preparations with HFIP pretreatment, closed symbols –  $A\beta_{42}$  NaOH form without HFIP pretreatment.

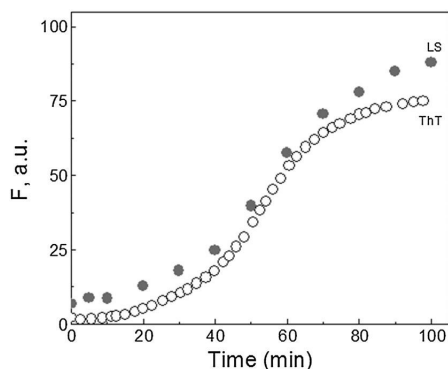


**Figure 3.** The fibrillization of  $A\beta_{40}$  followed by ThT fluorescence and light scattering. Aggregation of  $10\ \mu\text{M}$   $A\beta_{40}$  in 20 mM HEPES and 100 mM NaCl, pH 7.4 at  $50\ ^\circ\text{C}$  in the presence of  $3.3\ \mu\text{M}$  ThT with irregular stirring at a constant stirring rate of 250 rpm. Fluorescence measurements were carried out on a Perkin-Elmer LS-45 fluorescence spectrophotometer in a Hellma semimicro cells. ThT fluorescence was measured at 480 nm using excitation at 445 nm. Light scattering measured at  $90^\circ$  angle at 540 nm using excitation at 270 nm.

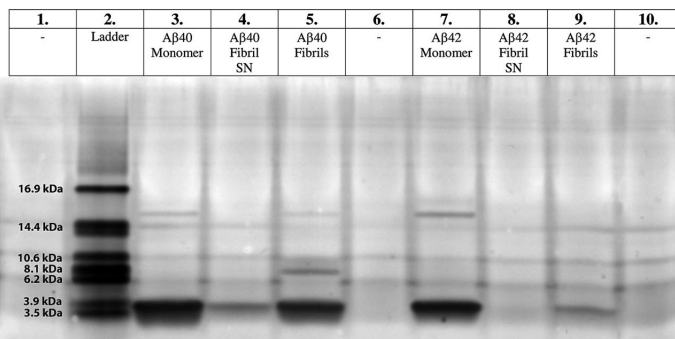


**Figure 4.** The SDS-PAGE analysis of  $A\beta$  fibrils. Monomers – HFIP treated  $A\beta_{40}$  and  $A\beta_{42}$  was dissolved in 10 mM NaOH and diluted two times with 40 mM HEPES and 200 mM NaCl buffer, pH 7.4 with concentration of  $10\ \mu\text{M}$ . Fibrils –  $10\ \mu\text{M}$   $A\beta_{40}$  and  $A\beta_{42}$  fibrils were centrifuged for 30 min, 21 130 g. Supernatant (SN) was collected, and precipitate (fibrils) was dissolved in equal amounts of 10 mM NaOH and 40 mM HEPES buffer containing 200 mM NaCl, pH 7.4 with concentration of  $10\ \mu\text{M}$ . SDS-PAGE was performed using 15%T/5%C gel on Mini-PROTEAN Tetra System (Bio-Rad) over 1.5 h and visualized by silver staining.

demonstrating that the aggregation is parallel to the formation of  $\beta$ -structures. The aggregates were centrifugated at 21 130 g for 30 min, and the SDS-PAGE analysis shows that all the peptide is sedimented (Figure 4). This means that there is no detectable amounts of soluble peptide either in monomeric or in oligomeric form after fibrillization is completed. It has been shown earlier that a fast fibrillization of the HFIP treated  $A\beta_{42}$  peptide can be initiated by stirring [12] or by the addition of preformed fibrillar seeds [14]. A typical sigmoidal fibrillization curve observed under the conditions of intensive stirring is presented in Figure 5A occurring with  $t_0 = 10$  min and  $k = 0.50\ \text{min}^{-1}$  (average values given in Table 1). Figure 5A shows that in the case of  $A\beta_{42}$ , stopping the stirrer after the fluorescence has achieved 25% of its maximum value had no effect on the rate of the process: In some experiments, a small 10% decrease in the rate of increase of ThT fluorescence was detected, which is presumably caused by sedimentation of larger aggregates.

Thus, for the fibrillization of  $A\beta_{42}$ , the agitation is crucial only in the initial exponential phase of the process, where new fibrils are forming and stirring is not required in the following first-order growth phase, where the major process is fibril elongation. When the stirrer was turned off earlier, for instance, at the level of 5% of the final fluorescence intensity, the exponential phase and the increase in the fibrillization rate ended abruptly, and the fibril growth continued with the rate achieved at that time point. These results show clearly that in the case of  $A\beta_{42}$ , agitation affects the formation of new seeds and/or fibrils but not the fibril growth.

Similar to  $A\beta_{42}$ , the  $A\beta_{40}$  peptide was also stable under quiescent conditions at pH 7.4 for several days, and its fast fibrillization was induced by stirring with a magnetic stirrer. However, the response of  $A\beta_{40}$  to the stopping of agitation in the fibril growth phase was different from that of  $A\beta_{42}$ . Figure 5B shows that stopping the stirring almost halted the fibril growth independently of the depth of the reaction; thus,  $A\beta_{40}$  needed agitation for fibrillization throughout the whole process including the fibril growth phase. From the rates of  $A\beta_{40}$  fibrillization after stopping the stirrer, it was estimated that in nonagitated conditions, reaction proceeded with 5%–20% of the rate in agitated conditions. When the stirring was turned on again, the fibrillization rate quickly returned to the value it had before the stirrer was turned off. It has been demonstrated that the fibrillization of  $A\beta_{40}$  initiated by shearing continues when shearing was stopped, however at a much slower (approximately fourfold to fivefold)



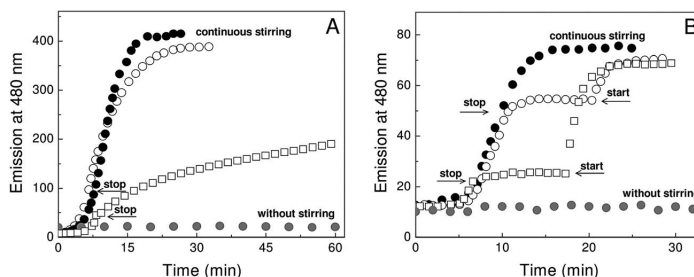


**Figure 5.** The effect of agitation on the  $A\beta$  fibrillization followed by ThT fluorescence. Fluorescence measurement was carried out on a Perkin-Elmer LS-45 fluorescence spectrophotometer equipped in house with a magnetic stirrer with constant stirring rate 250 rpm in a Hellma semimicro cells. Closed symbols – continuous stirring, open symbols – stirrer was turned off on at the points indicated by the first arrow and turned on again at the points indicated by the second arrow; gray symbols correspond to quiescent conditions. (A) Aggregation of  $5 \mu\text{M}$   $A\beta_{42}$  in 20 mM HEPES and 100 mM NaCl, 25 °C, pH 7.4; other conditions and sample preparation as described earlier [12]. (B) Aggregation of  $10 \mu\text{M}$   $A\beta_{40}$  in 20 mM HEPES and 100 mM NaCl, 50 °C pH 7.4. The decrease of the fibrillization rate after stopping the agitation was estimated from the slopes of the kinetic curves.

**Table 1.** The fibrillization parameters of  $A\beta_{40}$ ,  $A\beta_{42}$ , insulin and amylin.

Peptide	Reaction conditions	$k$ (per minute)	$t_0$ (min)
$A\beta_{42}$ ( $n=9$ )	$5 \mu\text{M}$ peptide; 25 °C	$0.45 \pm 0.09$	$11.5 \pm 4.9$
$A\beta_{40}$ ( $n=3$ )	$10 \mu\text{M}$ peptide; 50 °C	$1.11 \pm 0.37$	$7.6 \pm 1.5$
Insulin ( $n=5$ )	$2.5 \mu\text{M}$ peptide; 50 °C	$4.00 \pm 0.71$	$26.4 \pm 5.2$
Amylin ( $n=4$ )	$10 \mu\text{M}$ peptide; 40 °C	$2.51 \pm 0.83$	$13.4 \pm 0.6$

pace than with continuous shearing [15]. However, the lag period of the shear-induced fibrillization was several hours under similar temperature and pH, and the overall process was slower.

### Effect of Stirring on the Fibrillization of Insulin and Amylin

It has been shown recently that fast insulin fibrillization may occur at physiologically relevant pH, temperature and ionic strength under agitated conditions without added denaturing agents [16]. Figure 6A and B show that insulin and amylin are forming fibrils under agitated conditions in the same time scale as  $A\beta$  peptides. No fibril formation was observed during the incubation of these peptides under quiescent conditions at the same temperature and pH for at least 2–3 days. Insulin and amylin behaved similarly to  $A\beta_{40}$ , where intensive agitation was necessary during the whole fibrillization process, e.g. the

fibril growth when the stirrer was turned off was 11% and 5%, respectively, of the rate in agitated conditions. Fibrillization continued with high rate at the point where stirrer was turned on again (Figure 6A and B).

### Discussion

It has been generally accepted that the agitation of the solution substantially accelerates the peptide and protein fibrillization; however, the origin of the accelerating effect has remained elusive. Historically, the first explanation for this rate enhancement was that mixing causes the fragmentation of fibrils and increases the number of fibril ends available for monomer addition. This explanation links the acceleration with a phenomenon called secondary (e.g., fibril depending) nucleation that is crucial in the exponential phase of the fibrillization. It has been demonstrated

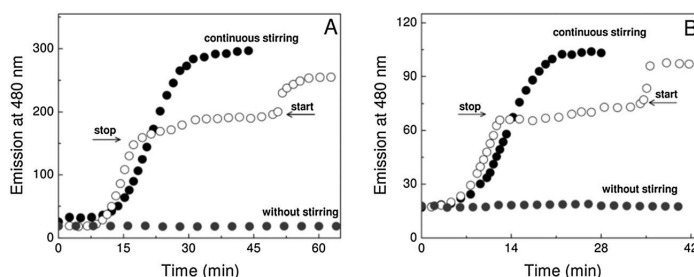


**Figure 6.** The effect of agitation on the fibrillization of insulin (A) and amylin (B) followed by ThT fluorescence. (A) Insulin concentration  $2.5 \mu\text{M}$  50 °C. (B) Amylin concentration  $10 \mu\text{M}$ , 40 °C; 20 mM HEPES and 100 mM NaCl, pH 7.4, stirring speed 250 rpm. Closed symbols – continuous stirring; open symbols – stirrer was turned off at the points indicated by the first arrow and turned on again at the points indicated by the second arrow, gray symbols correspond to the process in quiescent conditions. The decrease of fibrillization rate after stopping the agitation was estimated from the slopes of the kinetic curves.

that the fibrillization curves for several peptides cannot be described without assuming intensive secondary nucleation during fibrillization [5,17–20]; thus, secondary nucleation is a common phenomenon in peptide fibrillization in agitated as well as in nonagitated conditions. The fibril fragmentation by agitation is not the only mechanism that can lead to secondary nucleation. Interactions of peptide/protein fibrils with water–air and water–solid interfaces may also be involved in the acceleration of fibrillization because of catalyzing both secondary and primary nucleation events *in vitro* [8]. Our experiments also demonstrated the importance of interface effects because a regular stirring vortex generated by magnetic stirrer at 250 rpm had a significantly lower impact on the fibrillization rate than putative ‘grinding’ of fibrils when stirrer contacts the cell walls. However, as the fibrillization process is also accelerated by shear generated by Couette flow [6], the secondary nucleation can also occur in bulk solution. The origin of primary nucleation both *in vitro* and *in vivo* remains unknown. As the duration of lag phase is relatively insensitive to the increase in the peptide concentration [21,22] and the process is enhanced by stirring, it is reasonable to speculate that in practice, the primary fibrils start to grow on the interface of the test tube. *In vivo* the process can be triggered by metal ions [12,23,24] or, for instance, by lipid membranes [25].

The impact of agitation on the fibrillization of  $A\beta_{42}$  can be described assuming that the enhanced secondary nucleation is the only impact of agitation; however, it remains elusive why the fibrils of other peptides required agitation throughout the whole process. It can be hypothesized that they need secondary nucleation because of some kind of extensive ‘autoinhibition’, which may result from accidental association of peptide molecules to the fibril end in a ‘nonproductive’ way or incorrect or slow ‘locking’ (in the framework of docking and locking model) that blocks the growth of the individual fibrils temporarily. This assumption is based on the finding that assembly of individual amyloid fibrils is discontinuous: Bursts of rapid growth phases are interrupted with pauses, e.g. the process involves fluctuation between fast-growing and blocked states in which fibril is somehow kinetically trapped [26]. It might be suggested that in agitated conditions, the pauses between bursts are shorter as compared with the fibrillization in nonagitated conditions. The *in vitro* fibrillization rates of the peptides studied were relatively similar in the agitated conditions (Table 1). However, only  $A\beta_{42}$ , which has the highest amyloidogenicity among these peptides *in vivo*, showed high fibrillization rate in the absence of intensive agitation in the fibril growth phase. We suggest that the high *in vivo* amyloidogenicity of  $A\beta_{42}$  might be causatively related to the ability of  $A\beta_{42}$  fibrils to grow under quiescent conditions.

### Acknowledgements

This work was supported by the Estonian Ministry of Education and Research (grant SF0140055s08), Estonian Science Foundation grants no. 9318 (V.T.) and 8811 (P.P.) and World Federation of Scientists scholarships to A.T. and A.N.

### References

- Harrison RS, Sharpe PC, Singh Y, Fairlie DP. Amyloid peptides and proteins in review. *Rev. Physiol. Biochem. Pharmacol.* 2007; **159**: 1–77.
- Dobson CM. Protein folding and misfolding. *Nature* 2003; **426**(6968): 884–90.
- Harper JD, Lansbury PT, Jr. Models of amyloid seeding in Alzheimer's disease and scrapie: mechanistic truths and physiological consequences of the time-dependent solubility of amyloid proteins. *Annu. Rev. Biochem.* 1997; **66**: 385–407.
- Lomakin A, Chung DS, Benedek GB, Kirschner DA, Teplow DB. On the nucleation and growth of amyloid beta-protein fibrils: detection of nuclei and quantitation of rate constants. *Proc. Natl. Acad. Sci. USA* 1996; **93**(3): 1125–1129.
- Knowles TPJ, Waudby CA, Devlin GL, Cohen SIA, Aguzzi A, Vendruscolo M, Terentjev EM, Welland ME, Dobson CM. An analytical solution to the kinetics of breakable filament assembly. *Science* 2009; **326**(5959): 1533–1537.
- Dunstan DE, Hamilton-Brown P, Asimakis P, Ducker W, Bertolini J. Shear flow promotes amyloid- $\beta$  fibrillization. *Protein Eng. Des. Sel.* 2009; **22**(12): 741–746.
- Mahler HC, Friess W, Grauschopf U, Kiese S. Protein aggregation: pathways, induction factors and analysis. *J. Pharm. Sci.* 2009; **98**(9): 2909–2934.
- Morinaga A, Hasegawa K, Nomura R, Ookoshi T, Ozawa D, Goto Y, Yamada M, Naiki H. Critical role of interfaces and agitation on the nucleation of beta amyloid fibrils at low concentrations of beta monomers. *Biochim. Biophys. Acta* 2010; **1804**(4): 986–95.
- Stine WB, Jr., Dahlgren KN, Krafft GA, LaDu MJ. *In vitro* characterization of conditions for amyloid-beta peptide oligomerization and fibrillogenesis. *J. Biol. Chem.* 2003; **278**(13): 11612–22.
- Wiltfang J, Smirnov A, Schmierstein B, Kelemen G, Matthies U, Klafki HW, Staufenbiel M, Hübner G, Rübner E, Kornhuber J. Improved electrophoretic separation and immunoblotting of beta-amyloid (a beta) peptides 1-40, 1-42, and 1-43. *Electrophoresis* 1997; **18**(3-4): 527–32.
- Dunn M. Detection of proteins in polyacrylamide gels by silver staining. In *The Protein Protocols Handbook*, Walker J (ed.). Humana Press, New York, 1996; 229–233.
- Töugu V, Karafin A, Zovo K, Chung RS, Howells C, West AK, Palumaa P. Zn(II)- and Cu(II)-induced non-fibrillar aggregates of amyloid-beta (1-42) peptide are transformed to amyloid fibrils, both spontaneously and under the influence of metal chelators. *J. Neurochem.* 2009; **110**(6): 1784–95.
- Nielsen L, Frokjaer S, Brange J, Uversky VN, Fink AL. Probing the mechanism of insulin fibril formation with insulin mutants. *Biochemistry* 2001; **40**(28): 8397–409.
- Zovo K, Helk E, Karafin A, Töugu V, Palumaa P. Label-free high-throughput screening assay for inhibitors of Alzheimer's amyloid-beta peptide aggregation based on MALDI MS. *Anal. Chem.* 2010; **82**(20): 8558–8565.
- Hamilton-Brown P, Bekard I, Ducker WA, Dunstan DE. How does shear affect a beta fibrillogenesis? *J. Phys. Chem. B* 2008; **112**(51): 16249–16252.
- Noormägi A, Gavrilova J, Smirnova J, Töugu V, Palumaa P. Zn(II) ions co-secreted with insulin suppress inherent amyloidogenic properties of monomeric insulin. *Biochem. J.* 2010; **430**: 511–518.
- Hofrichter J. Kinetics of sickle hemoglobin polymerization. III. Nucleation rates determined from stochastic fluctuations in polymerization progress curves. *J. Mol. Biol.* 1986; **189**(3): 553–71.
- Larson JL, Miranker AD. The mechanism of insulin action on islet amyloid polypeptide fiber formation. *J. Mol. Biol.* 2004; **335**(1): 221–231.
- Librizzi F, Rischel C. The kinetic behavior of insulin fibrillation is determined by heterogeneous nucleation pathways. *Protein Sci.* 2005; **14**(12): 3129–34.
- Padrick SB, Miranker AD. Islet amyloid: phase partitioning and secondary nucleation are central to the mechanism of fibrillogenesis. *Biochemistry* 2002; **41**(14): 4694–703.
- Hellstrand E, Boland B, Walsh DM, Linse S. Amyloid beta-protein aggregation produces highly reproducible kinetic data and occurs by a two-phase process. *ACS Chem. Neurosci.* 2010; **1**(1): 13–18.
- Karafin A, Palumaa P, Töugu V. Monitoring of amyloid-beta fibrillization using an improved fluorimetric method. In *New Trends in Alzheimer and Parkinson Related Disorders: ADPD 2009*, Fisher A, Hanin I (eds). Medimond International Proceedings: Bologna, Italy, 2009; 255–261.
- Sarell CJ, Wilkinson SR, Viles JH. Substoichiometric levels of Cu<sup>2+</sup> ions accelerate the kinetics of fiber formation and promote cell toxicity of amyloid-beta from Alzheimer disease. *J. Biol. Chem.* 2010; **285**(53): 41533–41540.

- 24 Bush AI, Pettingell WH, Multhaup G, d Paradis M, Vonsattel JP, Gusella JF, Beyreuther K, Masters CL, Tanzi RE. Rapid induction of Alzheimer a beta amyloid formation by zinc. *Science* 1994; **265**(5177): 1464–7.
- 25 Murray IV, Liu L, Komatsu H, Uryu K, Xiao G, Lawson JA, Axelsen PH. Membrane-mediated amyloidogenesis and the promotion of oxidative lipid damage by amyloid beta proteins. *J. Biol. Chem.* 2007; **282**(13): 9335–45.
- 26 Kellermayer MS, Karsai A, Benke M, Soos K, Penke B. Stepwise dynamics of epitaxially growing single amyloid fibrils. *Proc. Natl. Acad. Sci. U.S.A.* 2008; **105**(1): 141–4.

## **Publication II**

**Friedemann, M.**, Helk, E., Tiiman, A., Zovo, K., Palumaa, P., & Tõugu, V. (2015). Effect of methionine-35 oxidation on the aggregation of amyloid-beta peptide. *Biochem Biophys Rep*, 3, 94-99. doi: 10.1016/j.bbrep.2015.07.017





## Effect of methionine-35 oxidation on the aggregation of amyloid- $\beta$ peptide



Merlin Friedemann, Eneken Helk, Ann Tiiman<sup>1</sup>, Kairit Zovo, Peep Palumaa, Vello Tõugu\*

Department of Gene Technology, Tallinn University of Technology, Akadeemia tee 15, 12618 Tallinn, Estonia

### ARTICLE INFO

#### Article history:

Received 18 June 2015

Received in revised form

22 July 2015

Accepted 28 July 2015

Available online 30 July 2015

#### Keywords:

Alzheimer's disease

$\beta$ -amyloid

Copper(II) ion

Methionine oxidation

### ABSTRACT

Aggregation of A $\beta$  peptides into amyloid plaques is considered to trigger the Alzheimer's disease (AD), however the mechanism behind the AD onset has remained elusive. It is assumed that the insoluble A $\beta$  aggregates enhance oxidative stress (OS) by generating free radicals with the assistance of bound copper ions. The aim of our study was to establish the role of Met35 residue in the oxidation and peptide aggregation processes. Met35 can be readily oxidized by H<sub>2</sub>O<sub>2</sub>. The fibrillization of A $\beta$  with Met35 oxidized to sulfoxide was three times slower compared to that of the regular peptide. The fibrils of regular and oxidized peptides looked similar under transmission electron microscopy. The relatively small inhibitory effect of methionine oxidation on the fibrillization suggests that the possible variation in the Met oxidation state should not affect the in vivo plaque formation. The peptide oxidation pattern was more complex when copper ions were present: addition of one oxygen atom was still the fastest process, however, it was accompanied by multiple unspecific modifications of peptide residues. Addition of copper ions to the A $\beta$  with oxidized Met35 in the presence of H<sub>2</sub>O<sub>2</sub>, resulted a similar pattern of non-specific modifications, suggesting that the one-electron oxidation processes in the peptide molecule do not depend on the oxidation state of Met35 residue. Thus, it can be concluded that Met35 residue is not a part of the radical generating mechanism of A $\beta$ -Cu(II) complex.

© 2015 The Authors. Published by Elsevier B.V. This is an open access article under the CC BY license (<http://creativecommons.org/licenses/by/4.0/>).

### 1. Introduction

Alzheimer's disease (AD) is characterized by progressive neuronal death and the accumulation of protein aggregates in certain brain areas. The aggregation of amyloid- $\beta$  (A $\beta$ ) peptide into extracellular amyloid plaques is identified as the key molecular event in AD, however, the molecular cascade leading to the death of neurons remains elusive. The increase of oxidative stress (OS) levels in certain brain areas is also characteristic to the disease and this increase is assumed to be an early event in AD [1,2]. The major risk factor for the pathogenesis of AD is aging and according to the free radical hypothesis the major cause of aging is the accumulation of ROS and the accumulation of oxidative damage [3]. The relationship between OS and AD progression is a complex one: elevated levels of OS can be both, the risk factor and the consequence of AD progression [4,5]. The toxicity of A $\beta$  aggregates is

assumed to arise from their ability to generate free radicals [6,7], which depends on the presence of copper ions.

Considering the involvement of A $\beta$  in oxidative processes, the Met35 is one of the most intriguing amino acid residues in the peptide molecule. Met35 has the most easily oxidized side chain in the peptide and it is partially oxidized in post mortem amyloid plaques [8,9]. There has been many speculations about the role of Met35 in the formation of amyloid plaques and peptide toxicity: it has been suggested that A $\beta$  mediated generation of ROS is initiated by the Met 35 residue [10]. On the other hand, a particular function in neuroprotection is also proposed for Met35 due to the antioxidant character of the thioether group [11,12]. The suggestions about the involvement of Met35 in toxic mechanisms is supported by the observation that Met35 oxidation state is critical for A $\beta$  synaptotoxicity – the oxidized form was clearly less toxic than the reduced one [13]. It has been shown that oxidation of Met35 reduces the A $\beta$ 42 toxicity in human neuroblastoma cells [14,15], however, the substitution of Met35 to valine and norleucine had no effect on the toxicity of A $\beta$  [16,17].

Methionine residues can be oxidized by two different mechanisms [18]. First, they can be spontaneously oxidized to methionine sulfoxide in a two electron process by some oxidants such as H<sub>2</sub>O<sub>2</sub> and molecular oxygen. This oxidation pathway can be considered relatively benign since no reactive oxygen species or

Abbreviations: A $\beta$ , Alzheimer's amyloid peptide; AD, Alzheimer's disease; HFIP, 1,1,1,3,3,3-hexafluoro-2-propanol; OS, oxidative stress; ROS, reactive oxygen species; ThT, Thioflavin T

\* Corresponding author.

E-mail address: [vello.tougu@ttu.ee](mailto:vello.tougu@ttu.ee) (V. Tõugu).

<sup>1</sup> Present address: Department of Clinical Neuroscience, Center for Molecular Medicine CMM L8:01, Karolinska Institutet, Stockholm, 17176, Sweden.

free radicals are formed. The oxidation of methionine to sulfoxide is a common reaction in living organism and the oxidation can be reversed by the methionine sulfoxide reductases, enzymes that reduce the sulfoxide and are an essential part of redox detoxification mechanisms in the living organisms. Methionine oxidation to sulfoxide is demonstrated to inhibit fibril formation [12] and this observation has also led to various speculations about the essential role of the oxidation of Met35 in AD. The sulfoxide can be further oxidized to sulfone, however, this reaction does not occur in physiological environments.

From the viewpoint of AD progression the second mechanism, one-electron oxidation of methionine to a highly reactive radical cation intermediate, is more intriguing. The single-electron mechanism can be catalyzed by copper ions that can have an essential role in AD etiology since they bind to A $\beta$  with high affinity and enhance its aggregation whereas the electrochemically active copper ions buried within the aggregates can generate ROS and cause OS [19,20]. An intriguing question is whether the radical cation generated from Met35 is an essential intermediate in the pathway of A $\beta$  generated oxidative stress or is this just a supplementary process that does not contribute to ROS generation and OS. In order to answer these questions we studied the kinetics and products of the oxidation of A $\beta$  by H<sub>2</sub>O<sub>2</sub> in the presence and absence of copper ions as the catalysts of one electron oxidation processes. Methionine oxidation slightly decreased the rate of in vitro fibrillization of the A $\beta$  peptides but did not changed its ability to catalyze the formation of ROS.

## 2. Materials and methods

### 2.1. Materials

Lyophilized A $\beta$ 40 and A $\beta$ 42 peptides (ultra pure, recombinant) NaOH salts or HFIP forms were purchased from rPeptide (Athens, USA). HEPES, Ultrapure, MB Grade was from USB Corporation (Cleveland, USA), 1,1,1,3,3,3-hexafluoro-2-propanol (HFIP) and Thioflavin T (ThT) were from Sigma Aldrich (St. Louis, USA). NaCl was extra pure from Scharlau (Barcelona, Spain). All solutions were prepared in fresh MilliQ water.

### 2.2. Sample preparation

Stock solution of A $\beta$  peptides was prepared as follows: 1 mg of the peptide was dissolved in HFIP at a concentration 500  $\mu$ M to disassemble preformed aggregates [21]. The solution was divided into aliquots, HFIP was evaporated in vacuum and the tubes with the peptide film were kept at  $-80^{\circ}\text{C}$  until used. Before using the A $\beta$  HFIP film was dissolved in water containing 10 mM NaOH at a concentration of 10–20  $\mu$ M. After 5 min incubation the A $\beta$  stock solution was dissolved with buffer and used for experiments.

### 2.3. Fluorescence spectroscopy

Fluorescence spectra were collected on a Perkin-Elmer LS-45 fluorescence spectrophotometer equipped with a magnetic stirrer. Fibrillation was monitored using ThT fluorescence. If not otherwise stated, fresh A $\beta$  stock solution was diluted in 20 mM HEPES and 100 mM NaCl, pH 7.4 containing 3.3  $\mu$ M of ThT to a final concentration of 5  $\mu$ M. 400  $\mu$ l of each sample was incubated at 40  $^{\circ}\text{C}$  if not otherwise stated. ThT fluorescence was measured at 480 nm using excitation at 445 nm.

### 2.4. Data analysis and kinetics of fibril formation

The kinetics of A $\beta$  fibrillation could be described as sigmoid

curves and the aggregation parameters were determined by fitting the plot of fluorescence intensity versus time to Boltzmann curve

$$y = \frac{A_2 - A_1}{1 + e^{-k(t-t_0)}} + A_1 \quad (1)$$

where  $A_1$  is the initial fluorescence level,  $A_2$  corresponds to the fluorescence at maximal fibrillation level,  $t_0$  is the time  $t$  when fluorescence is reached half maximum and  $k$  is the rate constant of fibril growth.

### 2.5. Transmission electron microscopy (TEM)

An aliquot of 5  $\mu$ l of sample was loaded on a Formvar-coated, carbon-stabilized copper grid (300 mesh from Ted Pella Inc., Redding CA). After 1 min, the excess solution was drained off using a Whatman filter paper. The grid was briefly washed and negatively stained with 5  $\mu$ l of 2% uranyl acetate. The grid was air-dried and then viewed on a Tecnai G2 BioTwin transmission electron microscope (FEI, Japan) operating with an accelerator voltage of 80 kV. Typical magnifications ranged from 20,000 to 60,000  $\times$ .

### 2.6. Kinetics of A $\beta$ oxidation

20 A $\beta$  M of alkaline A $\beta$  solution in 0.1% NaOH was diluted with equal volume of 0.1 M phosphate buffer containing hydrogen peroxide (H<sub>2</sub>O<sub>2</sub>) and Cu(II). Final concentrations of H<sub>2</sub>O<sub>2</sub> was 1% and the concentrations of copper ions were 0.1 and 10  $\mu$ M. The kinetics of A $\beta$  oxidation and the disappearance of monomers from the solution were monitored with matrix-assisted laser desorption/ionization mass spectrometry (MALDI MS) using the energy absorbing matrix  $\alpha$ -cyano-4-hydroxycinnamic acid (CHCA) [22]. Matrix CHCA was dissolved in 60% acetonitrile and 0.3% trifluoroacetic acid to a concentration of 10 mg/ml, containing 0.3  $\mu$ M bovine insulin as an internal standard. Samples were mixed with matrix (1:3 ratio of sample: matrix) and 1  $\mu$ l was spotted on the MALDI plate. MALDI MS spectra were acquired by Voyager-DE™ STR Biospectrometry Workstation in linear mode using automated program. Instrument parameter/settings: accelerating voltage 25,000 V; mass range ( $m/z$ ) 1500–10,000 Da; delay time 485 ns; grid voltage 93%; laser intensity 2200 V, shots per spectrum – 40; accumulated spectrum – 10.

The site of oxidation was determined by sequencing the oxidized peptide on ESI-MS. 10  $\mu$ M Ab42 in 100 mM ammonium acetate buffer (pH 7.5) was injected into the electrospray ion source of QATAR Elite ESI-Q-TOF MS instrument (Applied Biosystems) by a syringe pump at 7  $\mu$ l/min. ESI MS spectra were recorded for 5 min in the  $m/z$  region from 300 to 1500 Da with the following instrument parameters: ion spray voltage 5500 V; source gas 45 l/min; curtain gas 20 l/min; declustering potential 45 V; focusing potential 260 V; detector voltage 2450 V; collision energy 50 V; collision gas 5 l/min; precursor-ion mode.

Sodium dodecyl sulfate polyacrylamide gel electrophoresis (SDS-PAGE) was performed using Mini-PROTEAN Tetra System (Bio-Rad). Samples were mixed with loading buffer (0.36 M BisTris, 0.053 M Bicine, 1% glycerol, 1% SDS, 0.004% bromophenol blue), maintained at room temperature, applied to Bicine-Tris 15%T/5%C gel and resolved in a cathode buffer with 0.25% SDS (110 V) [23]. Gels were fixated in glutaraldehyde/borate buffer solution for 45 minutes and stained with silver according to a protocol [24].



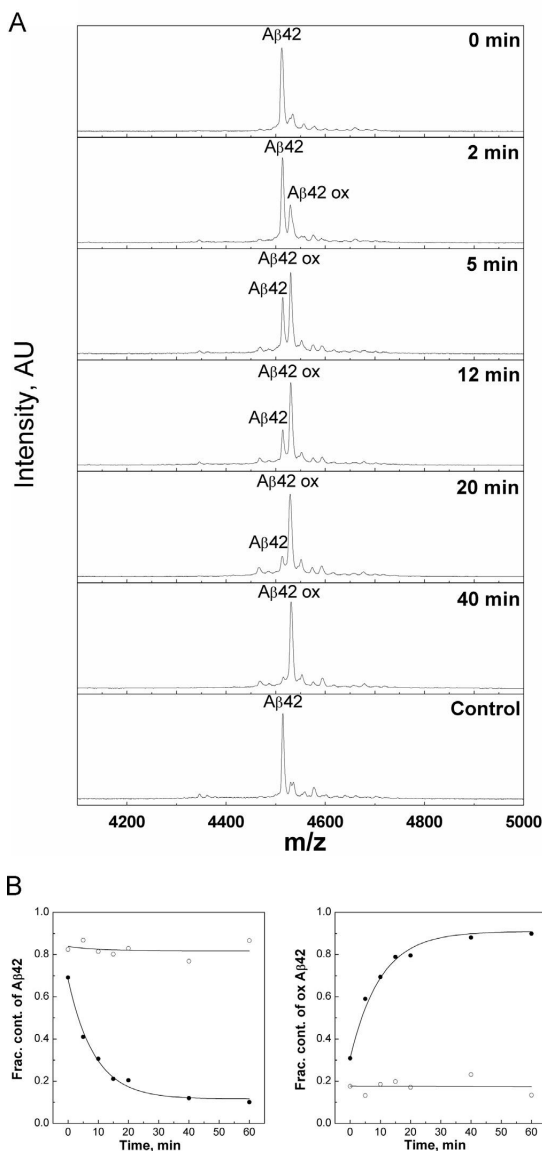


**Fig. 1.** Oxidation of A $\beta$ 42 peptide with H<sub>2</sub>O<sub>2</sub> in the absence of copper ions. (A) MALDI MS spectra of A $\beta$ 42 incubated in 20 mM HEPES at pH 7.3 in the presence of 1% H<sub>2</sub>O<sub>2</sub>. Samples were taken at time intervals shown in the legend; (B) kinetics of oxidation. ● – 1% H<sub>2</sub>O<sub>2</sub>, ○–control;  $k=(0.114 \pm 0.012) \text{ min}^{-1}$ .

### 3. Results

#### 3.1. Oxidation of Met35 by H<sub>2</sub>O<sub>2</sub>

The oxidation of A $\beta$ 42 by H<sub>2</sub>O<sub>2</sub> was studied by MALDI mass spectrometry. Fig. 1 shows that the peptide was easily oxidized in the presence of 200 mM H<sub>2</sub>O<sub>2</sub>. During the incubation with hydrogen peroxide the molecule mass of the peptide increased by 16 units and the process was almost complete within 40 min. The oxidation of Met35 residue was confirmed by ESI MS/MS

sequencing of the resulting oxidized peptide (Supplementary Fig. 1). Kinetic analysis of the MALDI MS data (Fig. 1B) showed that the disappearance of reduced A $\beta$  and the increase of A $\beta$ Met35ox followed the first order kinetics. In the absence of copper ions A $\beta$ Met35ox was the only product of the oxidation: no side products were detected in a significant amount.

The oxidation pattern of A $\beta$  in the presence of copper ions was more complex. As the copper complex of A $\beta$ 42 tends to form a precipitate during 30 min of incubation [25] the oxidation in the presence of copper ions was studied using A $\beta$ 40 peptide. Fig. 2 shows that the addition of a single oxygen atom was still the fastest process; however, the widening of the peptide peak in MS showed that subsequently a large number of non-specific modifications (oxygen additions and elimination) reactions in the A $\beta$  molecule occurred. When Cu(II) ions were added to the reaction mixture after the oxidation of Met35 by H<sub>2</sub>O<sub>2</sub> (Fig. 2B), a similar pattern of nonspecific modifications was observed, suggesting that the single-electron oxidation processes in A $\beta$  does not depend on the oxidation state of Met35. In principle, a peptide dimer can also form by di-tyrosine crosslinking during peptide oxidation. SDS PAGE (Fig. 2C for A $\beta$  40 and Supplementary Fig. 2 for A $\beta$ 42) shows that peptide dimers do not form under our experimental conditions, peaks of dimers and trimers were also not detected by MALDI MS.

#### 3.2. Fibrillization of A $\beta$ Met35ox

The fibrillization of A $\beta$  was studied under the conditions of intensive agitation where the fast fibrillization of the peptide proceeds with good reproducibility [25,26]. Incubation of unpurified oxidized peptide under these conditions did not reveal an increase in ThT fluorescence; however, the peptide peak in the MALDI MS spectrum disappeared showing fibrillation [22] and in a TEM image typical non-matured fibrils were observed. As the oxidizing agent can interfere with the ThT based detection method we repeated the experiments after removing the oxidizing solution by lyophilization and redissolving the peptide in HEPES buffer. Both oxidized peptides, A $\beta$ 42 and A $\beta$ 40, showed a typical sigmoidal fibrillization curve (Fig. 3A and B), whereas the value of the fibrillization rate constant,  $k$ , was threefold lower than that of the regular peptide. The lag-phase for the oxidized peptide was also longer however, the resulting fibrils look similar in TEM (Fig. 3C).

### 4. Discussion

In this work we studied the oxidation of A $\beta$  in the presence of two physiologically relevant redox-active compounds H<sub>2</sub>O<sub>2</sub> and copper ions. Low concentrations of H<sub>2</sub>O<sub>2</sub> are always present in living organisms and take part in various redox processes; copper ions bind to A $\beta$  with high affinity in a catalytically active form and are present in amyloid plaques. The aim of the study was to establish the role of the Met35 residue in the oxidation and peptide aggregation processes. In the absence of copper ions the Met35 residue in A $\beta$  molecule was readily oxidized to sulfoxide (Fig. 1 and Supplementary Fig. 1) and this was almost the only modification observed. Met35 oxidation only slightly inhibited A $\beta$  fibrillization, thus, we suggest that the possible variation in the Met oxidation state should not have a large effect on the plaque formation in vivo. The amyloid fibril formation is a complex auto-catalytic process and the fibrillization in agitated solutions models the fibril growth phase, but not the initiation of the fibrillization process or the formation of the protofibrils and first fibrils.

In the presence of copper ions that form a high affinity complex with A $\beta$ , the oxidation was more complex, the addition of the first oxygen was still the fastest process, however, it was accompanied



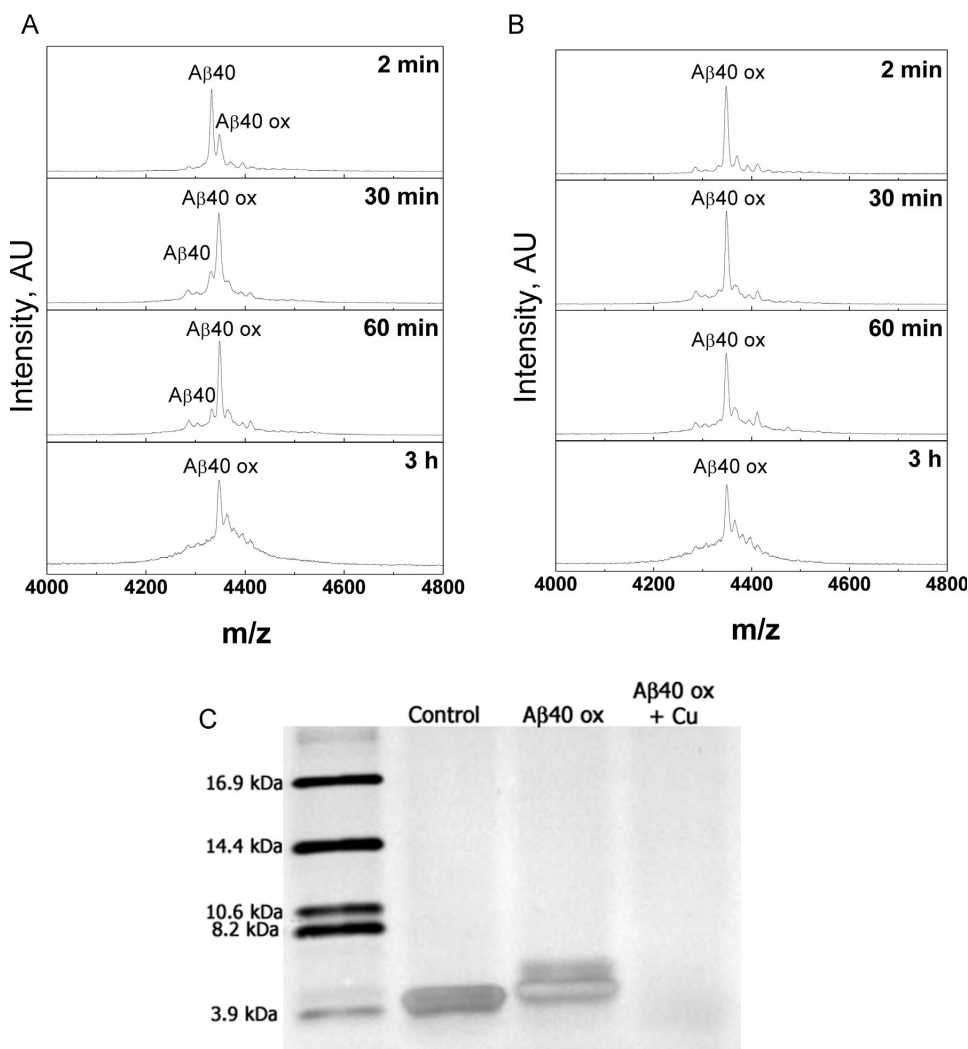


**Fig. 2.** Oxidation of A $\beta$ 40 peptide with H<sub>2</sub>O<sub>2</sub> in the presence of copper ions. MALDI MS spectra of A $\beta$ 42 incubated in the presence of 1% H<sub>2</sub>O<sub>2</sub> at pH 7.3 in 20 mM HEPES. Samples were taken at time intervals shown in the legend; A – native peptide; B – peptide was oxidized with H<sub>2</sub>O<sub>2</sub> for 40 min before adding copper ions. C–SDS Page of A $\beta$ 40: Control, untreated peptide, A $\beta$ ox, oxidized with H<sub>2</sub>O<sub>2</sub> in the absence of copper ions and A $\beta$  ox + Cu refers to oxidized peptide treated with H<sub>2</sub>O<sub>2</sub> in the presence of copper ions for 3 h.

by unspecific modifications of several residues in the peptide. Met35 oxidation had no effect on the oxidative behavior of A $\beta$  complex with copper ions – when Met35 was oxidized in the absence of copper, the addition of copper still lead to the appearance of diverse spectrum of oxidized peptides. These modifications may include the oxidation of His and Phe residues in A $\beta$  and Glu 1 decarboxylation observed in the presence of oxygen and ascorbic acid [27]. Thus, it can be concluded that Met35 residue is not a part of the radical generating mechanism of the A $\beta$ –Cu(II) complex.

The oxidation state of Met35 enhances the toxicity of the artificial truncated A $\beta$ 25–35, which affects mitochondria [28]. However, the high toxicity of this derivative is dependent on the C-terminal position of methionine and does not apply to the longer A $\beta$  variants such as 25–36 [29], thus, this process is not

related to the toxic effect of the full-length A $\beta$  and amyloid plaques. It should also be noted that we did not observed the formation of potentially highly toxic A $\beta$  dimers under our experimental conditions e. g. the oxidative dimerization of A $\beta$  due to tyrosine crosslinking did not occur at considerably higher concentrations of the peptide and H<sub>2</sub>O<sub>2</sub> than those in the brain. However, the oxidative dimerization of A $\beta$  in vivo can be catalyzed by enzymes [30]. It should also be noted that the A $\beta$  “dimers” from biological material have never been analyzed chemically e. g. they are not necessarily dimers, but they can be longer peptides containing the A $\beta$  sequence [31].

Methionine added to the environment also does not serve as a reducing agent for the Cu(II)–A $\beta$  complex [32], thus, it can be concluded that from the viewpoint of redox ability and fibril formation the possible oxidation of Met35 residue is not an

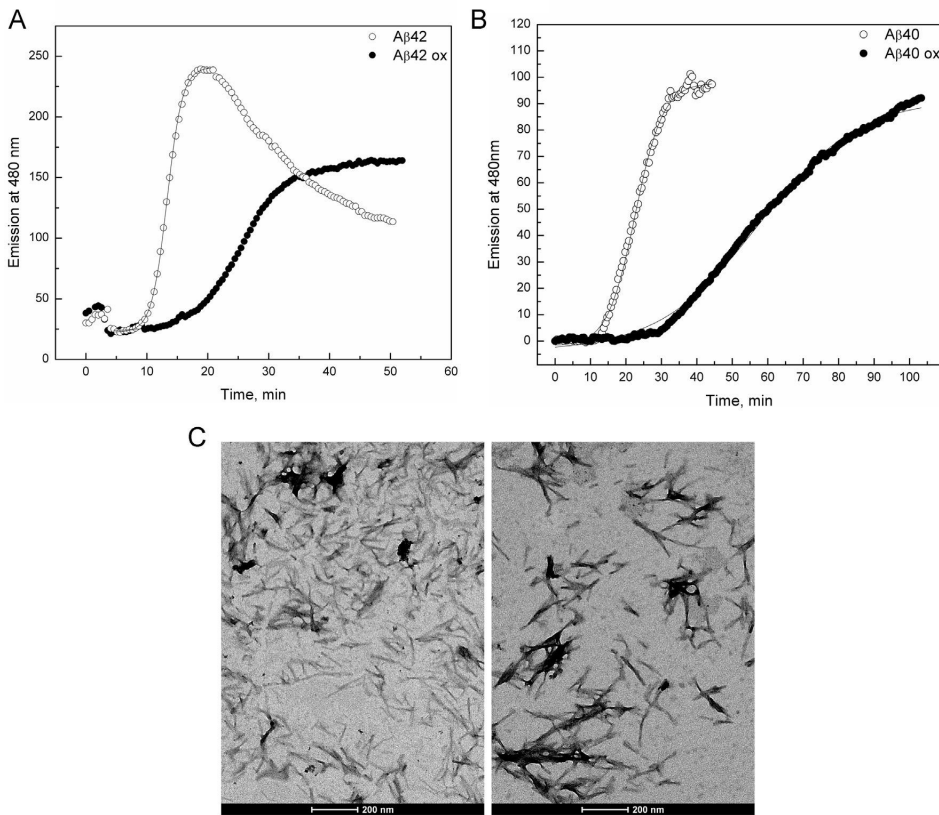


**Fig. 3.** Fibrillization of A $\beta$  peptides with reduced and oxidized Met35 residues at pH 7.3, 20 mM HEPES, 100 mM NaCl, 5  $\mu$ M ThT. A – Fibrillization of A $\beta$ 42: 4  $\mu$ M A $\beta$ 42 37 °C: Curves correspond to  $k=(1.30 \pm 0.02) \text{ min}^{-1}$ ,  $t_{lag}=11.8 \text{ min}^{-1}$  for reduced and  $k=(3.83 \pm 0.05) \text{ min}^{-1}$ ,  $t_{lag}=24.9 \text{ min}^{-1}$  for Met35ox peptide. B–Fibrillization of A $\beta$ 40: 5  $\mu$ M A $\beta$ 40; 50 °C: Curves correspond to  $k=(3.92 \pm 0.09) \text{ min}^{-1}$ ,  $t_{lag}=22.6 \text{ min}^{-1}$  for reduced peptide and  $k=(14.1 \pm 0.3) \text{ min}^{-1}$ ,  $t_{lag}=14.0$  for the oxidized peptide; C–TEM images of A $\beta$ 40 fibrils, left A $\beta$ 40ox; right – A $\beta$ 40 control.

important property of the peptide. However, Met35 can play a role in AD pathogenesis due to putative interactions in the biological systems. It has been shown that in a *Caenorhabditis elegans* model of inclusion body myositis the knockout of MSRA-1 reduces the aggregation of A $\beta$  into insoluble aggregates [33], however in this case the aggregation is intracellular. Even small differences in the peptide aggregation properties may be crucial in triggering the molecular events leading to the disease, however the lower amyloidogenicity and the unaffected ability to catalyze redox reactions when bound to copper ions suggest that Met35 oxidation is most likely not essential in AD. Recently it has been shown that A $\beta$  with oxidized Met 35 that does not cross the neuronal plasma membrane and is not uploaded from the extracellular space has no effect on synaptic plasticity when applied extracellularly [34].

#### Acknowledgments

This work was supported by the Institutional Research Funding IUT (Grant IUT 19-8) of the Estonian Research Council, Estonian Science Foundation Grant nos. 8811, 8385 and 9318.

#### Appendix A. Supplementary material

Supplementary data associated with this article can be found in

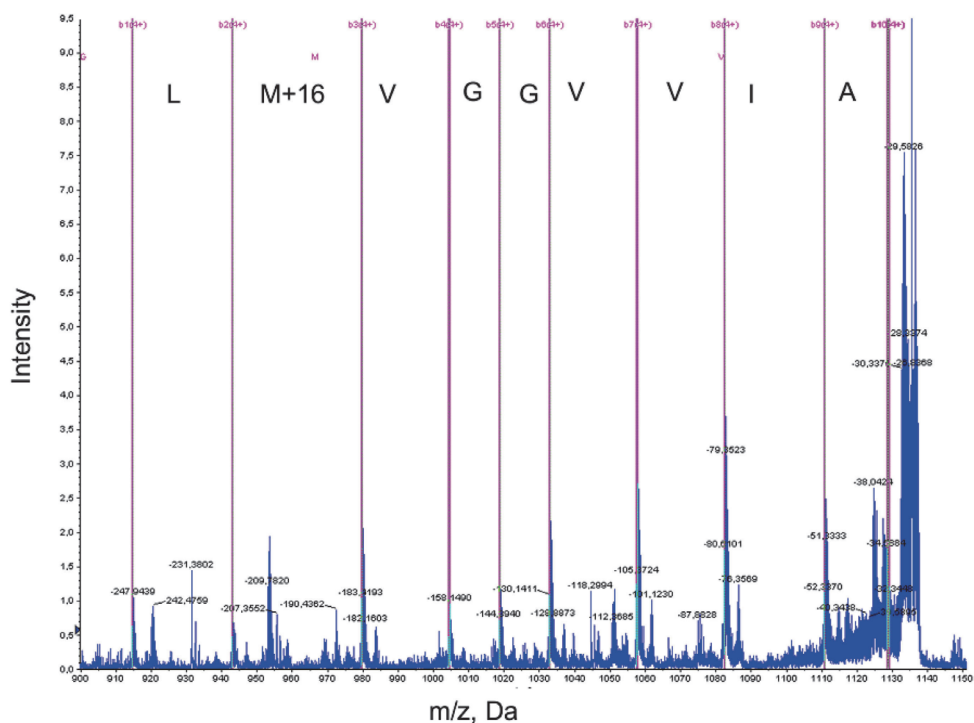
the online version at <http://dx.doi.org/10.1016/j.bbrep.2015.07.017>.

#### References

- [1] A. Nunomura, G. Perry, G. Aliev, K. Hirai, A. Takeda, E.K. Balraj, P.K. Jones, H. Ghanbari, T. Wataya, S. Shimohama, S. Chiba, C.S. Atwood, R.B. Petersen, M. A. Smith, Oxidative damage is the earliest event in Alzheimer disease, *J. Neuropathol. Exp. Neurol.* 60 (2001) 759–767.
- [2] A.M. Swomley, S. Forster, J.T. Keeney, J. Triplett, Z. Zhang, R. Sultana, D. A. Butterfield, Abeta, oxidative stress in Alzheimer disease: evidence based on proteomics studies, *Biochim. Biophys. Acta* 1842 (2014) 1248–1257.
- [3] S. Varadarajan, S. Yatin, M. Aksenova, D.A. Butterfield, Review: Alzheimer's amyloid beta-peptide-associated free radical oxidative stress and neurotoxicity, *J. Struct. Biol.* 130 (2000) 184–208.
- [4] E. Tamagno, M. Guglielmo, D. Monteleone, M. Tabaton, Amyloid- $\beta$  production: major link between oxidative stress and BACE1, *Neurotox. Res.* 22 (2012) 208–219.
- [5] D.A. Butterfield, R. Sultana, Methionine-35 of Abeta(1–42): importance for oxidative stress in Alzheimer disease, *J. Amino Acids* 2011 (2011) 198430.
- [6] K. Hensley, J.M. Carney, M.P. Mattson, M. Aksenova, M. Harris, J.F. Wu, R. A. Floyd, D.A. Butterfield, A model for beta-amyloid aggregation and neurotoxicity based on free radical generation by the peptide: relevance to Alzheimer disease, *Proc. Natl. Acad. Sci. USA* 91 (1994) 3270–3274.
- [7] D.A. Butterfield, J. Kanski, Methionine residue 35 is critical for the oxidative stress and neurotoxic properties of Alzheimer's amyloid beta-peptide 1–42, *Peptides* 23 (2002) 1299–1309.
- [8] J. Naslund, A. Schierhorn, U. Hellman, L. Lannfelt, A.D. Roses, L.O. Tjernberg, J. Silberring, S.E. Gandy, B. Winblad, P. Greengard, et al., Relative abundance of Alzheimer A beta amyloid peptide variants in Alzheimer disease and normal aging, *Proc. Natl. Acad. Sci. USA* 91 (1994) 8378–8382.

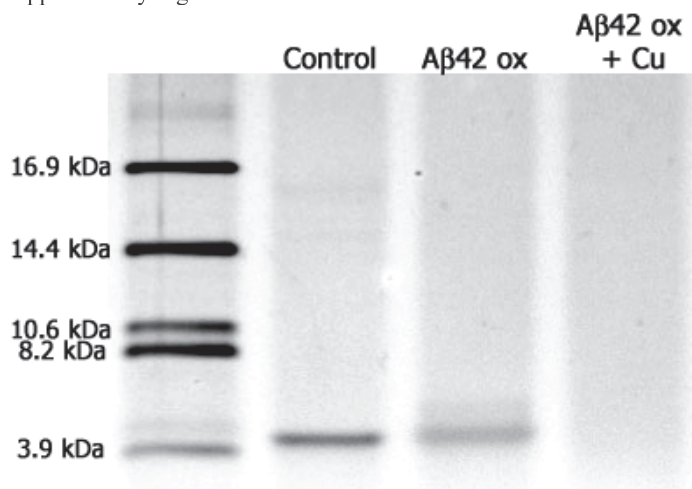
- [9] Y.M. Kuo, T.A. Kokjohn, T.G. Beach, L.I. Sue, D. Brune, J.C. Lopez, W.M. Kalback, D. Abramowski, C. Sturchler-Pierrat, M. Staufenbiel, A.E. Roher, Comparative analysis of amyloid-beta chemical structure and amyloid plaque morphology of transgenic mouse and Alzheimer's disease brains, *J. Biol. Chem.* 276 (2001) 12991–12998.
- [10] D.G. Smith, R. Cappai, K.J. Barnham, The redox chemistry of the Alzheimer's disease amyloid beta peptide, *Biochim. Biophys. Acta* 2007 (1768) 1976–1990.
- [11] A.A. Watson, D.P. Fairlie, D.J. Craik, Solution structure of methionine-oxidized amyloid beta-peptide (1–40). Does oxidation affect conformational switching? *Biochemistry* 37 (1998) 12700–12706.
- [12] L. Hou, I. Kang, R.E. Marchant, M.G. Zagorski, Methionine 35 oxidation reduces fibril assembly of the amyloid abeta-(1–42) peptide of Alzheimer's disease, *J. Biol. Chem.* 277 (2002) 40173–40176.
- [13] C. Ripoli, R. Piacentini, E. Riccardi, L. Leone, D.D. Li Puma, G. Bitan, C. Grassi, Effects of different amyloid beta-protein analogues on synaptic function, *Neurobiol. Aging* 34 (2013) 1032–1044.
- [14] F. Misiti, M.E. Clementi, B. Giardina, Oxidation of methionine 35 reduces toxicity of the amyloid beta-peptide(1–42) in neuroblastoma cells (IMR-32) via enzyme methionine sulfoxide reductase A expression and function, *Neurochem. Int.* 56 (2010) 597–602.
- [15] M.E. Clementi, M. Pezzotti, F. Orsini, B. Sampaolese, D. Mezzogori, C. Grassi, B. Giardina, F. Misiti, Alzheimer's amyloid beta-peptide (1–42) induces cell death in human neuroblastoma via bax/bcl-2 ratio increase: an intriguing role for methionine 35, *Biochem. Biophys. Res. Commun.* 342 (2006) 206–213.
- [16] G.D. Ciccotosto, D. Tew, C.C. Curtain, D. Smith, D. Carrington, C.L. Masters, A. I. Bush, R.A. Cherny, R. Cappai, K.J. Barnham, Enhanced toxicity and cellular binding of a modified amyloid beta peptide with a methionine to valine substitution, *J. Biol. Chem.* 279 (2004) 42528–42534.
- [17] P. Maiti, A. Lomakin, G.B. Benedek, G. Bitan, Despite its role in assembly, methionine 35 is not necessary for amyloid beta-protein toxicity, *J. Neurochem.* 113 (2010) 1252–1262.
- [18] C. Schoneich, D. Pogocki, G.L. Hug, K. Bobrowski, Free radical reactions of methionine in peptides: mechanisms relevant to beta-amyloid oxidation and Alzheimer's disease, *J. Am. Chem. Soc.* 125 (2003) 13700–13713.
- [19] K.P. Kepp, Bioinorganic chemistry of Alzheimer's disease, *Chem. Rev.* 112 (2012) 5193–5239.
- [20] V. Tõugu, A. Tiiman, P. Palumaa, Interactions of Zn(II) and Cu(II) ions with Alzheimer's amyloid-beta peptide. Metal ion binding, contribution to fibrillization and toxicity, *Metallomics* 3 (2011) 250–261.
- [21] W.B. Stine Jr., K.N. Dahlgren, G.A. Krafft, M.J. LaDu, In vitro characterization of conditions for amyloid-beta peptide oligomerization and fibrillogenesis, *J. Biol. Chem.* 278 (2003) 11612–11622.
- [22] K. Zovo, E. Helk, A. Karafin, V. Tõugu, P. Palumaa, Label-free high-throughput screening assay for inhibitors of Alzheimer's amyloid-beta peptide aggregation based on MALDI MS, *Anal. Chem.* 82 (2010) 8558–8565.
- [23] J. Wiltfang, A. Smirnov, B. Schmierstein, G. Kelemen, U. Matthies, H.W. Klafki, M. Staufenbiel, G. Huther, E. Ruther, J. Kornhuber, Improved electrophoretic separation and immunoblotting of beta-amyloid (A beta) peptides 1–40, 1–42, and 1–43, *Electrophoresis* 18 (1997) 527–532.
- [24] J.M. Dunn, Detection of Proteins in Polyacrylamide Gels by Silver Staining, in: J. M. Walker (Ed.), Humana Press, Totowa NJ, 2002, pp. 265–271.
- [25] V. Tõugu, A. Karafin, K. Zovo, R.S. Chung, C. Howells, A.K. West, P. Palumaa, Zn(II)- and Cu(II)-induced non-fibrillar aggregates of amyloid-beta (1–42) peptide are transformed to amyloid fibrils, both spontaneously and under the influence of metal chelators, *J. Neurochem.* 110 (2009) 1784–1795.
- [26] A. Tiiman, A. Noormägi, M. Friedemann, J. Krishtal, P. Palumaa, V. Tõugu, Effect of agitation on the peptide fibrillization: Alzheimer's amyloid-beta peptide 1–42 but not amylin and insulin fibrils can grow under quiescent conditions, *J. Pept. Sci.* 19 (2013) 386–391.
- [27] L.E. Cassagnes, V. Herve, F. Nepveu, C. Hureau, P. Fallier, F. Collin, The catalytically active copper-amyloid-beta state: coordination site responsible for reactive oxygen species production, *Angew. Chem. Int. Ed.* 52 (2013) 11110–11113.
- [28] M.E. Clementi, S. Marini, M. Coletta, F. Orsini, B. Giardina, F. Misiti, Abeta(31–35) and Abeta(25–35) fragments of amyloid beta-protein induce cellular death through apoptotic signals: role of the redox state of methionine-35, *FEBS Lett.* 579 (2005) 2913–2918.
- [29] S. Varadarajan, J. Kanski, M. Aksenoova, C. Lauderback, D.A. Butterfield, Different mechanisms of oxidative stress and neurotoxicity for Alzheimer's A beta (1–42) and A beta(25–35), *J. Am. Chem. Soc.* 123 (2001) 5625–5631.
- [30] L. Galeazzi, P. Ronchi, C. Franceschi, S. Giunta, In vitro peroxidase oxidation induces stable dimers of beta-amyloid (1–42) through dityrosine bridge formation, *Amyloid-Int. J. Exp. Clin. Investig.* 6 (1999) 7–13.
- [31] A.D. Watt, K.A. Perez, A. Rembach, N.A. Sherratt, L.W. Hung, T. Johanssen, C. A. McLean, W.M. Kok, C.A. Hutton, M. Fodero-Tavoletti, C.L. Masters, V. L. Villemagne, K.J. Barnham, Oligomers, fact or artefact? SDS-PAGE induces dimerization of beta-amyloid in human brain samples, *Acta Neuropathol.* (2013).
- [32] G.F. da Silva, V. Lykourinou, A. Angerhofer, L.J. Ming, Methionine does not reduce Cu(II)-beta-amyloid! – rectification of the roles of methionine-35 and reducing agents in metal-centered oxidation chemistry of Cu(II)-beta-amyloid, *Biochim. Biophys. Acta* 1792 (2009) 49–55.
- [33] A.N. Minniti, M.S. Arrazola, M. Bravo-Zehnder, F. Ramos, N.C. Inestrosa, R. Aldunate, The protein oxidation repair enzyme methionine sulfoxide reductase A modulates abeta aggregation and toxicity in vivo, *Antioxid. Redox Signal.* 22 (2014) 48–62.
- [34] C. Ripoli, S. Cocco, D.D. Li Puma, R. Piacentini, A. Mastrodonato, F. Scala, D. Puzzo, M. D'Ascenzo, C. Grassi, Intracellular accumulation of amyloid-beta (Abeta) protein plays a major role in Abeta-induced alterations of glutamatergic synaptic transmission and plasticity, *J. Neurosci.* 34 (2014) 12893–12903.

Supplementary Figure 1



ESI-MS-MS spectrum of oxidized A $\beta$  42. Mass of Met residue is increased by 16 units showing the oxidation of Met35.

Supplementary Figure 2.



SDS Page of A $\beta$ 42: Control, untreated peptide, A $\beta$ ox, oxidized with H<sub>2</sub>O<sub>2</sub> in the absence of copper ions and A $\beta$  ox + Cu refers to oxidized peptide treated with H<sub>2</sub>O<sub>2</sub> in the presence of copper ions for 3 hour.



### **Publication III**

Tõugu, V., **Friedemann, M.**, Tiiman, A., & Palumaa, P. (2014). Copper(II) ions and the Alzheimer's amyloid- $\beta$  peptide: Affinity and stoichiometry of binding. *AIP Conference Proceedings*, 1618(1), 109-111. doi: 10.1063/1.4897689



# Copper(II) Ions and the Alzheimer's Amyloid- $\beta$ Peptide: Affinity and Stoichiometry of Binding

Vello Tõugu<sup>a</sup>, Merlin Friedemann<sup>a</sup>, Ann Tiiman<sup>a,b</sup> and Peep Palumaa<sup>a</sup>

<sup>a</sup>*Department of Gene Technology, Tallinn University of Technology, Akadeemia 15, Tallinn, 12618, Estonia.*

<sup>b</sup>*Department of Biochemistry and Biophysics, Stockholm University, 106 91 Stockholm, Sweden*

**Abstract.** Deposition of amyloid beta (A $\beta$ ) peptides into amyloid plaques is the hallmark of Alzheimer's disease. According to the amyloid cascade hypothesis this deposition is an early event and primary cause of the disease, however, the mechanisms that cause this deposition remain elusive. An increasing amount of evidence shows that the interactions of biometal ions can contribute to the fibrillization and amyloid formation by amyloidogenic peptides. From different anions the copper ions deserve the most attention since it can contribute not only to amyloid formation but also to its toxicity due to the generation of ROS. In this thesis we focus on the affinity and stoichiometry of copper(II) binding to the A $\beta$  molecule.

**Keywords:** Alzheimer's amyloid, copper, fibrillization.

**PACS:** 87.15.nr; 87.15.bk; 87.14.em; 82.30.

## COPPER(II) IN ALZHEIMER'S DISEASE

The accumulation of the A $\beta$  peptides into amyloid plaques is considered as the key step in the pathology of Alzheimer's disease (AD). Copper as well as zinc and iron ions are enriched within these extracellular aggregates consisting mainly of fibrillar forms of A $\beta$  in cross- $\beta$  structure<sup>1</sup>. The electrochemically active copper ions can catalyze a large variety of unspecific redox reactions that substantially contribute to the oxidative stress in the brains of AD patients. Copper ions can also directly contribute to the plaque formation since they can enhance the peptide aggregation and fibril formation *in vitro*<sup>2-4</sup>. Imbalance in cerebral Cu homeostasis plays a role in the pathogenesis of AD and is also important in animal models of AD<sup>5</sup>. The absence of copper ions and the inability to produce ROS may be the main reason for the low toxicity of *in vitro* fibrillar aggregates in multiple experiments that has led to the search for other toxic forms of amyloid peptides and formulation of a large variety of "oligomer" hypothesis for AD<sup>6</sup>. Recent findings have clearly pointed out the strong autocatalytic nature of the initially formed amyloid fibrils and their "prion-like" behavior inside the brain<sup>7-8</sup>, which leaves very little space for the formation of nonfibrillar aggregates in highly toxic amounts: once the first fibrils are formed the process will spread in the brain and lower the concentration of monomeric A $\beta$  in CSF. Zinc and copper ions are regulators of synaptic function in the brain, they are easily exchangeable and weakly coordinated after their release into the synaptic cleft, thus they have the potential to bind to A $\beta$  and cause its aggregation. The identification of various copper-A $\beta$  complexes and the description of their structure and the thermodynamics helps to understand the molecular events leading to sporadic forms of AD and may also provide clues for the development of a potential therapy for AD by the chelation of metal ions.

## COPPER(II)-ABETA COMPLEX FORMATION

The affinity of metal ion binding to A $\beta$  is quantitatively characterized by a dissociation constant. The first conditional (e. g. "buffer independent") dissociation constant value for Cu(II)-A $\beta$  complex equal to 33 nM was estimated from the fluorimetric titration of Y10 and published in 2008<sup>9</sup>. Later on a substantially higher affinity was determined by microcalorimetric methods and the  $K_D$  value has been suggested to be within the range 10 pm to 100 nM<sup>10</sup>. Since then the value has been continuously under dispute. The main concern about the fluorimetric titration is whether the titration curve corresponds to the binding of the first Cu(II) to the A $\beta$  molecule. Prof. Fallner and coworkers<sup>11</sup> have demonstrated that when A $\beta$ 16 is titrated with copper ions the Y10 fluorescence change corresponds to the binding of three copper ions. The fit of experimental data to the titration curves in the case of the



titration of A $\beta$  with Cu(II) usually shows a small systematic deviation from the model (see Fig.1), however, the binding of multiple copper ions is not the only possible cause for these relatively small deviations. A $\beta$  does not have any preformed well defined copper binding sites and the copper binding to this molecule is pleiomorphic, thus, the structure of the complex may vary with the copper concentration and more than one A $\beta$  molecules can coordinate the same copper ion at low copper concentrations. We have titrated A $\beta$ 16 with copper ions under different experimental conditions, hoping that the models expecting the binding of one and three copper ions can be discriminated, since the buffer added or a change in the pH affect the apparent binding affinity. Fig. 1 shows that in all cases the experimental data can still be fitted to the binding curve expecting the binding of one copper ion and a small linear decrease in Y10 fluorescence with increasing copper concentration (Equation 1).

$$I = I_0 + \frac{(I_0 - I_\infty)}{2 \cdot [A]} \times \left( [A] + [Cu^{2+}] + K_D + \sqrt{([A] + [Cu^{2+}] + K_D)^2 - 4 \times [A] \times [Cu^{2+}]} \right) + C \cdot [Cu^{2+}] \quad (1)$$

where [A] and [Cu<sup>2+</sup>] are the total concentrations of the peptide and Cu<sup>2+</sup> ions, K<sub>D</sub> is the dissociation constant of Cu(II)-A $\beta$  complex and I<sub>0</sub>, I and I<sub>∞</sub> are the Y10 fluorescence intensities of the peptide sample in the absence, the presence, and the saturation of Cu<sup>2+</sup> ions.

It should be noted that in the alternative approach suggesting a high affinity binding of multiple copper ions, a quite complicated compensation mechanism between the effects of buffer and pH of the solution on the fluorescence of Y10 and binding affinity has to be postulated.

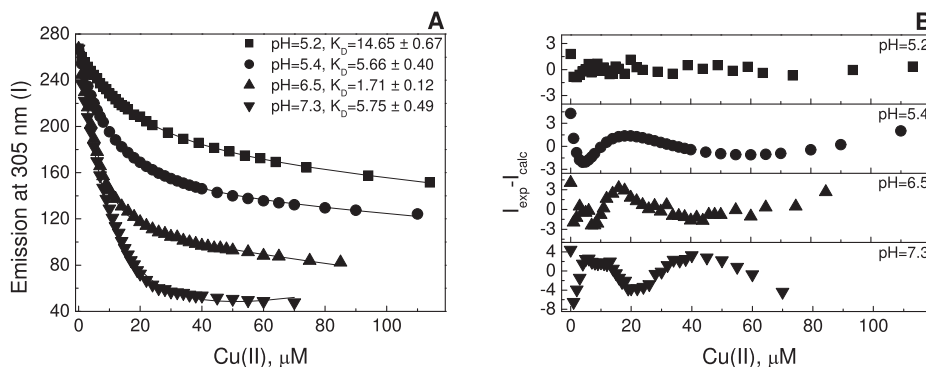


**FIGURE 1.** Titration of A $\beta$ <sub>16</sub> with Cu(II) ions. Changes in Y10 fluorescence with increasing Cu(II) concentration (A). Peptide concentration 8 $\mu$ M, 20 mM Hepes . The data are fitted to Equation 1 and residuals are plotted in panel B.

Thus, it can be concluded that independent experiments are required to demonstrate or rule out the binding of additional copper ions under particular experimental conditions. It has been shown that titration of a fluorescent copper-sensitive dye Phen Green in the presence of A $\beta$  does not show the “high affinity“ copper-binding to the peptide<sup>9</sup>. However, copper bound to A $\beta$  was not directly measured and therefore the possible formation of nonfluorescent ternary complex does not allow to exclude the high affinity binding of Cu(II) to A $\beta$ . Cu(II) induces the aggregation of A $\beta$ 40 and especially A $\beta$ 42 peptides. We have made an attempt to estimate the stoichiometry of Cu(II) binding by A $\beta$  after aggregation. Fig. 2 shows that one equivalent of the peptide can precipitate 2 equivalents of Cu(II), however, in the presence of a small amount of glycine the amount of Cu(II) coprecipitating with A $\beta$  decreases to one. Thus, we can conclude that *in vivo* the peptide cannot bind more than one copper ion, however, we did not get a decisive answer to the question about the binding stoichiometry (and accordingly about the binding affinity) in the solution. As the measurements of A $\beta$  affinity towards copper ions have been always carried out in the presence of weak copper binding ligands that can form ternary complexes with A $\beta$  and Cu(II) which can result in a huge overestimation of the affinity, the correct value of the copper(II) binding affinity of A $\beta$  even in its monomeric form still remains elusive.

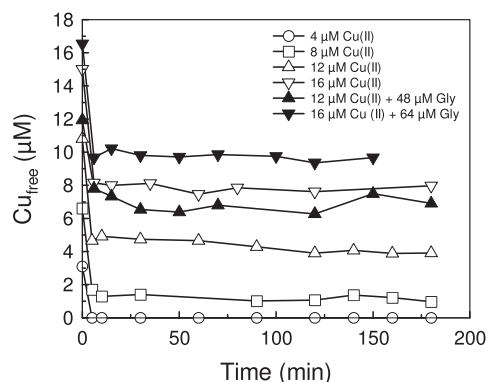


**FIGURE 2.** Stoichiometry of the binding of Cu(II) to A $\beta$ . 4 $\mu$ M of A $\beta$ 40 peptide was mixed with appropriate amounts of copper in 20 mM Hepes pH 7.3 and the concentration of metal ions was determined in the supernatant after 20 min centrifugation at 10 000 rpm was determined spectrophotometrically with Zincon dye.

## ACKNOWLEDGMENTS

This work was supported by the Estonian Ministry of Education and Research (Grant SF0140055s08), Estonian Science Foundation Grants No 8811 to P.P. and 9318 to V.T., and World Federation of Scientists scholarship to A.T and M.F.

## REFERENCES

1. M. A. Lovell; J. D. Robertson; W. J. Teesdale; J. L. Campbell; W. R. Markesbery. *J Neurol Sci*, 158, pp. 47-52 (1998).
2. C. S. Atwood; R. D. Moir; X. Huang; R. C. Scarpa; N. M. Bacarra; D. M. Romano; M. A. Hartshorn; R. E. Tanzi; A. I. Bush. *J.Biol.Chem.*, 273, pp. 12817-12826 (1998).
3. V. Tõugu; A. Karafin; K. Zovo; R. S. Chung; C. Howells; A. K. West; P. Palumaa. *J. Neurochem.*, 110, pp. 1784-1795 (2009).
4. C. J. Sarell; S. R. Wilkinson; J. H. Viles. *J.Biol.Chem.*, 285, pp. 41533-41540 (2010).
5. I. Singh; A. P. Sagare; M. Coma; D. Perlmutter; R. Gelein; R. D. Bell; R. J. Deane; E. Zhong; M. Parisi; J. Ciszewski; R. T. Kasper; R. Deane. *P. Natl. Ac.Sci. USA*, 110, pp. 14771-14776 (2013).
6. A. Tiiman; P. Palumaa; V. Tõugu. *Neurochem. Int.*, 62, pp. 367-378 (2013).
7. J.-X. Lu; W. Qiang; W.-M. Yau; Charles D. Schwieters; Stephen C. Meredith; R. Tycko. *Cell*, 154, pp. 1257-1268 (2013).
8. T. P. J. Knowles; C. A. Waudby; G. L. Devlin; S. I. A. Cohen; A. Aguzzi; M. Vendruscolo; E. M. Terentjev; M. E. Welland; C. M. Dobson. *Science*, 326, pp. 1533-1537 (2009).
9. V. Tougu; A. Karafin; P. Palumaa. *J. Neurochem.*, 104, pp. 1249-1259 (2008).
10. P. Faller; C. Hureau. *Dalton Trans.*, pp. 1080-1094 (2009).
11. B. Alies; E. Renaglia; M. Rozga; W. Bal; P. Faller; C. Hureau. *Anal. Chem.*, 85, pp. 1501-1508 (2013).



#### **Publication IV**

**Friedemann, M.**, Tõugu, V., & Palumaa, P. (2020). Cu(II) partially protects three histidine residues and the N-terminus of amyloid-beta peptide from diethyl pyrocarbonate (DEPC) modification. *FEBS Open Bio*. doi: 10.1002/2211-5463.12857



# Copper(II) partially protects three histidine residues and the N-terminus of amyloid- $\beta$ peptide from diethyl pyrocarbonate (DEPC) modification

Merlin Friedemann , Vello Tõugu  and Peep Palumaa 

Department of Chemistry and Biotechnology, Tallinn University of Technology, Estonia

## Keywords

amyloid-beta peptide; Cu(II) ions; diethyl pyrocarbonate; ESI Q-TOF MS; insulin; MALDI-TOF MS; MS

## Correspondence

M. Friedemann, Department of Chemistry and Biotechnology, Tallinn University of Technology, Akadeemia 15, 12618, Tallinn, Estonia

Tel: (+372) 6204412

E-mail: merlin.friedemann@taltech.ee

(Received 15 October 2019, revised 9 March 2020, accepted 31 March 2020)

doi:10.1002/2211-5463.12857

Diethyl pyrocarbonate (DEPC) has been primarily used as a residue-specific modifying agent to study the role of His residues in peptide/protein and enzyme function; however, its action is not specific, and several other residues can also be modified. In the current study, we monitored the reaction of DEPC with amyloid-beta ( $A\beta$ ) peptides and insulin by matrix-assisted laser desorption/ionization time-of-flight mass spectrometry (MALDI-TOF MS) and determined the modification sites by electrospray ionization quadrupole time-of-flight tandem MS (ESI Q-TOF MS/MS). Our results indicate that five residues in  $A\beta$ 1–42 are modified in the presence of 30-fold molar excess of DEPC. After hydroxylamine treatment (which removes modifications from three His residues), two labels remain bound at the peptide N terminus and Lys16. DEPC treatment of  $A\beta$ 1–42 promotes peptide aggregation, as monitored through the loss of soluble  $A\beta$ 42 in a semi-quantitative MALDI-TOF MS assay. It has been previously proposed that Cu(II) ions protect  $A\beta$ 1–16 from DEPC modification through binding to His6. We confirmed that Cu(II) ions decrease the stoichiometry of  $A\beta$ 1–16 modification with the excess of DEPC being lower as compared to the control, which indicates that Cu(II) protects  $A\beta$  from DEPC modification. Sequencing of obtained Cu(II)-protected  $A\beta$ 1–16 samples showed that Cu(II) does not protect any residues completely, but partially protects all three His residues and the N terminus. Thus, the protection by Cu(II) ions is not related to specific metal binding to a particular residue (e.g. His6), but rather all His residues and the N terminus are involved in binding of Cu(II) ions. These results allow us to elucidate the effect of DEPC modification on amyloidogenicity of human  $A\beta$  and to speculate about the role of His residues in these processes.

Alzheimer disease (AD) is the most common neurodegenerative disease, which is believed to start with the pathological build-up of cerebral extracellular amyloid plaques, comprised of aggregated amyloid- $\beta$  peptides ( $A\beta$ ) [1]. Enormous efforts have been directed

to unravelling the factors initiating the formation of amyloid plaques, which is of crucial importance for understanding the pathological mechanisms of AD and for drug design. According to the accumulated knowledge, the path of protein/peptide self-assembly is

## Abbreviations

AD, Alzheimer's disease;  $A\beta$ , amyloid beta; DEPC, diethyl pyrocarbonate; ESI Q-TOF MS/MS, electrospray ionization quadrupole time-of-flight tandem mass spectrometry; HEPES, 4-(2-hydroxyethyl)-1-piperazineethanesulfonic acid; HFIP, 1,1,1,3,3,3-hexafluoro-2-propanol; MALDI-TOF MS, matrix-assisted laser desorption/ionization time-of-flight mass spectrometry; ThT, thioflavin T;  $\alpha$ -CHCA,  $\alpha$ -cyano-4-hydroxycinnamic acid.

determined by a multitude of factors including the composition and sequence of its amino acid residues, concentration and by environmental conditions and interactions with external ligands such as metal ions. It is firmly established that metal ions such as Zn(II) and Cu(II) interact with A $\beta$  peptides and initiate peptide aggregation mainly into nonfibrillar aggregates [2,3]. These aggregates tend to fibrillize, and according to many authors, such pathway might initiate the formation of amyloid plaques also *in vivo* conditions [3,4].

Structural and metal-binding studies have demonstrated that the metal binding to A $\beta$  peptides is at large extent determined by His residues located in positions 6, 13 and 14 of human A $\beta$  [2-3,5,6]. Replacement of His13 with Arg in rat A $\beta$  peptide is assumed to be responsible for its lower sensitivity towards Zn (II)-induced aggregation as compared with human A $\beta$  [7]. It has also been shown that substoichiometric amounts of Cu(II) accelerate fibrillization [8] through binding to all three His residues, whereas His6 has been identified as a key ligand together with peptide N terminus [9]. Modification of these His residues can inhibit Cu(II)-induced aggregation [10]. In addition, a large body of evidence indicates that binding of Cu(II) ions to A $\beta$  peptides is not characterized by a single coordination mode but occurs through a population of multiple binding modes, which depends on solution pH and the nature of the residues in the N-terminal region. In result, several distinct combinations of all three His residues, terminal Asp, N-terminal amino and other groups can act as co-ligands for Cu(II) [3,11–13].

Chemical modification of amino acid residues is a classical protein chemistry approach for studies of the role of amino acid residues in the functioning of proteins/peptides, whereas several different reagents have been elaborated for all chemically reactive amino acid residues. Standard reagent for modification of His residues in proteins [14–16] is diethyl pyrocarbonate (DEPC), which results in the formation of *N*-ethoxyformylimidazole [6,14,17] (Fig. 1).

It should be noted that DEPC is not absolutely selective to His and can also modify other amino acid residues such as Lys, Tyr, Ser, Thr and also the N terminus at neutral pH [14]. Most of the DEPC modifications (except Lys and N terminus) are reversible and could be removed by nucleophilic agents such as hydroxylamine [18–20]. As a rule, DEPC can modify up to 30% of all amino acid residues in the average protein [21], and because of bulkiness, DEPC can react only with amino acid residues located on the surface of the protein [20]. DEPC has also been used for modification of amyloidogenic peptides [6,17,22,23], which

affects in case of insulin also peptide amyloidogenicity [6]. A $\beta$  has also been modified by DEPC, and it has been demonstrated that Cu(II) binding with the participation of His6 protects A $\beta$  from modification [24]. However, the reaction stoichiometry has not been carefully analysed and it was not considered that DEPC can modify in A $\beta$  at least four residues, involved in the binding of metal ions – three His and N terminus. Moreover, the effect of DEPC modification on amyloidogenicity of A $\beta$  has not been evaluated.

In the current study, we monitored the products of A $\beta$  modification with DEPC in the presence and absence of Cu(II) ions by matrix-assisted laser desorption/ionization time-of-flight mass spectrometry (MALDI-TOF MS), determined the sites of modification by electrospray ionization quadrupole time-of-flight tandem MS (ESI Q-TOF MS/MS) and performed comparative fibrillization studies of modified and native peptide. Obtained results allow to elucidate the effect of DEPC modification on inherent and metal-induced amyloidogenicity of human A $\beta$  and to speculate about the role of His residues in these processes.

## Materials and methods

### Materials

Lyophilized A $\beta$ 1–42 and A $\beta$ 1–16 peptide were purchased from rPeptide (Watkinsville, GA, USA). Bovine insulin, DEPC; 1,1,1,3,3,3-hexafluoro-2-propanol (HFIP); sodium chloride; sodium hydroxide; ammonium hydroxide; sodium phosphate monohydrate; disodium phosphate heptahydrate;  $\alpha$ -cyano-4-hydroxycinnamic acid ( $\alpha$ -CHCA); acetonitrile; trifluoroacetic acid; thioflavin T (ThT); and hydroxylamine hydrochloride (NH<sub>2</sub>OH·HCl) were purchased from Sigma-Aldrich (St. Louis, MO, USA).

### Sample preparation

Lyophilized A $\beta$ 1–42 and A $\beta$ 1–16 were dissolved in HFIP at a concentration of 100  $\mu$ M, divided into aliquots, HFIP was evaporated in vacuum, and the tubes with A $\beta$  film were stored at –80 °C. HFIP treatment is used to disassemble peptide aggregates into monomers.

### Preparation of samples for MALDI-TOF MS

HFIP-treated A $\beta$ 1–42 and A $\beta$ 1–16 aliquots were dissolved in 10 mM NaOH, incubated for 10 min on ice and diluted to the final concentration of 10  $\mu$ M with 50 mM phosphate buffer. DEPC was dissolved in ethanol and aliquoted in the argon-filled glovebox to the required concentrations to avoid hydrolysis of DEPC by the moisture in the air.

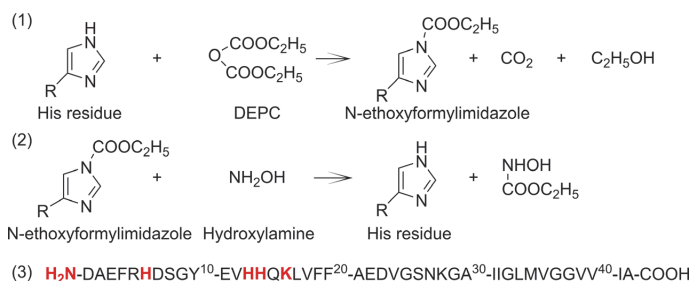


**Fig. 1.** Chemical modification of His side chain with DEPC (1) and its removal by hydroxylamine (2) [27]. The sequence of human A $\beta$ 42 (3).

Aliquots were closed airtight in an argon atmosphere and stored at  $-20^{\circ}\text{C}$ . DEPC was added to the mixed sample (final concentration 20–300  $\mu\text{M}$ ) so that the volume of ethanol did not exceed 5% of total sample volume. Samples were incubated at  $25^{\circ}\text{C}$ , and at distinct time points, 1  $\mu\text{L}$  of the sample was mixed with 3  $\mu\text{L}$  of  $\alpha$ -CHCA matrix (10  $\text{mg}\cdot\text{mL}^{-1}$ ) and analysed with MALDI-TOF MS. In the case of Cu(II) protection experiments, three times molar excess of Cu(II) acetate was added to A $\beta$ 1–16 before the addition of DEPC.

Bovine insulin was weighed out and dissolved in 50 mM phosphate buffer to a final concentration of 10  $\mu\text{M}$ .

To study the effect of hydroxylamine on DEPC modification, hydroxylamine (final concentration 0.5 M) was added to the samples, and at distinct time points (5–30 min), samples were analysed with MALDI-TOF MS.

For semi-quantitative MALDI-TOF MS experiments, 1  $\mu\text{L}$  was taken from the fluorescence spectroscopy samples, previously desalted with 1 mL PD SpinTrap G-25 Column, and mixed with 3  $\mu\text{L}$  of  $\alpha$ -CHCA matrix.

The MALDI-TOF MS matrix  $\alpha$ -CHCA was dissolved in 60% acetonitrile containing 0.3% trifluoroacetic acid concentration 10  $\text{mg}\cdot\text{mL}^{-1}$ . Hydroxylamine stock solution was prepared in ultrapure water at a concentration of 10 M.

### Preparation of samples for fluorescence spectroscopy

A $\beta$ -4242 was dissolved in 10 mM NaOH, incubated 10 min on ice and diluted with 50 mM phosphate buffer, pH 7.4, to a final concentration of 40  $\mu\text{M}$  and total volume of 140  $\mu\text{L}$ . In the case of DEPC modification, DEPC was added (30 times excess), the sample was incubated for 30 s or 60 min, and the reaction was stopped with the addition of 10 mM imidazole. All samples (control, 30-second DEPC-modified and 60-min DEPC-modified A $\beta$ 1–42) were applied to 1 mL PD SpinTrap G-25 Column (GE Healthcare, Chicago, IL, USA) equilibrated with 20 mM 4-(2-hydroxyethyl)-1-piperazineethanesulfonic acid (HEPES) buffer containing 100 mM NaCl, pH 7.3, and spun down for 1 min at 800 *g*. The desalted fraction of A $\beta$ 1–42 (140  $\mu\text{L}$ )

was diluted with 20 mM HEPES buffer containing 100 mM NaCl, pH 7.3, to required volume of 500  $\mu\text{L}$ .

### Preparation of samples for ESI Q-TOF MS/MS sequencing

To locate DEPC modifications in A $\beta$  by ESI Q-TOF MS/MS sequencing, A $\beta$ 1–16 was used. Five different samples were prepared: (a) A $\beta$ 1–16 control, (b) DEPC-modified A $\beta$ 1–16, (c) DEPC-modified and hydroxylamine-treated A $\beta$ 1–16, (d) copper protected DEPC-modified A $\beta$ 1–16 and (e) copper-protected, DEPC-modified and hydroxylamine-treated A $\beta$ 1–16.

DEPC-modified samples were prepared as follows: A $\beta$ 1–16 film was dissolved in 10 mM NaOH, incubated 10 min on ice, diluted with 50 mM phosphate buffer, pH 7.4, to a final concentration of 40  $\mu\text{M}$  and DEPC was added in 30 times molar excess. DEPC modification was carried out for 1 hour, and reaction products were monitored with MALDI-TOF MS. This procedure resulted in A $\beta$ 1–16 modified with DEPC in 4 and 5 positions. This sample was treated with hydroxylamine (final concentration 0.5 M) to remove DEPC modifications from His residues. Hydroxylamine treatment was carried out for 30 min and monitored with MALDI-TOF MS. This resulted in A $\beta$ 1–16 modified by DEPC in 1 and 2 positions.

Cu(II)-protected DEPC-modified A $\beta$ 1–16 was prepared as follows: A $\beta$ 1–16 was dissolved in 10 mM NaOH, incubated 10 min on ice, diluted with 50 mM phosphate buffer, pH 7.4, to a final concentration of 40  $\mu\text{M}$ , 120  $\mu\text{M}$  copper (II)acetate was added and the sample was incubated for 10 min. DEPC modification with 30 times molar excess was then carried out for 1 hour, and the reaction was monitored with MALDI-TOF MS. This procedure resulted in A $\beta$ 1–16 modified with DEPC in 2 and 3 positions. The resulting sample was further treated with hydroxylamine for 30 min and analysed with MALDI-TOF MS.

Before ESI Q-TOF MS/MS experiments, all samples were desalted with 1 mL PD SpinTrap G-25 Column (GE Healthcare), equilibrated with 20 mM ammonium acetate, pH 7.4. Resulting samples were diluted 3 times with 20 mM ammonium acetate, pH 7.4.



## Monitoring of peptide fibrillization by fluorescence spectroscopy

Fibrillization of A $\beta$ 1–42 and DEPC-modified A $\beta$ 1–42 was studied by using fluorescent ligand ThT, which fluorescence intensity at 480 nm (excitation at 440 nm) is increased upon binding to amyloid fibrils. ThT fluorescence was monitored on a Perkin Elmer (Waltham, MA, USA) LS45 fluorescence spectrophotometer in 500- $\mu$ L cuvette by constant stirring at 40 °C. To study the effect of DEPC modification on A $\beta$ 1–42 fibrillization, three samples were compared: desalted A $\beta$ 1–42 control, desalted 30-s DEPC-modified A $\beta$ 1–42 and desalted 1-hour DEPC-modified A $\beta$ 1–42.

## MALDI-TOF MS

The reaction mixtures were analysed by MALDI-TOF MS on Bruker Autoflex and Microflex LT instruments (Bruker Corporation, Billerica, MA, USA). One microliter of the reaction mixture was mixed with 3  $\mu$ L of  $\alpha$ -CHCA matrix, and 1  $\mu$ L of the mixture was pipetted to the MALDI-TOF MS plate and dried in air. In semi-quantitative experiments,  $\alpha$ -CHCA matrix contained 0.3  $\mu$ M bovine insulin as an internal standard. Parameters are as follows:  $m/z$  range from 100 to 10 000 in linear positive mode, 337-nm laser frequency 60 Hz, ions source voltages 10 and 9.1 kV, lens voltage 3 kV and 1000 shots accumulated per spectrum.

## ESI Q-TOF MS/MS

Samples of A $\beta$ 1–16 and DEPC-modified A $\beta$ 1–16 in 20 mM ammonium acetate buffer, pH 7.4, were injected into the electrospray ion source of an Agilent Technology 6540 UHD Accurate-Mass Q-TOF MS instrument by a syringe pump at 7  $\mu$ L $\cdot$ min<sup>-1</sup>. The spectrometer parameters were as follows: drying gas temperature 100 °C, drying gas 4 L $\cdot$ min<sup>-1</sup>, nebulizer 15 psig, skimmer voltage 65 V, capillary voltage 3500 V and fragmentor 400 V (capillary 3228 uA, Okt 1 RF Vpp 750 V). ESI MS spectra were recorded for 10 min in the region of 500–3000  $m/z$ , and fragmentation spectra were recorded in 50–3000  $m/z$  region. The peptides were fragmented with collision energy (CID) of 50 in case of DEPC-modified samples and 45 for the control sample. Obtained fragmentation spectra peaks were analysed by M $\alpha$ SS open-source MS tool [25] using 1% of the largest peaks from ESI Q-TOF MS/MS spectra with fragment matching error tolerance 0.01 Da.

## Results and Discussion

First, the conditions for the modification reaction were optimized, which was necessary for the determination of the maximal stoichiometry of the DEPC reaction and synthesis of peptides with defined modification

pattern for fibrillization studies. In an earlier study, a two-fold excess of DEPC in phosphate buffer at pH 6.8 was used for peptide modification [6]; however, in these conditions, the yield of modification is very low (Fig. S1A). The modification was substantially more efficient at pH 7.4 (See Fig. S1B), and therefore, the latter pH was selected for our studies.

Results presented in Fig. 2 demonstrate that the stoichiometry of DEPC modification depends substantially from the concentration of DEPC – after 1-hour incubation with two times molar excess of DEPC, the main peak in the spectrum still corresponded to the unmodified A $\beta$  (Fig. 2A,B), whereas modification of the peptide at four and five positions was achieved in the presence of 20- to 30-fold molar excess of DEPC (Fig. 2B,C,D). This result indicates that in addition to three His residues, maximums of two additional amino acid residues are modified in A $\beta$ 1–42 by DEPC.

It is known that hydroxylamine removes the carboxy group from all amino acid residues except Lys and peptide N terminus [19]. After hydroxylamine treatment, one and two modifications remained in case of A $\beta$ 1–42 carrying four and five DEPC modifications, respectively (Fig. 2,B,G,H). Most probably these two modifications occur at N-terminal amino group and the amino group of Lys16.

We also observed that treatment of A $\beta$ 1–42 with 20- and 30-fold molar excess of DEPC leads to the decrease in MALDI-TOF MS signal (Fig. 2,B,C,D), which might be caused by peptide aggregation since the fibrils do not show peptide peaks in MALDI-TOF MS under ordinary conditions [26]. A semi-quantitative MALDI-TOF MS experiment by using of 0.3  $\mu$ M insulin as an internal standard demonstrated that indeed, the decrease in signal intensity of DEPC-modified A $\beta$ 1–42 is connected with the decrease in the concentration of soluble A $\beta$ 1–42 (Fig. 3).

Fibrillization potential of A $\beta$  peptides was also studied in agitated conditions by using ThT fluorescence assay. Fibrillization of normal A $\beta$ 1–42 (Fig. 4 black line) was compared to DEPC-modified A $\beta$ 1–42 and incubated for 30 s (Fig. 4 green line) and 60 min (Fig. 4 blue line) with 30 $\times$  excess of DEPC. A $\beta$ 1–42 modified with DEPC for 30 s, which represents partially modified A $\beta$ 1–42, showed similar lag time but a two-fold slower elongation rate compared with the control sample. A $\beta$ 1–42 modified with DEPC for 60 min, representing fully modified A $\beta$ 1–42, exposes an initial increased fluorescence and even slower elongation rate. The initial fluorescence is indicative for the presence of fibrils in the sample and decreased fibrillization rate shows that higher modification level decreases the fibrillization rate under agitated

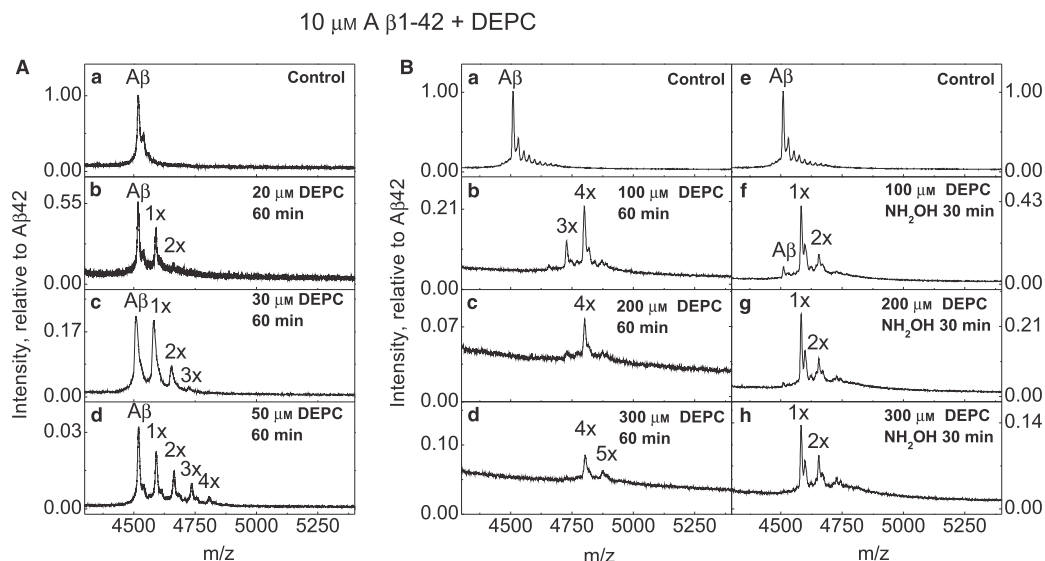


**Fig. 2.** MALDI-TOF MS spectra of A $\beta$ 1-42 modified by increasing concentrations of DEPC in phosphate buffer at pH 7.4: molar excess of two times (2 $\times$ ) (A, b), 3 $\times$  (A, c), 5 $\times$  (A, d), 10 $\times$  (B, b), 20 $\times$  (B, c) and 30 $\times$  (B, d) and hydroxylamine treatment of 10 $\times$ , 20 $\times$  and 30 $\times$  DEPC samples, respectively (B, f, g, h). Annotations 1-5 $\times$  denote the number of DEPC modifications bound to A $\beta$ . Intensity is relative to A $\beta$ 42 in the control sample.

conditions. Results indicate that DEPC modification decreases the fibrillization rate of A $\beta$ 1-42 in agitated conditions; however, it promotes peptide aggregation.

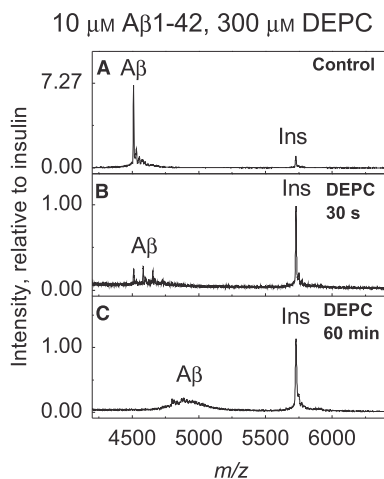


**Fig. 3.** Semi-quantitative MALDI-TOF MS assay for peptide aggregation. Desalted A $\beta$ 1-42 as control (A), desalted A $\beta$ 1-42 modified with 30 $\times$  DEPC for 30 s (B) and desalted A $\beta$ 1-42 modified with 30 $\times$  DEPC for 60 min (C). Intensity is relative to insulin in the control sample.

DEPC modification of insulin was faster as compared to A $\beta$ 1-42: in case of 10-fold molar excess of DEPC (Fig. 5B), the insulin modification was completed in 30 min and in case of 20- and 30-fold molar excess of DEPC (Fig. 5C,D), it was completed in 10 min. The main peak in all experiments was insulin modified with four DEPC molecules, and after hydroxylamine treatment, two modifications remained (Fig. 5F-H).

### Sequencing of DEPC-modified A $\beta$ with ESI Q-TOF MS/MS

In order to locate the DEPC modification sites in A $\beta$  peptide, shorter peptide A $\beta$ 1-16 was studied because of its better solubility and a lower tendency for aggregation. 10-fold (Fig. 6A), 20-fold (Fig. 6B) and 30-fold (Fig. 6C) molar excess of DEPC was studied by MALDI-TOF MS, showing the maximum level of modification to be reached in case of 30-fold molar excess of DEPC. We used ESI Q-TOF MS/MS and sequenced A $\beta$ 1-16 control (Fig. S2), the major A $\beta$ 1-16 form modified with four DEPC molecules and a minor form modified with five DEPC molecules (Fig. 6C,B). We also sequenced the A $\beta$ 1-16 with a single modification obtained from the major form after hydroxylamine treatment (Fig. 6C,C). Sequencing results obtained by

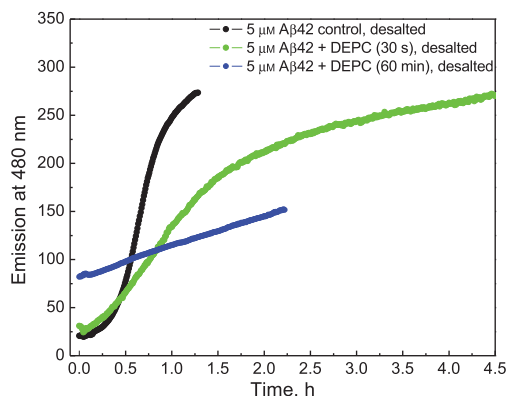


**Fig. 4.** The fibrillization of DEPC-modified A $\beta$ 1–42 in agitated conditions. Desalted A $\beta$ 1–42 control (black line), and A $\beta$ 1–42 incubated for 30 s (green line) and 60 min (blue line) with 30 $\times$  excess of DEPC. Conditions: 20 mM ammonium acetate, pH 7.4, temperature 40  $^{\circ}$ C, constant stirring.

MMAS indicate that in A $\beta$ 1–16 form carrying five DEPC modifications, three His residues, Lys16 and N terminus were modified (Fig. S5). In A $\beta$ 1–16 with four modifications, only two His residues (His6 and His14), N terminus and Lys were modified (Fig. S4). Sequencing of A $\beta$ 1–16 sample carrying one modification after hydroxylamine treatment indicated that only the N terminus was modified (Fig. S3) compared with A $\beta$ 1–16 control (Fig. S2). This result indicates that the N terminus of A $\beta$ 1–16 is modified faster than Lys16.

Our results showed that Cu(II) ions decrease the stoichiometry of A $\beta$ 1–16 modification with an excess of DEPC (Fig. 6,D,A,B) in average by two units, showing that Cu(II) protects A $\beta$  residue(s) from DEPC modification. Sequencing of obtained A $\beta$ 1–16 samples containing two and three modifications showed that there is a mixture of A $\beta$ 1–16 species with a different distribution of DEPC modifications, which indicates that Cu(II) does not protect any residues completely but it protected partially all three His residues and N terminus (Figs S6 and S7). Thus, the protection by Cu(II) ions indicates that all His residues, as well as N terminus of A $\beta$ 1–16, are involved in binding of Cu(II) ions. This is expected as Cu(II) ions prefer coordination with 4–6 groups, and moreover, A $\beta$  peptides do apparently not contain a specific binding site for metal ions like it exists in enzymes, but is assumingly binding Cu(II) ions into multiple coordination environments, which are energetically similar and in equilibrium [3,11–13]. In earlier work, the Cu(II) protection on DEPC modification of A $\beta$ 1–16 peptide was assumed to occur with the participation of His6 only [24]. However, in that work, only the peptide derivative with a single DEPC modification (mainly at His6) was used in Cu(II) protection experiment. Sequencing of corresponding peptides showed that His6 is protected by Cu(II); however, these data cannot show the protection of His13, His14 and N terminus since these residues were not modified in the absence of Cu(II) ions. Thus, our experiments with high-level DEPC-modified samples indicate that the protection by Cu(II) ions is

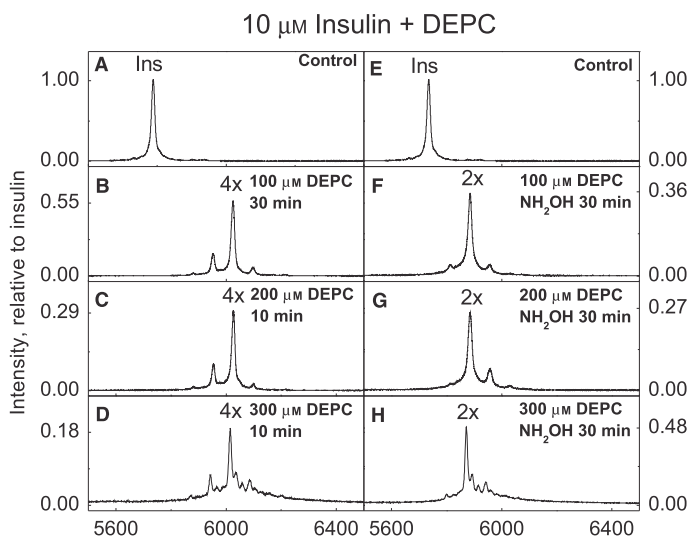


**Fig. 5.** MALDI-TOF MS spectra of bovine insulin modified with DEPC in phosphate buffer at pH 7.4: DEPC excess of 10 $\times$  (B), 20 $\times$  (C) and 30 $\times$  (D) and hydroxylamine treatment of 10 $\times$ , 20 $\times$  and 30 $\times$  DEPC-modified insulin samples, respectively (F, G, H), compared with insulin control (A, E). Annotations 1–5 $\times$  denote the number of DEPC modifications added to insulin. Intensity is relative to insulin in the control sample.

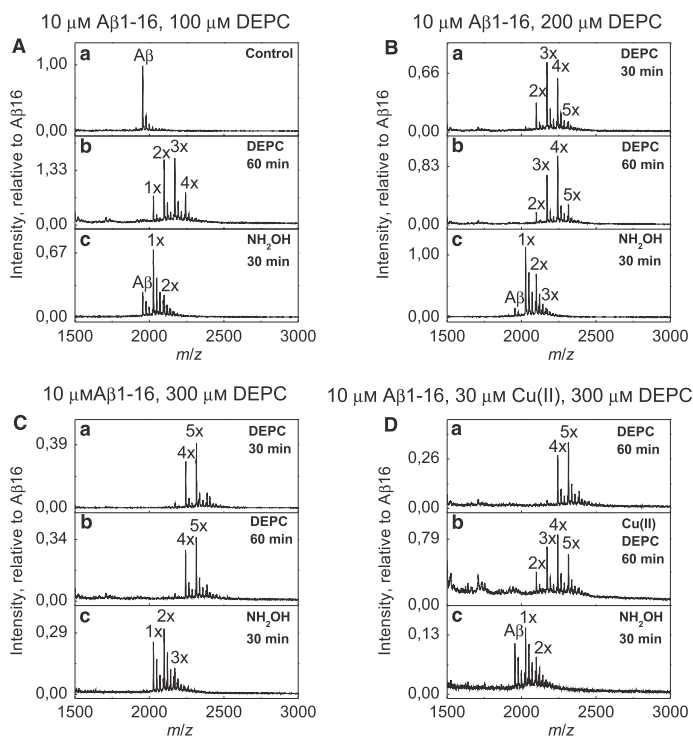


**Fig. 6.** MALDI-TOF MS spectra of A $\beta$ 1-16 DEPC modification in phosphate buffer pH 7.4 with different DEPC concentrations: excess of 10 $\times$  (A), 20 $\times$  (B) and 30 $\times$  (C) and Cu(II) protection of 30 $\times$  DEPC (D). Annotations 1–5 $\times$  denote the number of DEPC modifications added to A $\beta$ . Intensity is relative to A $\beta$ 16 in the control sample.

not connected with the involvement of only His6, but all His residues and N terminus are involved.

ESI Q-TOF MS/MS sequencing data in Figs S3 and S8 show that after hydroxylamine treatment of DEPC-modified A $\beta$ 1-16, only N terminus remained modified, whereas in the presence of Cu(II) a mixture of N terminus and Lys16-modified A $\beta$ 1-16 was detected.

## Conclusions

MALDI-TOF MS results show that A $\beta$ 1-42 could be modified with maximum five DEPC molecules, and our ESI Q-TOF MS/MS sequencing identified that three His residues, Lys16 and N terminus of A $\beta$  are modified. A $\beta$ 1-42 with four DEPC modifications had only two His residues (His6 and His14) modified in addition to Lys16 and N terminus. Hydroxylamine treatment removed only modifications from His residues.

DEPC treatment of A $\beta$ 1-42 promotes peptide aggregation monitored through the loss of soluble A $\beta$ 1-42 in a semi-quantitative MALDI-TOF MS assay; however, according to ThT assay, the DEPC modification decreased the rate of A $\beta$ 1-42 fibrillization.

Cu(II) ions decrease the stoichiometry of A $\beta$ 1-16 modification with an excess of DEPC by average 2 units, confirming that Cu(II) protects A $\beta$  from DEPC modification. Sequencing of Cu(II)-protected A $\beta$ 1-16 revealed that all three His residues and the N terminus of A $\beta$ 1-16 were partially protected, which indicates their involvement in the binding of Cu(II) ions.

## Acknowledgements

This work was supported by the Estonian Research Council grant IUT 19-8 to PP. We thank Ksenia Kozlova (Borissenkova) for participation in an early phase of this project and Julia Smirnova for the assistance during ESI Q-TOF MS/MS system operations.

## Conflict of interest

The authors declare no conflict of interest.

## Author contributions

VT and PP conceived and designed the project; MF acquired the data; MF, VT and PP analysed and interpreted the data; and MF, VT and PP wrote the paper.

## References

- Masters CL, Simms G, Weinman NA, Multhaup G, McDonald BL and Beyreuther K (1985) Amyloid plaque core protein in Alzheimer disease and Down syndrome. *Proc Natl Acad Sci USA* **82**, 4245–4249.
- Faller P, Hureau C and Berthoumieu O (2013) Role of metal ions in the self-assembly of the Alzheimer's amyloid-beta peptide. *Inorg Chem* **52**, 12193–12206.
- Tiiman A, Palumaa P and Tougu V (2013) The missing link in the amyloid cascade of Alzheimer's disease - metal ions. *Neurochem Int* **62**, 367–378.
- Irie K, Murakami K, Masuda Y, Morimoto A, Ohigashi H, Ohashi R, Takegoshi K, Nagao M, Shimizu T and Shirasawa T (2005) Structure of beta-amyloid fibrils and its relevance to their neurotoxicity: implications for the pathogenesis of Alzheimer's disease. *J Biosci Bioeng* **99**, 437–447.
- Tiiman A, Krishtal J, Palumaa P and Tõugu V (2015) *In vitro* fibrillization of Alzheimer's amyloid- $\beta$  peptide (1–42). *AIP Adv* **5**, 092401.
- Yang X, Li Y, Huang L, Zhang X, Cheng C, Gong H, Ma L and Huang K (2015) Diethylpyrocarbonate modification reveals HisB5 as an important modulator of insulin amyloid formation. *J Biochem* **157**, 45–51.
- Liu ST, Howlett G and Barrow CJ (1999) Histidine-13 is a crucial residue in the zinc ion-induced aggregation of the A beta peptide of Alzheimer's disease. *Biochemistry* **38**, 9373–9378.
- Sarell CJ, Wilkinson SR and Viles JH (2010) Substoichiometric levels of Cu<sup>2+</sup> ions accelerate the kinetics of fiber formation and promote cell toxicity of amyloid- $\beta$  from Alzheimer disease. *J Biol Chem* **285**, 41533–41540.
- Young TR, Kirchner A, Wedd AG and Xiao Z (2014) An integrated study of the affinities of the Abeta16 peptide for Cu(I) and Cu(II): implications for the catalytic production of reactive oxygen species. *Metallomics* **6**, 505–517.
- Leshem G, Richman M, Lisniansky E, Antman-Passig M, Habashi M, Gräslund A, Wärländer SKTS and Rahimpour S (2019) Photoactive chlorin e6 is a multifunctional modulator of amyloid-beta aggregation and toxicity via specific interactions with its histidine residues. *Chem Sci* **10**, 208–217.
- Cheignon C, Tomas M, Bonnefont-Rousselot D, Faller P, Hureau C and Collin F (2018) Oxidative stress and the amyloid beta peptide in Alzheimer's disease. *Redox Biol* **14**, 450–464.
- Stefaniak E and Bal W (2019) Cu(II) Binding properties of N-truncated Abeta peptides. Search of biological function. *Inorg Chem* **58**, 13561–13577.
- Yako N, Young TR, Cottam Jones JM, Hutton CA, Wedd AG and Xiao Z (2017) Copper binding and redox chemistry of the Abeta16 peptide and its variants: insights into determinants of copper-dependent reactivity. *Metallomics* **9**, 278–291.
- Hnizda A, Santrúček J, Sanda M, Strohal M and Kodíček M (2008) Reactivity of histidine and lysine side-chains with diethylpyrocarbonate – a method to identify surface exposed residues in proteins. *J Biochem Biophys Methods* **70**, 1091–1097.
- Kalkum M, Przybylski M and Glocker MO (1998) Structure characterization of functional histidine residues and carbethoxylated derivatives in peptides and proteins by mass spectrometry. *Bioconjug Chem* **9**, 226–235.
- Karmakar S and Das KP (2012) Identification of histidine residues involved in Zn(2+) binding to alphaA- and alphaB-crystallin by chemical modification and MALDI TOF mass spectrometry. *Protein J* **31**, 623–640.
- Zhang X, Liu J, Huang L, Yang X, Petersen RB, Sun Y, Gong H, Zheng L and Huang K (2016) How the imidazole ring modulates amyloid formation of islet amyloid polypeptide: a chemical modification study. *Biochim Biophys Acta* **1860**, 719–726.
- Evrard C, Fastrez J and Soumillion P (1999) Histidine modification and mutagenesis point to the involvement of a large conformational change in the mechanism of action of phage lambda lysozyme. *FEBS Lett* **460**, 442–446.
- Mendoza VL and Vachet RW (2009) Probing protein structure by amino acid-specific covalent labeling and mass spectrometry. *Mass Spectrom Rev* **28**, 785–815.
- Zhou Y and Vachet RW (2012) Increased protein structural resolution from diethylpyrocarbonate-based covalent labeling and mass spectrometric detection. *J Am Soc Mass Spectrom* **23**, 708–717.
- Mendoza VL and Vachet RW (2008) Protein surface mapping using diethylpyrocarbonate with mass spectrometric detection. *Anal Chem* **80**, 2895–2904.
- Arndt JR, Arndt JR, Kondalaji SG, Maurer MM, Parker A, Legleiter J and Valentine SJ (2015) Huntingtin N-terminal monomeric and multimeric structures destabilized by covalent modification of heteroatomic residues. *Biochemistry* **54**, 4285–4296.
- Qin K, Yang Y, Mastrangelo P and Westaway D (2002) Mapping Cu(II) binding sites in prion proteins by diethyl pyrocarbonate modification and matrix-assisted laser desorption/ionization-time of flight (MALDI-TOF) mass spectrometric footprinting. *J Biol Chem* **277**, 1981–1990.
- Ginotra YP, Ramteke SN, Srikanth R and Kulkarni PP (2012) Mass spectral studies reveal the structure of Abeta1-16-Cu<sup>2+</sup> complex resembling ATCUN motif. *Inorg Chem* **51**, 7960–7962.
- Strohal M, Kavan D, Novák P, Volný M and Havlíček V (2010) mMass 3: a cross-platform software environment for precise analysis of mass spectrometric data. *Anal Chem* **82**, 4648–4651.



- 26 Zovo K, Helk E, Karafin A, Töugu V and Palumaa P (2010) Label-free high-throughput screening assay for inhibitors of Alzheimer's amyloid-beta peptide aggregation based on MALDI MS. *Anal Chem* **82**, 8558–8565.
- 27 Fang J, Zhang B and Asai H (2003) Chemical modification of contractile 3-nm-diameter filaments in *Vorticella spasmoneme* by diethyl-pyrocabonate and its reversible renaturation by hydroxylamine. *Biochem Biophys Res Commun* **310**, 1067–1072.

## Supporting information

Additional supporting information may be found online in the Supporting Information section at the end of the article.

Since the MALDI-TOF MS analysis of the products of DEPC modification of insulin under the conditions reported in an earlier study (2-fold molar excess of DEPC, phosphate buffer pH 6.8) the reaction (Fig. S1A) showed that only a small amount of the peptide was modified by 1–3 DEPC molecules. Increasing the pH value from 6.8 to 7.4 increased the modification level substantially (Fig. S1B).

**Fig. S1.** MALDI-TOF MS spectra of bovine insulin modified with a two-times molar excess of DEPC in phosphate buffer at pH 6.8 (A) and pH 7.4 (B). Annotations 1–4 $\times$  denote the number of DEPC modifications added to insulin. Intensity is relative to insulin in the control sample.

**Fig. S2.** Sequencing of A $\beta$ 1–16 control. Above is a spectrum of identified fragments from M<sub>MASS</sub> and below is the table of M<sub>MASS</sub> results from ESI Q-TOF MS/MS spectrum where pink cells are false-positive results indicated by M<sub>MASS</sub> as DEPC modifications in A $\beta$ 1–16 control sample, grey cells are results found by M<sub>MASS</sub> software for A $\beta$ 1–16 control. '0 DEPC' row indicates peptide fragments without modifications and '1–5 DEPC' indicates the number of modifications found by M<sub>MASS</sub> software. The sample was in 20 mM ammonium acetate, pH 7.4; collision energy 45; auto sequencing.

**Fig. S3.** Targeted sequencing of A $\beta$ 1–16 modified with one DEPC molecule after hydroxylamine treatment. Above is a spectrum of identified fragments from M<sub>MASS</sub> and below is the table of M<sub>MASS</sub> results from ESI Q-TOF MS/MS spectrum where pink cells are false-positive results indicated by M<sub>MASS</sub> as DEPC modifications in A $\beta$ 1–16 control sample, grey cells are results found by M<sub>MASS</sub> software for A $\beta$ 1–16 modified with 1 DEPC molecule. '0 DEPC' row indicates peptide fragments without modifications and '1–5 DEPC'

indicates the number of modifications found by M<sub>MASS</sub> software. The sample was in 20 mM ammonium acetate, pH 7.4; precursor was peak 1014 *m/z* (once DEPC-modified A $\beta$ 1–16 with charge 2+), collision energy 50.

**Fig. S4.** Targeted sequencing data from the peak of A $\beta$ 1–16 modified with 4 DEPC molecules. Above are spectra of identified fragments from M<sub>MASS</sub> and below are tables of M<sub>MASS</sub> results from ESI Q-TOF MS/MS spectrum where pink cells are false-positive results indicated by M<sub>MASS</sub> as DEPC modifications in A $\beta$ 1–16 control sample, grey cells are results found by M<sub>MASS</sub> software for A $\beta$ 1–16 modified with four DEPC molecules. '0 DEPC' row indicates peptide fragments without modifications and '1–5 DEPC' indicates the number of modifications found by M<sub>MASS</sub> software. Samples were in 20 mM ammonium acetate, pH 7.4; precursor was peak 1122.5 *m/z* (four times DEPC-modified A $\beta$ 1–16 with charge 2+), collision energy 50.

**Fig. S5.** Targeted sequencing data from the peak of A $\beta$ 1–16 modified with 5 DEPC molecules. Above are spectra of identified fragments from M<sub>MASS</sub> and below are tables of M<sub>MASS</sub> results from ESI Q-TOF MS/MS spectrum where pink cells are false-positive results indicated by M<sub>MASS</sub> as DEPC modifications in A $\beta$ 1–16 control sample, grey cells are results found by M<sub>MASS</sub> software for A $\beta$ 1–16 modified with five DEPC molecules. '0 DEPC' row indicates peptide fragments without modifications and '1–5 DEPC' indicates the number of modifications found by M<sub>MASS</sub> software. Samples were in 20 mM ammonium acetate, pH 7.4; precursor was peak 1158.5 *m/z* (five times DEPC-modified A $\beta$ 1–16 with charge 2+), collision energy 50.

**Fig. S6.** Targeted sequencing data from the peak of copper protected A $\beta$ 1–16 modified with two DEPC molecules. Above are spectra of identified fragments from M<sub>MASS</sub> and below are tables of M<sub>MASS</sub> results from ESI Q-TOF MS/MS spectrum, where pink cells are false-positive results indicated by M<sub>MASS</sub> as DEPC modifications in A $\beta$ 1–16 control sample combined with results indicating higher modification level than the precursor. Grey cells are results found by M<sub>MASS</sub> software for copper protected A $\beta$ 1–16 modified with two DEPC molecules. '0 DEPC' row indicates peptide fragments without modifications and '1–5 DEPC' indicates the number of modifications found by M<sub>MASS</sub> software. Samples were in 20 mM ammonium acetate, pH 7.4; precursor was peak 1050.5 *m/z* (two times DEPC-modified A $\beta$ 1–16 with charge 2+), collision energy 50.

**Fig. S7.** Targeted sequencing data from the peak of copper protected A $\beta$ 1–16 modified with three DEPC

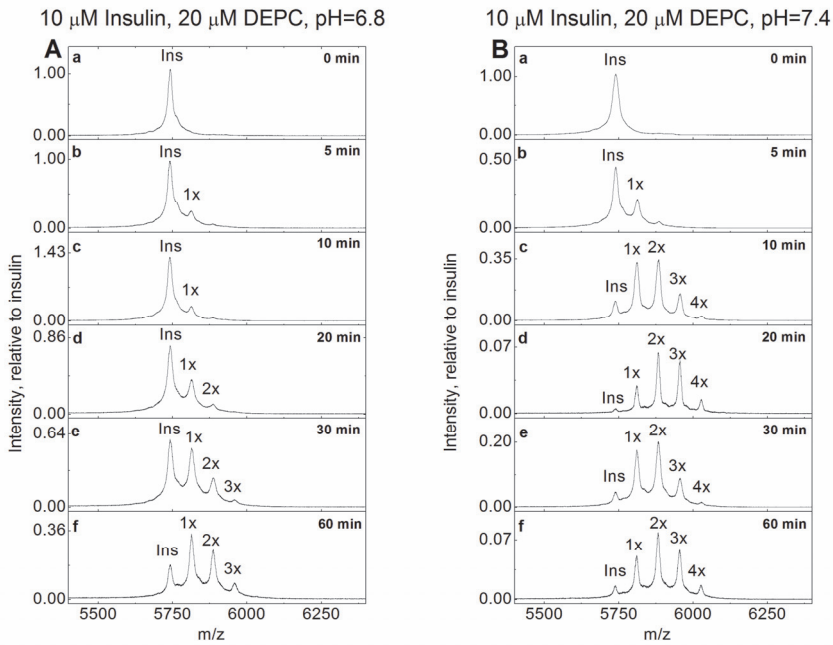
molecules. Above are spectra of identified fragments from *MMASS* and below are tables of *MMASS* results from ESI Q-TOF MS/MS spectrum, where pink cells are false-positive results indicated by *MMASS* as DEPC modifications in A $\beta$ 1–16 control sample combined with results indicating higher modification level than the precursor. Grey cells are results found by *MMASS* software for copper protected A $\beta$ 1–16 modified with three DEPC molecules. '0 DEPC' row indicates peptide fragments without modifications and '1–5 DEPC' indicates the number of modifications found by *MMASS* software. Samples were in 20 mM ammonium acetate, pH 7.4; precursor was peak 1086.5 *m/z* (three times DEPC-modified A $\beta$ 1–16 with charge 2+), collision energy 50.

**Fig. S8.** Targeted sequencing data from the peak of copper protected A $\beta$ 1–16 modified with 1 DEPC

molecules after hydroxylamine treatment. Above is a spectrum of identified fragments from *MMASS* and below is the table of *MMASS* results from ESI Q-TOF MS/MS spectrum, where pink cells are false-positive results indicated by *MMASS* as DEPC modifications in A $\beta$ 1–16 control sample combined with results indicating higher modification level than the precursor. Grey cells are results found by *MMASS* software for copper protected A $\beta$ 1–16 modified with 1 DEPC molecule. '0 DEPC' row indicates peptide fragments without modifications and '1–5 DEPC' indicates the number of modifications found by *MMASS* software. The sample was in 20 mM ammonium acetate, pH 7.4; precursor was peak 1014 *m/z* (one-time DEPC-modified A $\beta$ 1–16 with charge 2+), collision energy 50.

## Supplementary figures

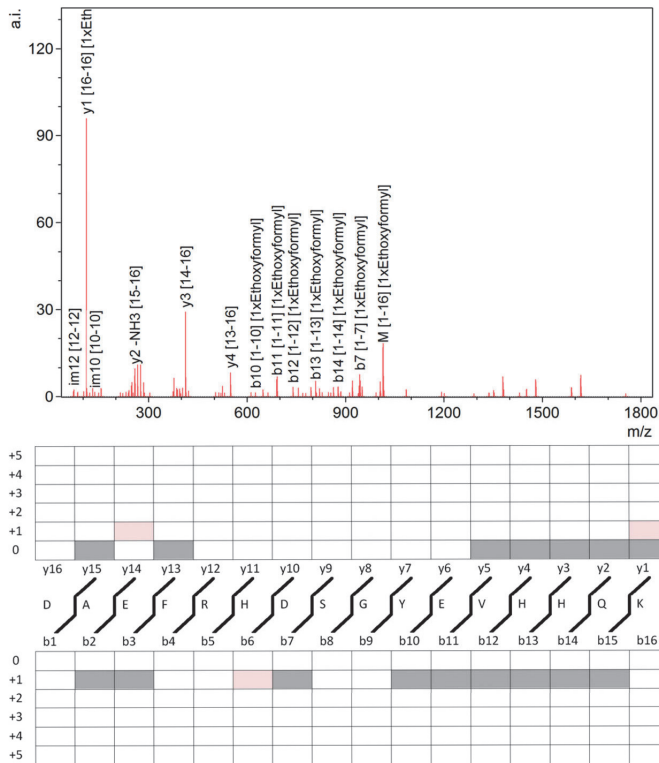
Since the MALDI-TOF MS analysis of the products of DEPC-modification of insulin under the conditions reported in an earlier study (2 fold molar excess of DEPC, phosphate buffer pH 6.8) the reaction (Suppl. Figure 1, A) showed that only a small amount of the peptide was modified by 1-3 DEPC molecules. Increasing the pH value from 6.8 to 7.4 increased the modification level substantially (Suppl. Figure 1, B).



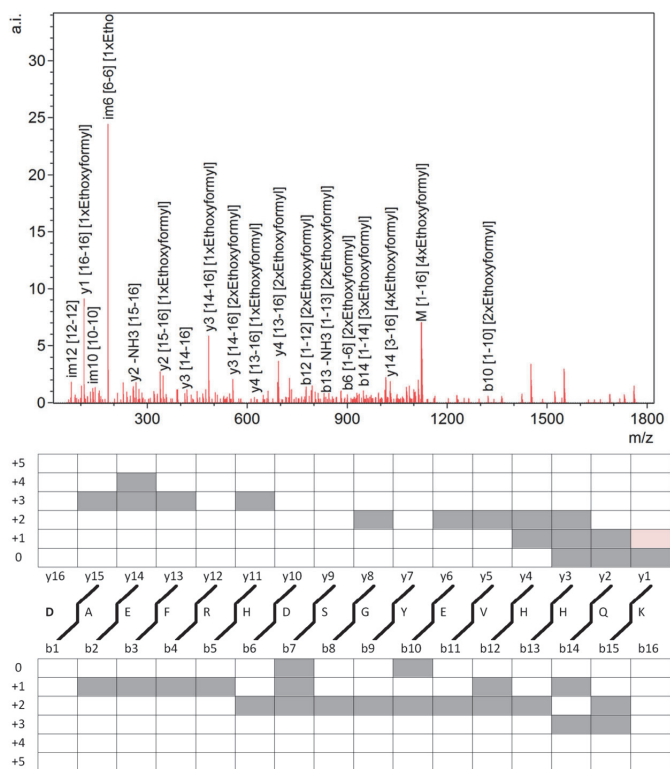
Suppl. Figure 1. MALDI-TOF MS spectra of bovine insulin modified with a 2-times molar excess of DEPC in phosphate buffer at pH 6.8 (A) and pH 7.4 (B). Annotations 1x to 4x denote the number of DEPC modifications added to insulin. Intensity is relative to insulin in the control sample.



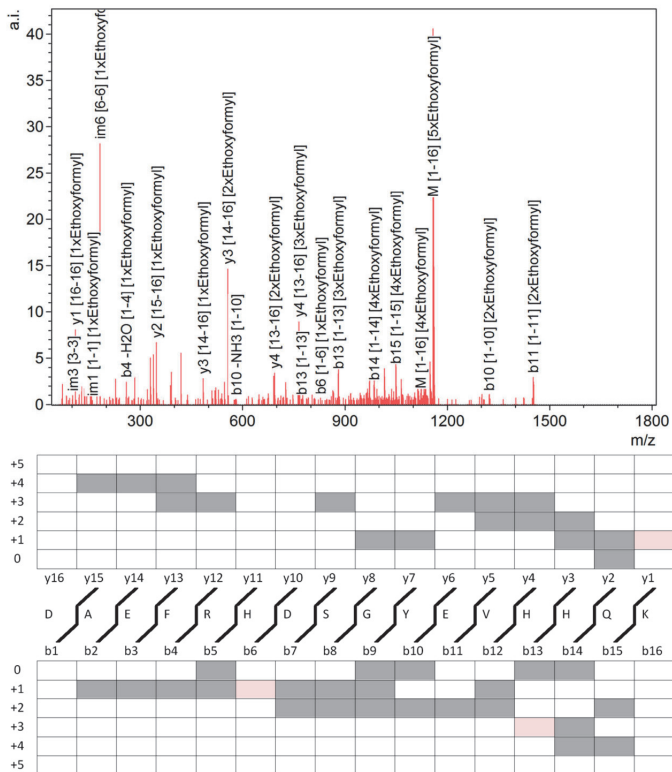




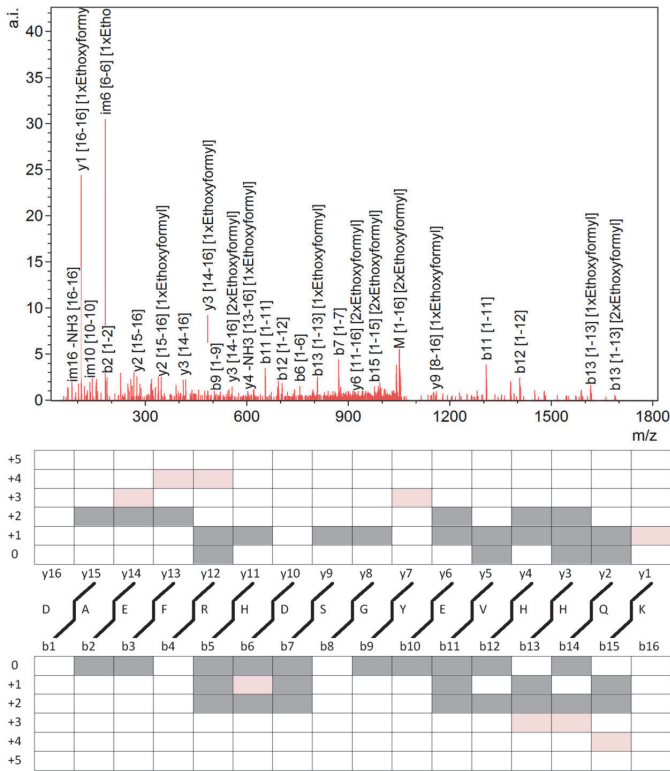
Suppl. Figure 3: Targeted sequencing of A $\beta$ 1-16 modified with 1 DEPC molecule after hydroxylamine treatment. Above is a spectrum of identified fragments from mMass and below is the table of mMass results from ESI Q-TOF MS/MS spectrum where pink cells are false-positive results indicated by mMass as DEPC modifications in A $\beta$ 1-16 control sample, grey cells are results found by mMass software for A $\beta$ 1-16 modified with 1 DEPC molecule. “0 DEPC” row indicates peptide fragments without modifications and “1-5 DEPC” indicates the number of modifications found by mMass software. The sample was in 20mM ammonium acetate, pH 7.4; precursor was peak 1014 m/z (once DEPC-modified A $\beta$ 1-16 with charge 2+), collision energy 50.



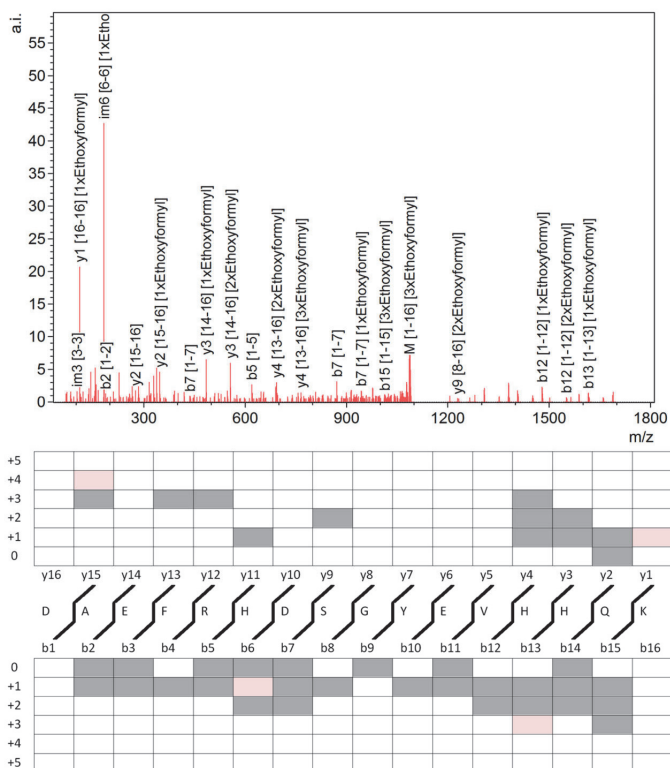
Suppl. Figure 4: Targeted sequencing data from the peak of A $\beta$ 1-16 modified with 4 DEPC molecules. Above are spectra of identified fragments from mMass and below are tables of mMass results from ESI Q-TOF MS/MS spectrum where pink cells are false-positive results indicated by mMass as DEPC modifications in A $\beta$ 1-16 control sample, grey cells are results found by mMass software for A $\beta$ 1-16 modified with 4 DEPC molecules. “0 DEPC” row indicates peptide fragments without modifications and “1-5 DEPC” indicates the number of modifications found by mMass software. Samples were in 20mM ammonium acetate, pH 7.4; precursor was peak 1122.5 m/z (4 times DEPC-modified A $\beta$ 1-16 with charge 2+), collision energy 50.



Suppl. Figure 5: Targeted sequencing data from the peak of Aβ1-16 modified with 5 DEPC molecules. Above are spectra of identified fragments from mMass and below are tables of mMass results from ESI Q-TOF MS/MS spectrum where pink cells are false-positive results indicated by mMass as DEPC modifications in Aβ1-16 control sample, grey cells are results found by mMass software for Aβ1-16 modified with 5 DEPC molecules. “0 DEPC” row indicates peptide fragments without modifications and “1-5 DEPC” indicates the number of modifications found by mMass software. Samples were in 20mM ammonium acetate, pH 7.4; precursor was peak 1158.5 m/z (5 times DEPC-modified Aβ1-16 with charge 2+), collision energy 50.



Suppl. Figure 6: Targeted sequencing data from the peak of copper protected Aβ1-16 modified with 2 DEPC molecules. Above are spectra of identified fragments from mMass and below are tables of mMass results from ESI Q-TOF MS/MS spectrum, where pink cells are false-positive results indicated by mMass as DEPC modifications in Aβ1-16 control sample combined with results indicating higher modification level than the precursor. Grey cells are results found by mMass software for copper protected Aβ1-16 modified with 2 DEPC molecules. “0 DEPC” row indicates peptide fragments without modifications and “1-5 DEPC” indicates the number of modifications found by mMass software. Samples were in 20mM ammonium acetate, pH 7.4; precursor was peak 1050.5 m/z (2 times DEPC-modified Aβ1-16 with charge 2+), collision energy 50.



Suppl. Figure 7: Targeted sequencing data from the peak of copper protected A $\beta$ 1-16 modified with 3 DEPC molecules. Above are spectra of identified fragments from mMass and below are tables of mMass results from ESI Q-TOF MS/MS spectrum, where pink cells are false-positive results indicated by mMass as DEPC modifications in A $\beta$ 1-16 control sample combined with results indicating higher modification level than the precursor. Grey cells are results found by mMass software for copper protected A $\beta$ 1-16 modified with 3 DEPC molecules. “0 DEPC” row indicates peptide fragments without modifications and “1-5 DEPC” indicates the number of modifications found by mMass software. Samples were in 20mM ammonium acetate, pH 7.4; precursor was peak 1086.5 m/z (3 times DEPC-modified A $\beta$ 1-16 with charge 2+), collision energy 50.



## CURRICULUM VITAE

Name: Merlin Sardis  
Date of birth: 21.04.1986  
Place of birth: Tallinn, Estonia  
Citizenship: Estonia  
E-mail: [merlin.sardis@gmail.com](mailto:merlin.sardis@gmail.com);  
[merlin.sardis@taltech.ee](mailto:merlin.sardis@taltech.ee)

### Education

2010–2019 Tallinn University of Technology, Ph.D. student  
2008–2010 Tallinn University of Technology, MSC  
2005–2008 Tallinn University of Technology, BSC  
2002–2005 Tallinn Technical Gymnasium

### Professional employment

2017–... Tallinn University of Technology, Department on Chemistry and Biotechnology, engineer  
2015–2017 Tallinn University of Technology, Department of Gene Technology, engineer

### Awards and stipends

February 2018 DoRa Plus Scholarship of Archimedes Academic Fund (activity T1.1)  
July 2013 DoRa Research Fellowship (activity 8)  
2011 World Federation of Scientists (WFS)

### Courses and conferences

February 2018 “Essential Operator Training Course – Proteomics” Bruker Daltonik, Bremen, Germany  
June 2015 “European Society for Neurochemistry” conference poster presentation, Tartu, Estonia  
July 2013 “FEBS Congress” conference poster presentation, St. Petersburg, Russia  
April 2013 “Protein Crystallography” course, Tartu, Estonia  
October 2011 “Transmission-, Scanning- and Immune electron microscopy” Theoretical and practical course, Tartu, Estonia  
August 2009 Molecular Biosciences International Student Programme (MOBIL) summer school, Aarhus, Denmark



## Publications

Tiiman, A., Noormagi, A., **Friedemann, M.**, Krishtal, J., Palumaa, P., & Tõugu, V. (2013). Effect of agitation on the peptide fibrillization: Alzheimer's amyloid-beta peptide 1-42 but not amylin and insulin fibrils can grow under quiescent conditions. *J Pept Sci*, *19*(6), 386-391. doi: 10.1002/psc.2513

Taler-Vercic, A., Kirsipuu, T., **Friedemann, M.**, Noormagi, A., Polajnar, M., Smirnova, J., Znidaric, M. T., Zganec, M., Skarabot, M., Vilfan, A., Staniforth, R. A., Palumaa, P., & Zerovnik, E. (2013). The role of initial oligomers in amyloid fibril formation by human stefin B. *International Journal of Molecular Sciences*, *14*(9), 18362-18384. doi: 10.3390/ijms140918362

Tõugu, V., **Friedemann, M.**, Tiiman, A., & Palumaa, P. (2014). Copper(II) ions and the Alzheimer's amyloid- $\beta$  peptide: Affinity and stoichiometry of binding. *AIP Conference Proceedings*, *1618*(1), 109-111. doi: 10.1063/1.4897689

**Friedemann, M.**, Helk, E., Tiiman, A., Zovo, K., Palumaa, P., & Tõugu, V. (2015). Effect of methionine-35 oxidation on the aggregation of amyloid-beta peptide. *Biochem Biophys Rep*, *3*, 94-99. doi: 10.1016/j.bbrep.2015.07.017

Wallin, C., **Friedemann, M.**, Sholts, S. B., Noormagi, A., Svantesson, T., Jarvet, J., Roos, P. M., Palumaa, P., Graslund, A., & Warmlander, S. (2019). Mercury and Alzheimer's Disease: Hg(II) Ions Display Specific Binding to the Amyloid-beta Peptide and Hinder Its Fibrillization. *Biomolecules*, *10*(1). doi: 10.3390/biom10010044

Kirsipuu, T., Zadoroznaja, A., Smirnova, J., **Friedemann, M.**, Plitz, T., Tõugu, V., & Palumaa, P. (2020). Copper(II)-binding equilibria in human blood. *Sci Rep*, *10*(1), 5686. doi: 10.1038/s41598-020-62560-4

**Friedemann, M.**, Tougu, V., & Palumaa, P. (2020). Cu(II) partially protects three histidine residues and the N-terminus of amyloid-beta peptide from diethyl pyrocarbonate (DEPC) modification. *FEBS Open Bio*. doi: 10.1002/2211-5463.12857

## ELULOOKIRJELDUS

Nimi: Merlin Sardis  
Sünniaeg: 21.04.1986  
Sünnikoht: Tallinn, Eesti  
Kodakondsus: Eesti  
E-post: [merlin.sardis@gmail.com](mailto:merlin.sardis@gmail.com);  
[merlin.sardis@taltech.ee](mailto:merlin.sardis@taltech.ee)

### Hariduskäik

2010–2019 Tallinna Tehnikaülikool, doktorant  
2008–2010 Tallinna Tehnikaülikool, MSC  
2005–2008 Tallinna Tehnikaülikool, BSC  
2002–2005 Tallinna Tehnikagümnaasium

### Teenistuskäik

2017–... Tallinna Tehnikaülikool, Keemia ja Biotehnoloogia instituut, insener  
2015–2017 Tallinna Tehnikaülikool, Geenitehnoloogia instutuut, insener

### Teaduspreemiad ja tunnustused

Veebruar, 2018 DoRa Pluss lühiajalise õpirände stipendium (tegevus T1.1), SA Archimedes  
Juuni, 2013 DoRa T8 stipendium “Noorteadlaste lühiajalised välisviisidid” (tegevus 8)  
2011 World Federation of Scientists (WFS)

### Kursused ja konverentsid

Veebruar 2018 “Essential Operator Training Course – Proteomics” Bruker Daltonik, Bremen, Saksamaa  
Juuni 2015 “European Society for Neurochemistry” konverentsi posterettekanne, Tartu, Estonia  
Juuli 2013 “FEBS Congress” konverentsi posterettekanne, Peterburi, Venemaa  
Aprill 2013 “Valkude Kristallograafia” kursus, Tartu, Eesti  
Oktoober 2011 Transmissioon-, skaneeriv- ja immunoelektronmikroskoopia” teoreetiline ja praktiline kursus, Eesti Maaülikool, Tartu, Eesti  
August 2009 “Molecular Biosciences International Student Programme” (MOBIL) suvekool, Aarhus, Taani

## Publikatsioonid

Tiiman, A., Noormagi, A., **Friedemann, M.**, Krishtal, J., Palumaa, P., & Tõugu, V. (2013). Effect of agitation on the peptide fibrillization: Alzheimer's amyloid-beta peptide 1-42 but not amylin and insulin fibrils can grow under quiescent conditions. *J Pept Sci*, 19(6), 386-391. doi: 10.1002/psc.2513

Taler-Vercic, A., Kirsipuu, T., **Friedemann, M.**, Noormagi, A., Polajnar, M., Smirnova, J., Znidaric, M. T., Zganec, M., Skarabot, M., Vilfan, A., Staniforth, R. A., Palumaa, P., & Zerovnik, E. (2013). The role of initial oligomers in amyloid fibril formation by human stefin B. *International Journal of Molecular Sciences*, 14(9), 18362-18384. doi: 10.3390/ijms140918362

Tõugu, V., **Friedemann, M.**, Tiiman, A., & Palumaa, P. (2014). Copper(II) ions and the Alzheimer's amyloid- $\beta$  peptide: Affinity and stoichiometry of binding. *AIP Conference Proceedings*, 1618(1), 109-111. doi: 10.1063/1.4897689

**Friedemann, M.**, Helk, E., Tiiman, A., Zovo, K., Palumaa, P., & Tõugu, V. (2015). Effect of methionine-35 oxidation on the aggregation of amyloid-beta peptide. *Biochem Biophys Rep*, 3, 94-99. doi: 10.1016/j.bbrep.2015.07.017

Wallin, C., **Friedemann, M.**, Sholts, S. B., Noormagi, A., Svantesson, T., Jarvet, J., Roos, P. M., Palumaa, P., Graslund, A., & Warmlander, S. (2019). Mercury and Alzheimer's Disease: Hg(II) Ions Display Specific Binding to the Amyloid-beta Peptide and Hinder Its Fibrillization. *Biomolecules*, 10(1). doi: 10.3390/biom10010044

Kirsipuu, T., Zadoroznaja, A., Smirnova, J., **Friedemann, M.**, Plitz, T., Tõugu, V., & Palumaa, P. (2020). Copper(II)-binding equilibria in human blood. *Sci Rep*, 10(1), 5686. doi: 10.1038/s41598-020-62560-4

**Friedemann, M.**, Tougu, V., & Palumaa, P. (2020). Cu(II) partially protects three histidine residues and the N-terminus of amyloid-beta peptide from diethyl pyrocarbonate (DEPC) modification. *FEBS Open Bio*. doi: 10.1002/2211-5463.12857

ISSN 2585-6901 (PDF)  
ISBN 978-9949-83-682-6 (PDF)